Learning Data Fusion for Indoor Localisation

Widyawan

Department of Electronic Engineering

Cork Institute of Technology

A thesis submitted for the degree of

Doctor of Philosophy

October 2009

Learning Data Fusion for Indoor Localisation

Widyawan

Department of Electronic Engineering
Cork Institute of Technology

Supervisor: Dr. Martin Klepal & Dr. Dirk Pesch

A thesis submitted for the degree of
Doctor of Philosophy

October 2009

Declaration

I hereby declare that this submission is my own work and that, to the best of my knowledge and belief, it contains no material previously published or written by another person nor material to a substantial extent has been accepted for the award of any other degree or diploma of the university of higher learning, except where due acknowledgement has been made in the text.

Signature of Author : .....

Certified by : .....

Date : .....

To Diana, Yasmeen and Rana ...

Foreword

Alhamdulillah, after several years of studies, the moment has come to close this PhD thesis. I would like to acknowledge the support from many colleagues I have received throughout that period of time.

First and foremost, I wish to sincerely thank my supervisors, Dr. Martin Klepal, for the invaluable guidance and help that he was always willing to give during my research. Thanks to Dr. Dirk Pesch, for the advice and encouragement during my research and the help for bringing my family here.

I would also like to offer my gratitude to Dr. Chris Bleakley and Dr. Alan McGibney as my external and internal reviewers, for their input perfecting this thesis.

Thanks to Gerald, Danielle, Carl and Chunlei for helping with the measurements and preparation of the demo in Passau, Munich, Bremen and Linz. Thanks to Dr. David Sheehan and Donal for the proof-reading of my thesis. Thanks to Marteen Wyen and Stephane for the good discussions we always had. Thanks to Dave Hamilton, John Harrington and Julie O'Shea for their support during my work.

Thanks to Martin Koubek, Rosta, Yamuna, David Lopez and Gloria, for the cheers they often gave. I will always welcome you as my guest in Indonesia. Thanks to all the members of the basket ball lads: Chong, Ciaran, Susan, Jian, Fei Fei, Boon, Derry, Dave and Anthony for giving a healthy-break from my cubical desk once a week.

To Sigit, Warsun, Bimo, Neta and Adi, thanks for constantly reminding me that I will never walk alone here. To the Ober's: Chriss, Ovie and lovely Kirantje and the Ulman's: Yulia, Sven and the kids,

thanks for always having the moments to cheer and food to share. To Salam, Ershad, Kucai, Shukry, Hamid, Silvia and Fabrice, thanks for the friendship they always offer.

Thanks to Bapak, Pak Jirjis and Ibu for their support and prayers. For the rest of family members, thanks you all for always caring and being supportive. And finally to my Diana, Yasmeen and Rana for their simple, yet amazing love, they deserve more thanks than I can say.

It has been a long journey not only through illness, being homesick and after-hours work but also laugh and joy. It is a path worth taken, a story worth remembrance. Eventually, it finished. I am a Doctor now.

Acknowledgement

This research was conducted within the context of the WearIT@Work project (EC IST IP2003 0004216)[1] and LocON project (EC FP7 FP7 224148)[2].

The author also wishes to acknowledge several partners for their support during this research as follows

1. Bremen University, Bremen, Germany
2. University of Passau, Passau, Germany
3. DoCoMo Comm. Lab. Europe GmbH, Munich, Germany
4. Lancaster University, Lancaster, United Kingdom
5. Swiss Federal Institute of Technology, ETH Zurich, Switzerland
6. Artesis University College of Antwerp, Antwerp, Belgium

[1] www.wearitatwork.com
[2] www.ict-locon.eu

Abstract

Indoor localisation systems is evolving towards systems that can take advantage of any readily available information in the environment and a mobile device. This type of localisation is called opportunistic localisation system.

Some aspects of opportunistic indoor localisation systems, utilising received signal strength (RSS) measurement, need to be enhanced in terms of accuracy and usability.

Usability is defined as ease of installation and maintenance of the system. Before an opportunistic localisation system can be used, system calibration must be performed. During calibration, RSS measurements throughout the coverage area (called a fingerprint) must be collected and saved in a database. However, building a fingerprint database is time consuming and cumbersome. Furthermore, building fingerprints in a large-scale indoor environment is not a trivial undertaking and is labour intensive.

Therefore, implementation of opportunistic based localisation with more advanced algorithms is crucial to the wider adoption of affordable, accurate, usable indoor localisation systems.

This research proposes a learning data fusion algorithm based on a particle filter to increase the accuracy and usability of opportunistic indoor localisation system. The particle filter algorithm is improved with map filtering and backtracking particle filtering to further increase accuracy of the system.

To address the usability problem, a learning data fusion algorithm was devised. This was able to automatically generate and calibrate a

RSS fingerprint. The algorithm maintained the fingerprint up-to-date, thus achieving self-calibration of the localisation system.

In addition, the algorithm furthermore is used to fuse different sensory data when more fine-grained accuracy is desirable or when a multi-modal localisation system is required for different application domains, such as localisation for first-responders in emergency scenarios. The algorithm was used for fusing different localisation modalities based on wireless local area network (WLAN), pedestrian dead reckoning (PDR), ultrasound and wireless sensor network (WSN).

The main contributions of this work are the self-calibration fingerprinting to enhance usability of the opportunistic indoor localisation, and a collection of algorithms (map filtering, backtracking particle filter and particle filter-based sensor data fusion) to increase the accuracy of opportunistic indoor localisation system. Those algorithms advance state of the art and will be described and evaluated in this thesis.

Contents

List of Publications

[1] **Widyawan** and M. Klepal, "Real time location and tracking terminal in IEEE802.11 network," in *Proceedings of the MUCS 2006*, Ireland, May 2006.

[2] S. Beauregard, M. Klepal, and **Widyawan**, "Positioning in WearIT@Work," in *Proceedings of the Joint ISHTAR/LIAISON Workshop*, Athens, Greece, September 2006.

[3] **Widyawan**, M. Klepal, and D. Pesch, "RF-based location system in harsh environment," in *Proceedings of the IFAWC 2007*, Tel Aviv, Israel, March 2007.

[4] S. Beauregard, M. Klepal, **Widyawan**, and D. L. Perez, "Progress in WearIT@Work positioning technologies," in *Proceedings of the IFAWC*, Tel Aviv, Israel, March 2007.

[5] **Widyawan**, M. Klepal, and D. Pesch, "Influence of predicted and measured fingerprint on the accuracy of RSSI-based indoor location systems," in *Proceedings of the 4th IEEE WPNC 2007*, Hannover, Germany, March 2007.

[6] **Widyawan**, M. Klepal, and D. Pesch, "A bayesian approach for RF-based indoor localisation," in *Proceedings of the 4th IEEE ISWCS 2007*, Trondheim, Norway, October 2007.

[7] **Widyawan**, M. Klepal, and S. Beauregard, "A backtracking particle filter for fusing building plans with PDR displacement estimates," in *Proceedings of the 5th IEEE WPNC 2008*, Hannover, Germany, 2008.

[8] S. Beauregard, **Widyawan**, and M. Klepal, "Indoor PDR performance enhancement using minimal map information and particle filters," in *Proceedings of the IEEE/ION PLAN*, Monterey, California, May 2008.

[9] **Widyawan**, M. Klepal, S. Beauregard, and D. Pesch, "A novel backtracking particle filter for pattern matching indoor localization," in *Proceedings of the 1st ACM MELT 2008*, San Fransisco, 2008.

[10] W. Najib, M. Klepal, **Widyawan**, and D. Pesc, "A software development model for localization system," in *Proceedings of the POCA*, Antwerp, Belgium, May 2009.

[11] M. Klepal, M. Weyn, W. Najib, I. Bylemans, S. Wibowo, **Widyawan**, and B. Hantono, "OLS - opportunistic localisation system for smart phones devices," in *Proceedings of the SIGCOMM*, Barcelona, August 2009.

[12] M. Wyen, M. Klepal, and **Widyawan**, "Adaptive motion model for a smart phone based opportunistic localization system," in *Proceedings of the 2nd ACM MELT*, Florida, September 2009.

List of Figures

List of Tables

List of Algorithms

Nomenclature

Greek Symbols

α	direction
ϵ	localisation error
π	$\simeq 3.14\ldots$
η	penalty
σ	standard deviation
ϖ	trajectory weight

Acronyms

ANN	Artificial Neural Network
AOA	Angle of Arrival
AP	Access Point
BPF	Backtracking Particle Filter
$DECT$	Digital Enhanced Cordless Telephone
EM	Expectation Maximisation
$GNSS$	Global Navigation Satellite System
GPS	Global Positioning System

KF Kalman Filter

MF Map Filtering

MM Motif Model

MWM Multi Wall Model

NN Nearest Neighbour

OSM One Slope Model

PDA Personal Digital Assistant

PDR Pedestrian Dead Reckoning

PF Particle Filter

$RFID$ Radio Frequency Identification

RSS Received Signal Strength

SIS Sequential Important Sampling

$TDOA$ Time Difference of Arrival

TOA Time of Arrival

TOF Time of Flight

UWB Ultra Wide Band

$WLAN$ Wireless Local Area Network

WSN Wireless Sensor Network

Chapter 1

Introduction

Growing interest in pervasive computing has been fostered further by the omnipresence of mobile computing devices, such as portable media players, mobile phones, personal digital assistants (PDA) and notebooks. Automatically ascertaining the physical location of people or devices is regarded as a key pervasive computing application [1]. Knowledge of physical location would open up a wide range of possible future applications; for example, tracking people and assets, safety and security, and indoor navigation.

The global positioning system (GPS) is the mainstream technology for location and tracking in outdoor environments [2]. However, GPS provides insufficient reliability and accuracy for indoor environments, since its signal is heavily attenuated by building structures such as roofs and walls. Consequently, indoor localisation systems have been proposed based on other technologies, such as radio frequency identification (RFID) [3] and ultra wideband radio [4].

A common disadvantage of many existing localisation systems is the requirement for a dedicated device and proprietary infrastructure in the operation area of the indoor localisation system. These systems are evolving to take advantage of any readily available information in the environment and a mobile device. This type of localisation is called an opportunistic localisation system. One of the most common characteristics of a mobile computing device that can be extracted for localisation purposes is the wireless communication channel.

Received signal strength (RSS) is one of the channel parameters of a wireless communication system that is relevant for localisation. Since virtually all

wireless communication devices are able to obtain and read RSS, the localisation system can be implemented in the off-the-shelf device with little or no hardware change. The system becomes a software and algorithmic solution. However, some aspects of opportunistic indoor localisation systems need to be enhanced, namely usability[1] of the system and accuracy of location estimation. Before a localisation system can be used, system calibration must be performed. During this calibration, RSS measurements throughout the coverage area must be collected and saved in a database called a fingerprint.

Building a fingerprint is an expensive undertaking. It is time-consuming and cumbersome and building a fingerprint in a large-scale indoor environment is especially labour-intensive. The effort required outweighs the value of having the localisation system in the first place, thus hindering large scale adoption of such systems.

1.1 Motivation and Thesis

The development of an algorithm to enhance the accuracy and usability is a foundation in achieving an affordable, accurate and usable indoor localisation system. Consequently, this area has received significant research interest in recent years. However, the proposed solutions are still suboptimal given the problems they are attempting to address.

The main motivation of the research is to address current drawbacks of the opportunistic system and to develop a viable algorithm to advance state of the art of the opportunistic indoor localisation system. It is achieved by enhancing current approaches based on a particle filter and devising novel algorithms to enhance accuracy and usability of opportunistic indoor localisation.

1.2 Research Objectives

The main objectives of the research presented here are summarised as follows:

[1] Usability is defined as the ease to install and to maintain the system.

1. A comprehensive review of the state of the art of indoor localisation systems, with a particular focus on highlighting opportunities for an affordable, accurate, and usable opportunistic indoor localisation system.

2. Development and evaluation of a filtering algorithm with a Bayesian approach to enhance the accuracy of opportunistic indoor localisation.

3. Development and evaluation of a learning data fusion algorithm to enhance the accuracy and usability of opportunistic indoor localisation.

4. Investigation of the sensor data fusion algorithm between different localisation technologies and also algorithm implementation in different application domain.

5. Evaluation and comparison of the developed algorithms against current approaches with a particular focus on the implementation of opportunistic indoor localisation.

1.3 Contribution

A learning data fusion algorithm is devised to address current problems in opportunistic localisation systems. To enable the implementation of a particle filter into opportunistic indoor localisation, novel motion and measurement models are developed.

The particle filter-based algorithm is adopted to improve the accuracy of the opportunistic system. Furthermore, map filtering and backtracking particle filter algorithm are devised to further improve the accuracy of the opportunistic indoor localisation system.

One of the most important contributions of this thesis is the self-calibration fingerprint algorithm. The novelty of the algorithm lies on the ability to automatically build and maintain the fingerprint up-to-date, thus significantly enhance the usability of the opportunistic indoor localisation.

In addition, the algorithm is used to fuse different sensory data when more fine-grained accuracy is desirable or when a multi-modal localisation system is required for different application domains, such as in localisation for first-responders

in emergency scenarios. Sensor-specific measurement models are developed to enable the fusion.

The application of particle filter-based data fusion for opportunistic indoor localisation which can also be implemented into different application domain is one of the original contributions of this research.

It will be demonstrated that this novel algorithm yields significant benefits not only for improving accuracy but also in the usability of the opportunistic indoor localisation.

1.4 Thesis Outline

The remainder of this thesis is organised as follows:

- Chapter 2 describes the state of the art in indoor localisation. It will review current systems and algorithms and address current approaches in opportunistic indoor localisation.
- Chapter 3 discusses one of the contributions of this thesis - a Bayesian approach for opportunistic indoor localisation. It will present the idea behind Bayesian inference, and its implementation as the particle filter algorithm.
- Chapter 4 presents the learning data fusion as the major contribution of the thesis. The proposed algorithms are used to advance further the accuracy and usability of opportunistic indoor localisation. It will be described how the algorithm was able to build and refine the fingerprint.
- Chapter 5 describes the sensor data fusion of different localisation technologies.
- Chapter 6 provides a detailed evaluation of the proposed algorithm.
- Chapter 7 summarises conclusions that can be derived from the work presented and assesses future perspectives and opportunities for this research. It also reflects on the overall conclusions that can be drawn from completing the research presented in this thesis.

Chapter 2

State of the Art

A range of localisation systems have been developed to meet distinctive requirements of differing applications and operating environments. This domain has evolved to utilise various physical phenomena and algorithms for location estimation. This chapter describes current approaches towards development of such localisation systems. Since various localisation systems exist, a localisation classification taxonomy is developed to make possible a more structured and comprehensive review of current approaches.

Section 2.1 describes the classification of localisation systems, which also presents advantages and disadvantages of each approach. This classification underlines the opportunities for affordable opportunistic indoor localisation systems.

Section 2.2 focuses on current approaches in opportunistic indoor localisation. It highlights the necessity for an algorithm that enhances the accuracy and usability of the opportunistic indoor localisation system.

2.1 Classification of Localisation System

A classification was developed using criteria that help to underline the opportunities for an affordable, accurate, and usable opportunistic indoor localisation system. These are:

1. Measured phenomena
2. Measured data processing

3. Performance

2.1.1 Measured Phenomena

Four phenomena which are typically measured to infer location have been identified:

1. Time of arrival (TOA) and time difference of arrival (TDOA)
2. Angle of arrival (AOA)
3. Received signal strength (RSS)
4. Inertial

Time of Arrival (TOA) and Time Difference of Arrival (TDOA)

Time of arrival (TOA), which is also sometimes called time of flight (TOF), is the travel time between synchronised transmitting and receiving devices. The receiver can find the time of arrival by subtracting the time at which the signal was transmitted from the time at which the signal was received. TOA can be measured directly using the ultra wideband (UWB) technique [5] [4] or by using a signalling technique such as spread spectrum [6] [7]. Time difference of arrival (TDOA) is the time difference of arrival between multiple synchronised transmitters measured at the receiver. GPS is the best-known example of a localisation system utilising TDOA measurement. Global system for mobile communications (GSM) localisation can also be implemented using TDOA [8].

The advantage The advantage of TOA and TDOA is that the estimation can be very accurate (to sub-meter levels). However, the complexity of the hardware and the time synchronisation required are important **disadvantages** of localisation with time measurements [9]. Localisation systems based on this phenomenon have low affordability.

Angle of Arrival (AOA)

Angle of arrival (AOA) is a method for obtaining the direction of propagation of an incident radio-frequency wave. AOA can be measured either with a mechanically-steered narrow beam width antenna, or with a fixed array of antennas [10] of which the antenna array approach is more common and practical. Another method for AOA, which has been used for ultrasound waves, is described in [11]. It used several ultrasound receivers in a device to infer the angle of incoming ultrasonic pulse.

The advantage of AOA is that the required number of devices is relatively low for localisation. Two measurement points are sufficient for two dimensional (2D) localisation or three measurement points for three dimensional (3D) localisation[1]. The estimation also can be very accurate. **Disadvantages** include the requirement for relatively large and complex hardware and the fact that accuracy degrades as the mobile target moves further from the measurement unit [12]. The hardware requirement will make localisation systems based on this phenomenon have low affordability.

Received Signal Strength (RSS)

RSS is the radio signal power present at the receiver a distance from the transmitter. In general, RSS decreases proportionately with this distance [13]. If the relationship of distance to signal strength is known, either analytically or empirically, the distance between two devices can be calculated.

There are several **advantages** of using RSS for indoor localisation. Firstly, it can be implemented in wireless communication systems with little or no hardware change. All that is needed is the capability to obtain and read RSS, which is provided by virtually all wireless communication devices. The localisation system can therefore be implemented in off-the-shelf devices. Secondly, it does not require synchronisation between transmitter and receiver. These advantages are key factors that contribute to *the greater affordability and usability* of using RSS for indoor localisation. The principal **disadvantage** is that RSS readings

[1]It assumes a priori knowledge of orientation

can show large variations due to interference and multipath on the radio channel. The accuracy is therefore lower than time measurement methods [14].

Inertial

Inertial is a measured phenomenon used to infer the direction, displacement or velocity of an object for navigational purposes[1]. A range of instruments can be utilised for such measurements including accelerometers, magnetometers, gyroscopes, compasses or odometers. A more detailed explanation of how the navigational instruments work can be found in [15] [16].

The advantage of using inertial measured phenomena is that the sensors are independent of any external infrastructure. Therefore, it is suitable for localisation or navigation where there is no localisation infrastructure inside the building, such as localisation for first responders [17]. **A disadvantage** is that these systems can only provide a relative position; to provide an absolute position the assistance of another system would be required.

Other

There are a variety of other measured phenomenon that can be used for localisation, such as images taken from a wearable camera [18] [19] or audio and video signals [20] as data supplemental to other localisation systems. Since these methods required specialised and costly hardware, this method has a low affordability. Therefore, these methods are beyond the scope of the present work and will not be discussed further here.

2.1.2 Measured Data Processing

Classification based on measured data processing looks into how localisation systems process measured phenomena to infer location. The most common data processing methods to infer location are:

1. Geometric

[1] *Navigation* is a determination of position and velocity of a moving vehicle.

2. Fingerprinting
3. Proximity
4. Dead reckoning

Geometric

Geometric properties may be used for location estimation. Common geometric methods for location estimation include lateration and angulation (Figure 2.1). In lateration, target location is estimated by measuring its distance from multiple reference points using TOA (Figure 2.1(a)), TDOA (Figure 2.1(b)) or RSS measurements (Figure 2.1(c)). Angulation uses intersections of several pairs of angle direction lines to estimate target location (Figure 2.1(d)) .

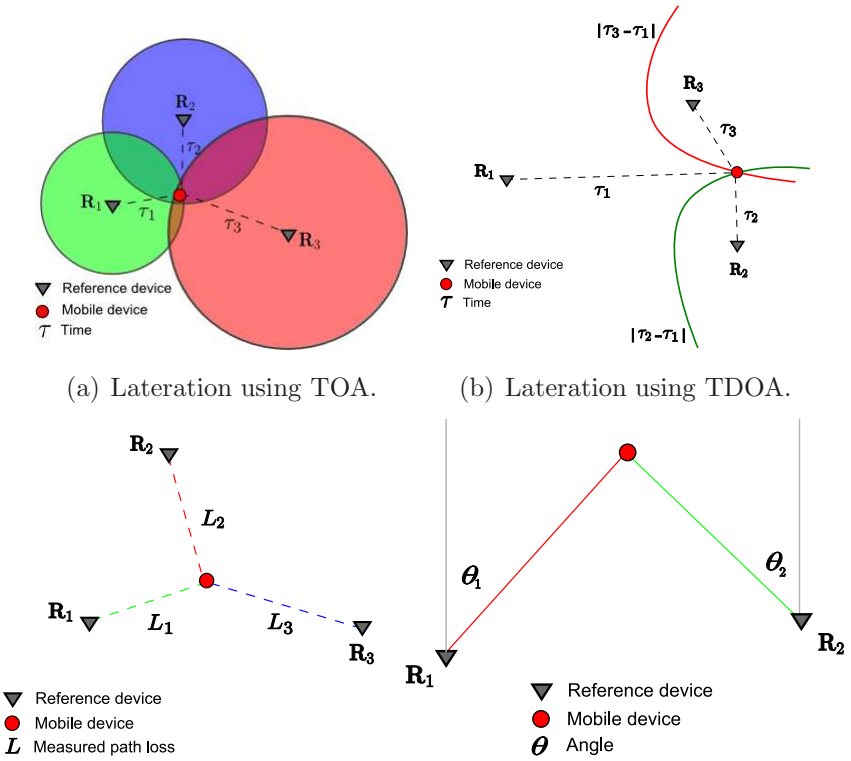

(a) Lateration using TOA.

(b) Lateration using TDOA.

(c) Lateration using RSS.

(d) Angulation using AOA.

Figure 2.1: Geometric methods for different types of measurements

Finding the circles' intersection points or minimising cost function using the least-square technique is a straightforward method with TOA [21]. A hyperbolic method (Figure 2.1(b)) may be used for TDOA measurements [22] whilst distances can be calculated from RSS measurements using a radio propagation model [23].

Fingerprinting

Fingerprinting is a method for mapping measured data (e.g.: RSS) to a known grid-point throughout the coverage area in the environment. Location is estimated from comparison between real-time RSS measurement and a RSS previously stored in the fingerprint. Fingerprinting is often used for RSS-based indoor localisation, especially when analytical correlation between RSS measurement and distance is not easily established due to multipath and interference [9].

Proximity

The proximity method provides symbolic location in terms of co-location with a known landmark. Mostly, it relies on the deployment of a dense grid antenna as the landmark. Mobile device location is determined as the antenna position which received the strongest signal. The proximity method is widely used for RFID [3], infra red localisation [24] or GSM positioning with cell identification (Cell-ID) or cell of origin (COO) method [25].

Dead Reckoning

Dead reckoning is a process for estimating location by advancing a known position using inertial sensory data translated to speed, time, course and distance travelled [13]. In other words, calculating where the target will be at a certain time if it maintains its speed (v) and course.

Figure 2.2 illustrates the dead reckoning principle to calculate target location x_t from previous known position x_{t-1} based on distance travelled ($d = v.\Delta t$) and course/angle.

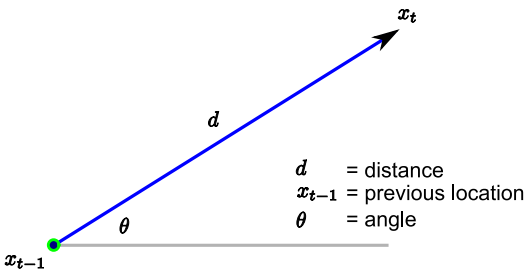

Figure 2.2: Dead reckoning principle.

2.1.3 Performance

Classification based on performance categorises various localisation systems based on the working environment and accuracy. A summary of this classification is illustrated in Figure 2.3. It was used to demonstrate the technology barrier of existing localisation technologies and it was an adaptation of the taxonomy found in [12].

It can be seen that indoor localisation systems based on UWB and microwave technology with time and angle measurements give the best accuracy. Nowadays, there are several commercially-available implementations of UWB [26] [27] [28] and proprietary microwave localisation [29] [30] available commercially. However, these systems require expensive and complex hardware, thus presenting a high technology barrier to wider implementation [29].

An alternative approach is to use existing wireless technology for indoor localisation. Some initiatives based on WSN technology [31] [32] technology, bluetooth [33] [34], digital enhanced cordless telephone (DECT) [35], and WLAN [36] have been proposed.

This approach utilises RSS of the wireless-communication channel for indoor localisation. It offers several important advantages, such as greater affordability (since RSS is virtually free to obtain) and the fact that it can be implemented with essentially off-the-shelf hardware. This approach, therefore, has a low technology barrier.

Recently, WLAN has become the dominant local wireless networking technology. It has coverage range of 50-100m, which is better than most local wireless

technologies such as Bluetooth or WSN. In consequence, many opportunistic indoor localisations use RSS of WLAN as the technology platform of choice.

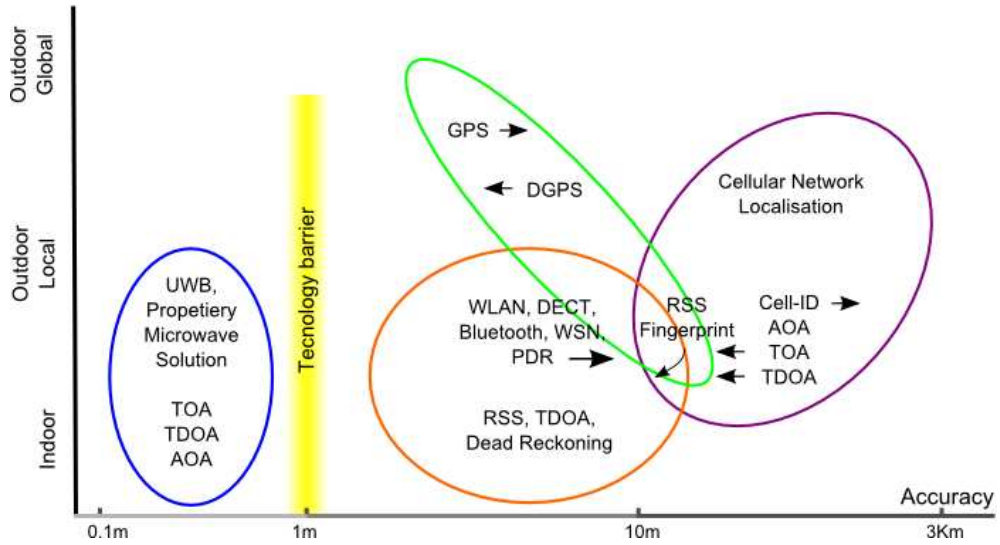

Figure 2.3: Operating environment and accuracy of various localisation systems.

2.1.4 Summary

This section described the classification of localisation systems and also presents advantages and disadvantages for each approach. It was shown that TOA, TDOA and AOA gave the best performance in terms of accuracy. The accuracy can be increased further by combining TOA-AOA or TDOA-AOA in one system. The disadvantages of these solutions are the requirement for time-synchronisation, and for complex or special-purpose hardware. Therefore, these options present a high technology barrier to wider implementation and exploitation of localisation systems. Since these solutions need dedicated hardware and infrastructure, it has lower affordability.

Using the RSS of the wireless-communication channel for indoor localisation offers several important advantages, such as greater affordability (since RSS is virtually free to obtain) and the fact that it can be implemented with essentially off-the-shelf hardware. RSS lateration methods are common in outdoor localisation based on cellular networks. To achieve better accuracy, fingerprinting is often

preferable, especially when analytical correlation between distance and RSS measurement is difficult to establish, such as in indoor environments. Fingerprinting, therefore, is method of choice for opportunistic indoor localisation.

The aforementioned advantages make RSS as the phenomenon of choice for opportunistic indoor localisation. However, the accuracy of RSS-based opportunistic indoor location still needs to be enhanced to meet requirements of typical applications. Furthermore, building an RSS fingerprint is not a trivial effort, especially in large scale indoor environment.

Enhancing the accuracy and usability of opportunistic indoor localisation becomes the objective of this research. Furthermore, using single type of measured phenomenon may not offer required accuracy, but they can be combined to achieve better accuracy.

WLAN has become the dominant local wireless networking technology. Accordingly, majority of the opportunistic indoor localisation systems use RSS of WLAN as the technology platform. The next section will review current approaches in opportunistic indoor localisation and identify problems that still need to be addressed.

2.2 Current Approaches to Opportunistic Indoor Localisation

There have been considerable research in the area of opportunistic indoor localisation particularly using WLAN as the technology platform. There are a number of methods commonly used to infer location from RSS measurement. Those methods will be presented in the following section.

2.2.1 Current Methods

Nearest Neighbour (NN)

An early implementation, called RADAR [36], adopted a method termed nearest neighbour (NN) distance in signal space. The location is estimated by a position

in the fingerprint which has smallest distance (d^*). The distance is governed by the following expressions:

$$d^* = \arg \min_{\mathbf{z}^+ \in \mathbf{Z}^+} M(\mathbf{z}^+, \mathbf{z}) \tag{2.1}$$

with

$$M(\mathbf{z}^+, \mathbf{z}) = \sum_{k \in (\mathbf{z}^+ \cap \mathbf{z})} |z^{+k} - z^k| \tag{2.2}$$

where d^* represents the distance, $\mathbf{Z}^+$ represents the fingerprint, $\mathbf{z}^+$and $\mathbf{z}$ represent a set of RSS in the fingerprint and measurement, respectively, k represents WLAN the access point (AP), $z^{+k}$and z^k represent the RSS value in the fingerprint and measurement, respectively.

The authors offered two approaches to building a fingerprint. First, make empirical measurements of RSS data throughout the coverage area in the indoor environment. Second, using a propagation model called multi-wall model (MWM) as suggested in [37]. Fingerprint prediction with a propagation model is explained in more detail in section 2.2.3.

The advantage of the NN method is its simplicity and its requirement for relatively low amount of computational power. **The Disadvantages** of the NN methods are that it only takes into account current measurements to estimate target location, and ignores other information (such as target behaviour, previous measurements, etc.). This approach often leads to poor estimation accuracy.

Motetrack

Motetrack [38] is a RSS-based indoor localisation using WSN as the technology platform. It uses a decentralised approach that runs on programmable beacon nodes. The fingerprint database is replicated across the beacon nodes to minimise per-node storage overhead and to achieve high robustness to failure.

To infer location, Motetrack extends NN method with a concept of penalty, termed adaptive signature distance metric. The distance metric is governed by:

$$d^* = \arg \min_{\mathbf{z}^+ \in \mathbf{Z}^+} M(\mathbf{z}^+, \mathbf{z}) \tag{2.3}$$

with

$$M(\mathbf{z}^+, \mathbf{z}) = \sum_{k \in (\mathbf{z}^+ \cap \mathbf{z})} |z^{+k} - z^k| + \sum_{k \in (\mathbf{z}^+ - \mathbf{z})} z^{+k} + \sum_{k \in (\mathbf{z} - \mathbf{z}^+)} z^k \tag{2.4}$$

where d^* represents the distance, $\mathbf{Z}^+$ represents the fingerprint, $\mathbf{z}^+$and $\mathbf{z}$ represent a set of RSS in the fingerprint and measurement, respectively, k represents a WSN beacon node, $z^{+k}$and z^k represent the RSS value in the fingerprint and measurement, respectively. **The advantages** of the Motetrack method is its simplicity and speed. The decentralised characteristic also makes it robust to failure. **The disadvantage** of the Motetrack is, like NN method, its simple approach to calculate the distance metric often leads to poor estimation accuracy.

Placelab

Placelab [39] tries to reduce barrier-to-entry to localisation systems by constructing community contributed radio-map. Radio map is a database of beacons position (GSM towers and WLAN APs).

Many of these beacon databases come from institutions that own a large number of wireless networking beacons or databases produced by the *war-driving* community. War-driving is the act of driving around with a mobile computer equipped with a GPS device and a radio (typically a WLAN card but sometimes a GSM phone or Bluetooth device) to collect beacons position.

Distance to known beacons position in the database is inferred by RSS-lateration method. The location can be calculated with finding the circles' intersection points similarly used in TOA (see section 2.1.2).

The advantages of Placelab is that it can be used to integrate outdoor and indoor localisation. The effort to build the radio map is also low since it is a community contributed database. **The disadvantage** is that it has low accuracy (15-20m).

Machine Learning

A machine learning approach has also been used for opportunistic indoor localisation. An artificial-neural-network (ANN) based classifier was used to infer

location from WLAN RSS [40]. The fingerprint is used as training data for ANN to build the localisation estimation model. The aforementioned study uses three-layer architecture with three input units, eight hidden layer units, and two outputs.

In [41] and [42], the authors proposed a statistical learning method based on the support vector machine (SVM) classifier. SVM is a supervised learning method which is mostly used as classification/regression. It uses a fingerprint as its training data to build a classification model. During the training phase, SVM constructs a classifier termed as hyper-plane which in turn is used to estimate the target location.

An important **disadvantage** of the machine learning approach is that it makes several assumptions which may not hold true in all situations [43]. Firstly, it requires large amounts of labelled data[1] to train the system. Secondly, the learned localisation model is static over time and across space. Moreover, static location estimation and tracking of moving targets will give significantly different results as this method does not properly consider a kinematic model of the target [12].

Horus

The Horus system [44] [45] proposed a joint clustering technique for location estimation. Each candidate location is regarded as a class or category. The fingerprint was stored as a collection of models for the joint probability distributions. The fingerprint is built using probabilistic aggregation, either based on a histogram method or on a kernel distribution method [46]. The estimated location is calculated by:

$$\arg\max_{\mathbf{x}} P(\mathbf{x}|\mathbf{z}) = \arg\max_{\mathbf{x}} P(\mathbf{z}|\mathbf{x}).P(\mathbf{z}) \tag{2.5}$$

where $P(\mathbf{x}|\mathbf{z})$ represents conditional probability of location $\mathbf{x}$ given measurement $\mathbf{z}$, $P(\mathbf{z}|\mathbf{x})$ represents conditional probability of measurement $\mathbf{z}$ given location $\mathbf{x}$, $P(\mathbf{z})$ represents probability of measurement $\mathbf{z}$.

[1] RSS with ground truth position, analogue to a fingerprint

The advantage of the Horus method is it can reduce required computational power by the clustering technique. **Disadvantages** of the Horus is it needs a large training data set (fingerprint) to properly construct the joint cluster. Therefore, it has poor usability. It also does not consider kinematic behaviour of target and assumed that the cluster probability always has Gaussian distribution, which can lead to reduced accuracy.

Kalman Filter

The Kalman filter is a probabilistic method based on Bayesian filter. It approximates the probability distribution of the target location by a Gaussian representation. It has been widely used in robotic mapping and localisation [47] [48]. The probability distribution is given by [49]:

$$p(x_t|z_t) \approx N(x_t; \mu_t, E_t) \tag{2.6}$$

$$= \frac{1}{(2\pi)^{d/2}|E_t|^{1/2}} \exp\left[-\frac{1}{2}(x_t - \mu_t)^T E_t^{-1}(x_t - \mu_t)\right] \tag{2.7}$$

where μ_t is the mean of the distribution, E_t is the d x d covariance matrix, d represents state's dimension. $N(x_t; \mu_t, E_t)$ denotes the probability of x_t given a Gaussian with mean μ_t and covariance E_t.

The principal **advantages** of Kalman filter lie in their computational efficiency compared to other variants of Bayesian filters. It is also suitable for systems with an accurate sensor measurement. A major **disadvantage** is that it only can represent unimodal Gaussian distribution and it only suitable in a system which has linear observation model and system dynamics.

Particle Filter

Among the family of Bayesian filtering, the most powerful algorithm comes from a Monte Carlo methods implemented as a particle filter. In [50], particle filtering is compared to other state of the art algorithms and it gives the best performance for state estimation. The particle filter robustness lies in the ability to handle non-linear system with non-Gaussian noise. The particle filter has been widely implemented in robotic localisation [49] [51].

The principal **advantages** of particle filter lie in its ability to handle non-linear system with non-Gaussian noise. The ability to incorporate a kinematic of the moving target and its inherent ability to combine various sensor measurements in its probability model make this method is naturally suitable for sensor data fusion. **The disadvantage** is that it requires relatively high computational power.

2.2.2 Accuracy and Sensor Data Fusion

Accuracy

Each method (described in section 2.2.1 previously) has its own claim about system performance in terms of accuracy. However, it can be problematic to compare the performance of different methods by this criterion, since they are usually implemented in different environments and with differing data sets. An attempt has been made to compare SVM with other methods, such as ANN, kNN and Bayesian probability in the same experimental platform [42].

The SVM method gave an accuracy of 3.96m with 75% probability, the ANN gave an accuracy of 4.01m with 75% probability and the kNN gave a value of 3.98m with 75% probability. In [52], the author developed a localisation test-bed for independently evaluating Ekahau[1] software [53] in a laboratory setting. He reported an x-axis Cartesian error of 5m and y-axis of 4.6m in a typical office environment with 7 APs.

Sensor Data Fusion

The accuracy of a single technology alone often cannot satisfy requirements for a higher degre of accuracy. For such situations, an additional localisation technology can help improve accuracy by means of sensor data fusion.

Fusion is defined as a technique to combine data from multiple sensors with related information from associated databases, to achieve improved accuracy and more specific inferences than could be achieved by the use of a single sensor alone.

[1] Ekahau is a commercial WLAN-based indoor localisation.

The data can come from sensors, history values of sensor data, information sources like a priori knowledge about the environment and human input [54] [55].

Most of the work on the sensor data fusion was performed in the field of robotic localisation [56] [57].

2.2.3 Limitations of the Fingerprinting Method

Another drawback of opportunistic localisation based on RSS measurements is the necessity to build a fingerprint. Building a fingerprint database is an exhaustive, time-consuming and cumbersome effort. Furthermore, a fingerprint is also bound to the indoor environment description and infrastructure at the time the fingerprint was generated. Therefore, major changes in the environment (movement of large pieces of furniture or appliances, adding or removing walls) will render a current fingerprint inaccurate and require re-building of a new fingerprint. In other words, *the current approach still has poor usability, evaluated from the effort needed to install and maintain it.*

There are two main approaches to overcome this problem: fingerprint prediction with a propagation model and fingerprint modelling with a machine learning approaches.

Fingerprint Prediction with Propagation Model

In [36] [58] [59] various propagation models such as one slope model (OSM) [60], multi wall model (WWM) and motif ray tracing model (MM) [61] have been used to predict the fingerprint. Figure 2.4 gives an example of a fingerprint prediction with the OSM model. The signal loss in OSM is given by:

$$L = L_1 + 10nlog(d) \tag{2.8}$$

where L is a signal loss, L_1 (dB) is a reference loss value of 1m distance, n is a power decay factor (path loss exponent) defining slope, and d is the distance in meters.

The principal **advantage** of fingerprint prediction is its speed in predicting the fingerprint compared to the measured fingerprint. A key **disadvantage** is that changes to the indoor environment (such as wall addition or removal) will

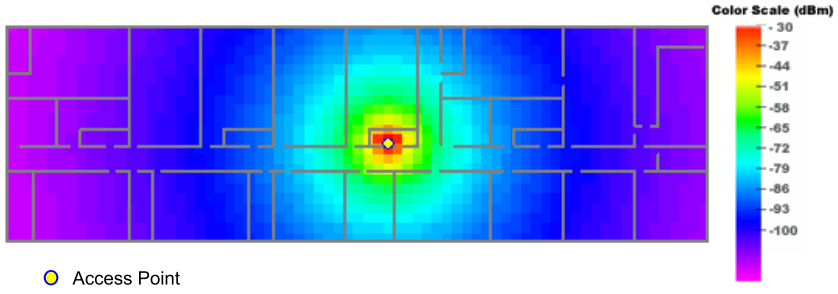

Figure 2.4: OSM prediction of a fingerprint [58].

require manual re-engineering work to accommodate it in the environment description (floor plan). Furthermore, the required parameter for the prediction model (such as wall loss for MWM) is often not accurate enough to represent the environment and still need a site survey to be performed to represent site specific wall parameter.

Fingerprint Modelling with Machine Learning Approach

In the machine learning approach, a sizeable training database is collected and subsequently used to train the system to estimate the complete fingerprint database. Various methods have been proposed for this, including expectation maximization (EM) algorithm [62], a model-based signal propagation distribution training (MSPDT) scheme [63] and location estimation using model trees (LEMT) [64].

In the EM algorithm, a sizeable unlabelled[1] RSS measurement is collected. Subsequently, the algorithm tries to label the data and include it in the fingerprint. In MSPDT, several fixed nodes are placed to monitor signal level between the nodes. The measurements are utilised to update parameters of the propagation model used to predict the fingerprint.

LEMT approach work in several steps: first, similar to MSPDT, a number of RF receivers are placed at fixed reference points to detect real-time RSS samples; second, a regression function between RSS measurements collected by the mobile device and the reference points are built; third, a NN-based method is used to find the most likely location.

[1]Measurements in unknown position.

The LEMT method is generally similar to the MSPDT method with the difference being that instead of using an indoor propagation model, it uses a machine learning approach to learn regression relationship between RSS and location to build a complete fingerprint.

These proposed methods offer a considerable **advantage** in that collection of the empirical fingerprint data is significantly reduced. In [62], the machine learning method used 50-75% less data compared to the empirical fingerprint. The **disadvantage** of the method is that the learned localisation model is static over time and/or across space. The model will therefore be rendered inaccurate if there are changes to the propagation environment or used in other environments. The system needs then to be re-trained with an updated training database to reflect the changes. In MSPDT and LEMT, a numbers of dedicated RF receivers are required to monitor RSS values all time (4-8 devices in their experiments).

2.2.4 Summary

This section described a detailed review of various methods that commonly used to infer location from RSS measurement. Based on the state of the art, the particle filter algorithm has been identified as the most viable method for the opportunistic system. The particle filter robustness lies in the ability to handle non-linear systems with non-Gaussian noise. The particle filter has been widely implemented in robotic localisation.

The accuracy of a single technology alone often cannot satisfy requirements for a higher granularity of accuracy. For such situations, an additional localisation technology can help improve accuracy by means of sensor data fusion.

A disadvantage of opportunistic localisation based on RSS measurement is the necessity to build a fingerprint. Building a fingerprint data base is an exhaustive, time-consuming and cumbersome effort. Furthermore, a fingerprint is also bound to the indoor environment description and infrastructure at the time the fingerprint was generated.

To address the fingerprinting problem, current methods use indoor propagation modelling or machine learning approach. Nevertheless, the proposed solu-

tions still have many disadvantages which hinder them from fully addressing the usability problem of the opportunistic system.

2.3 Summary of Motivation

This chapter described the state of the art of current approaches to indoor localisation. The developed taxonomy is utilised to help describe the current state of development of indoor localisation and underlines opportunities for an affordable, accurate, and usable opportunistic indoor localisation system. It was shown that localisation system based on time and angle measurement (TOA, TDOA and AOA) gave best performance in terms of accuracy. However, these solutions need dedicated hardware and infrastructure, therefore, it has lower affordability.

Utilising the RSS of the wireless-communication channel for opportunistic indoor localisation offers several advantages, such as affordability (since RSS is virtually free to obtain) and a low technology barrier to implementation (section 2.1). WLAN has become the dominant local wireless networking technology. Accordingly, opportunistic indoor localisation uses RSS of WLAN as the technology platform of choice.

However, there are some aspects of the current approaches in opportunistic indoor localisation that need to be addressed with more research; namely, further improvement in the accuracy and usability of the system. Furthermore, sensor data fusion capability is often overlooked in current approaches, even though accuracy of a single technology platform often cannot satisfy application requirements.

Some algorithms try to enhance the accuracy and to address the usability problem (section 2.2). However, the proposed solutions still have many disadvantages which restrict them from fully addressing the usability problem of the opportunistic system.

Hence, the drawbacks highlighted in the detail review of the state-of-the-art compound the need to enhance the accuracy and usability of opportunistic indoor localisation system.

It was found that the most advanced algorithm is the particle filter which comes from the family of Monte Carlo methods. This thesis offers a solution

of the accuracy problem by adopting a particle filter approach to opportunistic localisation (chapter 3).

This research also constructs novel algorithms for enhancing not only the accuracy but also the usability of opportunistic localisation (chapter 4). Furthermore, the algorithm is able to become a framework for the sensor data fusion between multi modal localisation technologies to improve the accuracy of indoor localisation system (chapter 5).

The collection of algorithms to improve the accuracy and usability of opportunistic indoor localisation system are the primary contribution of this thesis. The first contribution, that is the adoption of particle filter algorithm to opportunistic indoor localisation, will be described further in the next chapter.

Chapter 3

Particle Filter for Localisation

Based on the comprehensive review of the state of the art, it was found that the particle filter is the most advance algorithm. To achieve one of the thesis objectives, which is improving the accuracy, the particle filter algorithm is adopted to the opportunistic indoor localisation.

This chapter will describe the Bayesian probability approach implemented as the particle filter algorithm for opportunistic indoor localisation. Section 3.1 and 3.2 will present the theory that underlies the particle filter.

To enable the implementation of a particle filter into opportunistic indoor localisation, motion and measurement models have to be devised beforehand. These probabilistic models are one of the contributions of this research, which will be explained in section 3.4 and section 3.5 in more detail. Section 3.7 will conclude the chapter.

3.1 State Estimation

In order to clearly describe the problem during localisation, some terms are used in the following chapters. These are defined here for clarity and convenience. Firstly, *target*, is defined as an entity (e.g.: object, person) of which the state is being estimated. For example, it can be a person to whom the located mobile device is attached. Secondly *state*, is defined as the collection of the aspect of the target (such as location, velocity, or direction). The state will change over time. Thirdly, *measurement*, the observed phenomena obtained from a sensor which

carries information about the state. RSS measurement is utilised for opportunistic indoor localisation.

The main goal of an indoor localisation system is to estimate an unknown target's state based on the observed measurement. To conveniently describe the evolution of target state and its measurement during localisation, a statistical model so-called *hidden Markov model* [65] is used (Figure 3.1). Parameter $\mathbf{x}_t$ describes the state at time t, $\mathbf{x}$ is hidden and cannot be measured directly. Parameter $\mathbf{z}_t$ depicts the measurement at time t, $\mathbf{z}$ can be observed directly. One can only estimate the state $\mathbf{x}$ from the observed measurement $\mathbf{z}$.

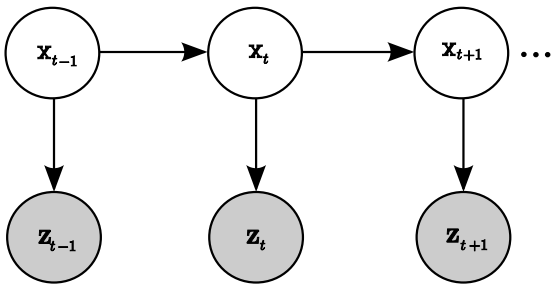

Figure 3.1: Graphical representation of hidden Markov model.

One of the important assumptions underlying this model is that the state $\mathbf{x}$ is complete. It has sufficient summary of all information that happened during a previous time-step. $\mathbf{x}_{t-1}$ has complete summary of past states and measurements, and is sufficient to predict the current state $\mathbf{x}_t$. This assumption, that the value of one temporal state is only influenced by the temporal state preceding it, is called a *Markov process* [66].

3.1.1 Probabilistic Representation of the Model

Evolution of the target state $\mathbf{x}_t$ and measurement $\mathbf{z}_t$ is formally described by the following discrete-time stochastic filtering model [67]:

$$\mathbf{x}_t = f_{t-1}(\mathbf{x}_{t-1}, \mathbf{n}_{t-1}) \tag{3.1}$$

$$\mathbf{z}_t = h_t(\mathbf{x}_t, \mathbf{e}_t) \tag{3.2}$$

where equation (3.1) and (3.2) represent a *state equation* and *measurement equation* respectively, $\mathbf{x}_t$ represents the state vector and $\mathbf{z}_t$ denotes the measurement

vector, f_{t-1} and h_t are known, possibly non-linear, time-varying functions, $\mathbf{n}_{t-1}$ and $\mathbf{e}_t$ are independent and identically-distributed noise.

The evolution of state and measurement is governed by a probabilistic principle. In order to obtain $\mathbf{x}_t$ and $\mathbf{z}_t$, probabilistic distributions, from which $\mathbf{x}_t$ and $\mathbf{z}_t$ can be generated, must be specified. In general, $\mathbf{x}_t$ is stochastically generated from the previous state $\mathbf{x}_{t-1}$. Since the system is assumed to be Markovian, the previous state $\mathbf{x}_{t-1}$ is a summary of past states and measurements and is sufficient to predict the current state $\mathbf{x}_t$. This can be expressed in the following equation:

$$p(\mathbf{x}_t|\mathbf{x}_{0:t-1}, \mathbf{z}_{1:t-1}) = p(\mathbf{x}_t|\mathbf{x}_{t-1}) \tag{3.3}$$

In probabilistic terms, this insight is called *transition probability*. Transition probability is a stochastic representation of equation (3.1).

The measurement also can be modelled as a conditional probability of the state $\mathbf{x}_t$. Once again, since $\mathbf{x}_t$ is complete, it is enough to utilise $\mathbf{x}_t$ to predict the potentially noisy measurement $\mathbf{z}_t$. The measurement model can be written as:

$$p(\mathbf{z}_t|\mathbf{x}_{0:t}, \mathbf{z}_{1:t-1}) = p(\mathbf{z}_t|\mathbf{x}_t) \tag{3.4}$$

Equation (3.4) is called the *measurement probability*. It is a probabilistic representation of equation (3.2).

Another important concept of the probabilistic representation for the HMM is *posterior probability* and *prior probability*. Posterior probability represents probability distribution of state $\mathbf{x}_t$ given all available measurements. It assigns a probabilistic value to each hypothesis of the true state. Posterior probability is expressed by:

$$p(\mathbf{x}_t|\mathbf{z}_{1:t}) = p(\mathbf{x}_t|\mathbf{z}_t) \tag{3.5}$$

This density is the probability distribution over state $\mathbf{x}_t$ at time t, given all past measurements $\mathbf{z}_{1:t}$.

Prior probability is a probability calculated based on the previous posterior, before incorporating measurement at the time t or denoted as $\mathbf{z}_t$. This probability is often referred to as a *prediction* since it is calculated from the previous posterior. The prediction probability can be written as:

$$p(\mathbf{x}_t|\mathbf{z}_{1:t-1}) = p(\mathbf{x}_t|\mathbf{z}_{t-1}) \tag{3.6}$$

Posterior probability can be calculated from the prior by correcting it with the new measurement $\mathbf{z_t}$. This step is often called *measurement update* or *correction*.

There are terms that need to be clarified before moving further. *Filtering* refers to state estimation $\mathbf{x}_t$ using measurements up to time t, i.e. $\{\mathbf{z}_1, \mathbf{z}_2, \mathbf{z}_3, \ldots, \mathbf{z}_t\}$. *Prediction* is an *a priori* form of estimation, using measurement available before t. *Smoothing* is estimation using measurements available after t [68].

3.2 Recursive Bayesian Filtering

The general algorithm for calculating the posterior distribution of $p(\mathbf{x}_t|\mathbf{z}_t)$ is given by Bayes' filter. From a Bayesian perspective, construction of posterior probability is achieved in two steps: *prediction* and *update*. The prediction stage is performed to obtain the prior probability $p(\mathbf{x}_t|\mathbf{z}_{t-1})$, whereas the update stage corrects the prediction with a new measurement to obtain the posterior $p(\mathbf{x}_t|\mathbf{z}_t)$.

The prediction is achieved through the the Chapman-Kolmogorov equation [69]:

$$p(\mathbf{x}_t|\mathbf{z}_{t-1}) = \int p(\mathbf{x}_t|\mathbf{x}_{t-1})p(\mathbf{x}_{t-1}|\mathbf{z}_{t-1})d\mathbf{x}_{t-1} \tag{3.7}$$

When the measurement $\mathbf{z}_t$ becomes available, Bayes' rule is utilised for the update stage:

$$p(\mathbf{x}_t|\mathbf{z}_t) = k^{-1}p(\mathbf{z}_t|\mathbf{x}_t)p(\mathbf{x}_t|\mathbf{z}_{t-1}) \tag{3.8}$$

with normalizing constant:

$$k = \int p(\mathbf{z}_t|\mathbf{x}_t)p(\mathbf{x}_t|\mathbf{z}_{t-1})d\mathbf{x}_t \tag{3.9}$$

$p(\mathbf{z}_t|\mathbf{x}_t)$ represents the measurement probability, $p(\mathbf{x}_t|\mathbf{x}_{t-1})$ is the transition probability and $p(\mathbf{x}_t|\mathbf{z}_{t-1})$ is the previous posterior probability.

Algorithm 3.1 describes the prediction and update stages of Bayes' filter. The algorithm input is the previous posterior and a current measurement. In line 2, prediction is obtained by integration of two probability distributions: previous posterior and transition probability. The measurement update is described in line 3, where Bayes' algorithm updates the prior probability with the measurement probability. The result is the posterior probability which is returned in line 5

Algorithm 3.1 BayesFilter ($p(\mathbf{x}_{t-1}|\mathbf{z}_{t-1})$, $\mathbf{z}_t$)

1: **for** all $\mathbf{x}_t$ **do**
2: $p(\mathbf{x}_t|\mathbf{z}_{t-1}) = \int p(\mathbf{x}_t|\mathbf{x}_{t-1})\ p(\mathbf{x}_{t-1}|\mathbf{z}_{t-1}) d\mathbf{x}_{t-1}$
3: $p(\mathbf{x}_t|\mathbf{z}_t) = k^{-1} p(\mathbf{z}_t|\mathbf{x}_t)\ p(\mathbf{x}_t|\mathbf{z}_{t-1})$
4: **end for**
5: **return** $p(\mathbf{x}_t|\mathbf{z}_t)$

of the algorithm. The recursive nature of the Bayesian filter is due to the fact that the posterior probability $p(\mathbf{x}_t|\mathbf{z}_t)$ is calculated form the previous posterior $p(\mathbf{x}_{t-1}|\mathbf{z}_{t-1})$.

Knowledge of the posterior probability enables an estimation of the state to be made, for instance to obtain the mean of $\mathbf{x}_t$ [70].

$$\hat{\mathbf{x}}_t^{ME} = \int \mathbf{x}_t\ p(\mathbf{x}_t|\mathbf{z}_t) dx_t \tag{3.10}$$

while the maximum *a posteriori* (MAP) estimate is the maximum of $p(\mathbf{x}_t|\mathbf{z}_t)$

$$\hat{\mathbf{x}}_t^{MAP} = \arg\max_{\mathbf{x}_t} p(\mathbf{x}_t|\mathbf{z}_t) \tag{3.11}$$

The aforementioned recursive propagation of the posterior density is only a conceptual solution in that, in general, it cannot be determined analytically. Only in a highly restrictive case when the system is linear and Gaussian, does an analytical solution exist in the form of the Kalman filter and its numerous variants [71] [72].

Since the analytical solution is intractable for most practical situations, an approximate solution to the Bayesian filter is required. The current state of the art of such approximate solutions is the particle filter [73] [74].

3.3 Particle Filter

The particle filter is a non-parametric implementation of the Bayes' filter. It approximates the posterior probability by a finite number of discrete samples with associated weights, called *particles*. The approximation of the posterior density is non-parametric. Therefore, it can represent a wider distribution than the parametric one, such as Gaussian. The particle filter is also known as the bootstrap filter [75], condensation algorithm [76] and survival of the fittest [77].

The particle filter directly estimates the posterior probability of the state expressed in the following equation [74]:

$$p(\mathbf{x}_t|\mathbf{z}_t) \approx \sum_{i=1}^{N} w_t \delta(\mathbf{x}_t - \mathbf{x}_t^i) \tag{3.12}$$

where $\mathbf{x}_t^i$ is the i-th sampling point or particle of the posterior probability with $1 < i < N$ and w_t^i is the weight of the particle. N represents the number of particles in the particle set, denoted by $\mathcal{X}_t$.

$$\mathcal{X}_t := \mathbf{x}_t^1, \mathbf{x}_t^2, \mathbf{x}_t^3, \ldots, \mathbf{x}_t^N \tag{3.13}$$

Each particle is a concrete instantiation of the state at time t, or put differently, each particle is a hypothesis of what the true state $\mathbf{x}_t$ might be, with a probability given by its weight.

The property of equation (3.12) holds for $N \uparrow \infty$. In the case of finite N, the particles are sampled from a slightly different distribution. However, the difference is negligible as long as the number of particles is not too small [65]. Based on recent finding [74], N value above 500 is suggested. In this work, N value of 1000 is used and remain static over time.

Algorithm 3.2 Particle_Filter ($\mathcal{X}_{t-1}$, $\mathbf{z}_t$)

1: $\bar{\mathcal{X}}_t = \mathcal{X}_t = \emptyset$
2: **for** $i = 1$ to N **do**
3: sample $\mathbf{x}_t^i \sim p(\mathbf{x}_t|\mathbf{x}_{t-1}^i)$
4: assign particle weight $w_t^i = p(\mathbf{z}_t|\mathbf{x}_t^i)$
5: **end for**
6: calculate total weight $k = \sum_{i=1}^{N} w_t^i$
7: **for** $i = 1$ to N **do**
8: normalise $w_t^i = k^{-1} w_t^i$
9: $\bar{\mathcal{X}}_t = \bar{\mathcal{X}}_t + \{\mathbf{x}_t^i, w_t^i\}$
10: **end for**
11: $\mathcal{X}_t =$ **Resample** ($\bar{\mathcal{X}}_t$)
12: **return** $\mathcal{X}_t$

The algorithm 3.2 describes a generic particle filter algorithm. The input of the algorithm is the previous set of the particle $\mathcal{X}_{t-1}$, and the current measurement

$\mathbf{z}_t$, whereas the output is the recent particle set $\mathcal{X}_t$. The algorithm will process every particle $\mathbf{x}_{t-1}^i$ from the input particle $\mathcal{X}_{t-1}$ as follows.

1. Line 3 shows the prediction stage of the filter. The particle $\mathbf{x}_t^i$ is sampled from the transition distribution $p(\mathbf{x}_t|\mathbf{x}_{t-1})$. The set of particles resulting from this step has a distribution according to (denoted by $\sim$) the prior probability $p(\mathbf{x}_t|\mathbf{z}_{t-1})$.

2. Line 4 describes incorporation of the measurement $\mathbf{z}_t$ into the particle. It calculates for each particle $\mathbf{x}_t^i$ the *importance factor* or *weight* w_t^i. The weight is the probability of particle $\mathbf{x}_t^i$ received measurement $\mathbf{z}_t$ or $p(\mathbf{z}_t|\mathbf{x}_t)$. The construction process of the weight will be described in section 3.5.

3. Lines 7 to 10 are steps required to normalise the weight of the particles. The result is the set of particles $\bar{\mathcal{X}}_t$, which is an approximation of posterior distribution $p(\mathbf{x}_t|\mathbf{z}_t)$.

4. Line 11 describes the step which is known as *resampling* or *importance resampling*. The resampling procedure is described in algorithm 3.3 in the next section. After the resampling step, the particle set, which was previously distributed in a manner equivalent to prior distribution $p(\mathbf{x}_t|\mathbf{z}_{t-1})$ will now be changed to particle set $\mathcal{X}_t$ which is distributed in proportion to $p(\mathbf{x}_t|\mathbf{z}_t)$.

3.3.1 Resampling

The early implementation of particle filter is called sequential important sampling (SIS) [78]. Implementation of SIS is similar to algorithm 3.2, but without the resample step (algorithm 3.2 line 11). The SIS approach suffers an effect which is called the *degeneracy problem*.

This occurs when, after some sequence time t, all but one particle has nearly zero weight. The problem happen since generally impossible to sample directly from posterior distribution, particles are sampled from related distribution, termed importance sampling. The choice of importance sampling made the degeneracy

problem is unavoidable [79]. The degeneracy problem will increase the weight variance over time and has a harmful effect on accuracy [74].

Resampling is an important step to overcome the degeneracy problem. It will force the particle to distribute according to the posterior density $p(\mathbf{x}_t|\mathbf{z}_t)$.

Algorithm 3.3 Resample ($\bar{\mathcal{X}}_t$)

1: $\mathcal{X}_t^* = \emptyset$
2: **for** $j = 1$ to N **do**
3: $r =$ random number uniformly distributed on [0,1]
4: $s = 0.0$
5: **for** $i = 1$ to N **do**
6: $s = s + w_t^i$
7: **if** $s \geq r$ **then**
8: $\mathbf{x}_t^{*j} = \mathbf{x}_t^i$
9: $w_t^{*j} = 1/N$
10: $\mathcal{X}_t^* = \mathcal{X}_t^* + \{\mathbf{x}_t^{*j}, w_t^{*j}\}$
11: **end if**
12: **end for**
13: **end for**
14: replacement $\bar{\mathcal{X}}_t = \mathcal{X}_t^*$
15: **return** $\bar{\mathcal{X}}_t$

Algorithm 3.3 describes a resampling step of particles. It is taken with a slight modification from [80] to increase the efficiency of the method. The modification lies in the iteration to draw newly sampled particles. The input of the algorithm is a set of particles and the output is the new resampled particles.

1. Line 3 shows the generation of random number r.

2. Lines 5 to 8 show the resampling steps. Line 8 shows when a particle is resampled only if its weight contribution causes the summation in line 6 to exceed or equal to the random sample r. The probability of drawing[1] a particle is in proportion to its importance factor. Particles with lower weight will have a lower chance and some will not be resampled.

[1]Random selection

3. Since the resampling process is performed every time step, the new particles do not need to know the old weight and their weight will be set equally, as shown in line 9.

4. Line 14 shows when members of particle set $\bar{\mathcal{X}}_t$ is replaced by new resampled particles.

Although the resampling step reduces the effects of the degeneracy problem, it introduces other practical problems. Firstly, it limits the opportunity to implement the algorithm on a parallel computer since all the particles must be combined. Secondly, the particles that have high weights are statistically selected many times. This leads to a loss of diversity among the particles as the resultant sample will contain many repeated points.

This problem, which is known as *sample impoverishment*, is apparent when process noise in state dynamics is small[1]. If the process noise is zero, then using a particle filter is not entirely appropriate. Particle filtering is a method well suited to the estimation of dynamic states.

State dynamics of RSS-based opportunistic indoor localisation is large due to noisy RSS measurement. Therefore, particle filter is well suited for state estimation in opportunistic system.

3.3.2 Summary

The particle filter, which is a non-parametric implementation of Bayes' filter, is well suited for state estimation in opportunistic system for a number of reasons. Firstly, it is the state of the art algorithm for a non-linear system with non-Gaussian noise such as in RSS-based opportunistic indoor localisation. Secondly, it is suitable for state estimation for a system that has large process noise in state dynamics. Thirdly, the particle filter is the most powerful algorithm to date to improve the performance of an opportunistic system.

To enable the implementation of a particle filter into opportunistic indoor localisation, motion and measurement model have to be devised beforehand. These probabilistic models will be explained in section the following sections.

[1]Smoothing is one of the approaches to overcome sample impoverishment [81]

3.4 Motion Model

A motion model is one of the probabilistic models that need to be devised in order to implement a particle filter for opportunistic system. The motion model is a representation of the target's kinematics behaviour. It is used to construct the transition probability $p(\mathbf{x}_t|\mathbf{x}_{t-1})$ which has an important role for the prediction step in the particle filter.

Recent work in motion models is mostly applied to robotic localisation or locating people relative to robot position. Brownian movement [82] and a first-order motion model with the Kalman filter [83] have been used to locate people relative to a robot. Both of these approaches have limitations. Brownian movement is a conservative approach and does not attempt to model the kinematics of persons movement. It assumes that motion is random at every time step and only depends on the current state.

The first-order of person kinematics is less conservative than Brownian movement, in a way that the motion is not totally random as in Brownian movement. Therefore it is often more accurate. It assumes that target direction is the same as the last observing movement [84]. However, this assumption does not hold when people turn direction in a corner, enter a room or avoid obstacles. This kind of action therefore is difficult to represent.

In this thesis, the approach for the motion model in indoor localisation is taken from both Brownian movement and the first-order motion model. The motion model assumes that the kinematics of a target has random values in it. However, this randomness is constrained by the previous state.

This approach is novel and more accurately reflects the target's kinematics behaviour (i.e.: a person) in opportunistic system. Especially, in a system that only uses RSS measurement, without additional motion sensor.

Velocity

To accommodate simple human locomotion patterns (such as remaining stationary, walking and running) and its limitations, the target velocity is constrained to take place only between limited ranges of speed. The succeeding velocity also

takes into account the preceding one, since it is assumed that people tend not to change their kinematics abruptly in a normal condition.

Based on observation of peoples' movement in the standard environment, the target velocity is given by the following rule:

$$v_t = \mathcal{N}(v_{t-1}, \sigma_v) \text{ and } v_t = \begin{cases} v_t, & 0 \leq v_t \leq Max_{v_t} \\ v_t = |v_t|, & v_t < 0 \\ 2\ Max_{v_t} - v_t, & Max_{v_t} < v_t \end{cases} \tag{3.14}$$

with

$$\sigma_v = \min(Max_{\Delta_t}, \sqrt{\Delta_t}) \tag{3.15}$$

where $\mathcal{N}$ represents a Gaussian random number generator, Max_{v_t} represents the maximum speed. min is a function which returns the smallest component, Δ_t represents elapsed time, Max_{Δ_t} represents the maximum threshold of the Δ_t.

The value of Max_{v_t} is set to the fastest recorded human speed (≈ 10 m/s) [85] and $Max_{\Delta_t} = 3$ s. Figure 3.2 shows an example of the velocity probability distribution function (PDF) when $v_{t-1} = 0$ m/s with various Δ_t.

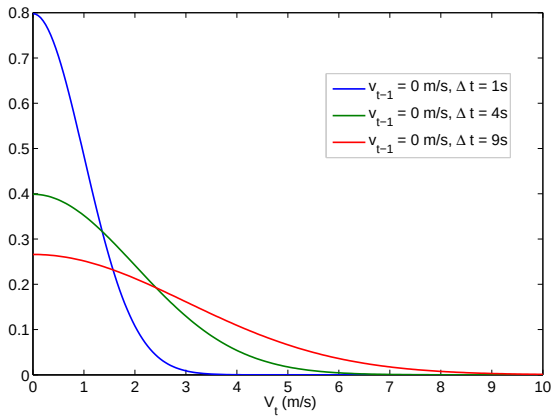

Figure 3.2: PDF of velocity with $v_{t-1} = 0$ m/s.

Direction

The succeeding direction also considers that preceding it. A velocity parameter is also included in the direction calculation. The motivation is to limit heading

variation based on preceding speed, since people tend to slow down when they want to change their direction of movement. The target direction is given by the following rule:

$$\alpha_t = \mathcal{N}(\alpha_{t-1}, \sigma_h) \text{ and } \alpha_t = \begin{cases} \alpha_t, & -\pi \leq \alpha_t \leq \pi \\ \alpha_t + 2\pi, & \alpha_t < -\pi \\ \alpha_t - 2\pi, & \alpha_t > \pi \end{cases} \tag{3.16}$$

with

$$\sigma_h = 0.4\pi - \arctan(\frac{\sqrt{v_{t-1}}}{2}) \tag{3.17}$$

where α_t represents direction at time t, σ_h represents the direction standard deviation.

Figure 3.3 shows the σ_h for different velocities. Figure 3.4 presents PDF of the direction based on different velocities with $\alpha_{t-1} = 0$. It can be seen that the heading variation is narrower when the velocity is increased.

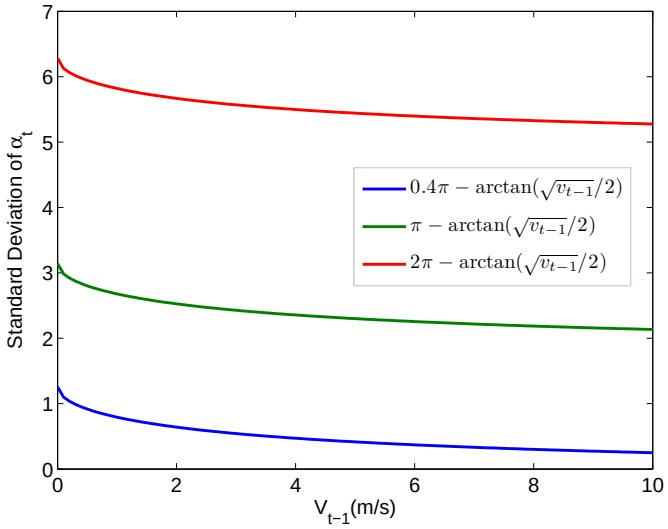

Figure 3.3: Standard deviation of target direction α_t.

Particle Motion Model

Each particle, which is a hypothesis of the target state in the real world, will have a kinematic characteristic according to the motion model during the prediction

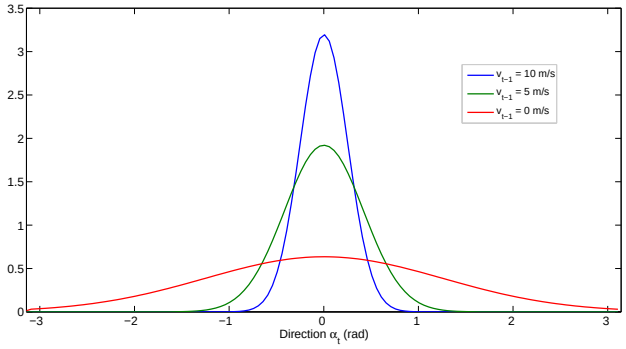

Figure 3.4: PDF of the direction with $\alpha_{t-1} = 0$.

stage. The particle state can be modelled with:

$$\mathbf{x}_t^i = \begin{bmatrix} x_t^i \\ y_t^i \end{bmatrix} = \begin{bmatrix} x_{t-1}^i + v_t^i cos(\alpha_t^i)\Delta t + n_t \\ y_{t-1}^i + v_t^i sin(\alpha_t^i)\Delta t + n_t \end{bmatrix} \tag{3.18}$$

where v_t denotes velocity, α_t describes particle direction at the time t, n_t is a noise with Gaussian distribution. The particles' velocity is governed by equation (3.14), whereas particles' direction is given by equation (3.16). The noise n_t is added to achieve a better distribution by preventing particles from collapsing into a single point. A n_t value of 0.5m is used for this work.

Figure 3.5 illustrates the evolution of particle distribution determined only by the motion model. The particle distribution is started from a known state in 2D space. The initial velocity $v_0 = 3$ m/s and number of particles are 2000. Since there is no RSS measurement update performed, the distribution will spread wider over time.

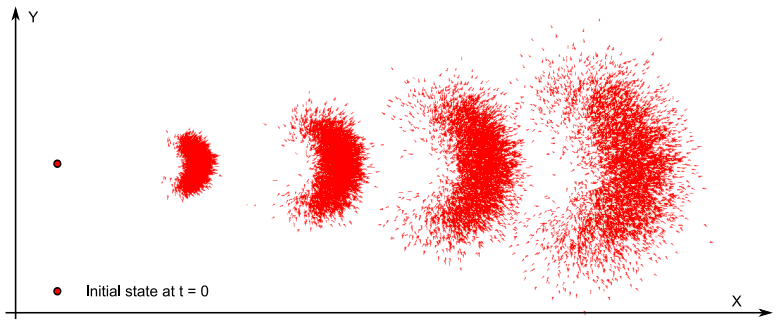

Figure 3.5: Evolution of particles with motion model.

The aforementioned particle distribution, which was constructed with the motion model, is a representation of transition probability. This density needs to be updated with the measurement probability $p(\mathbf{z}_t|\mathbf{x}_t)$ to obtain the posterior distribution. The construction of measurement probability with the measurement model in an opportunistic system is explained in the next section.

3.5 Measurement Model

The measurement model describes a construction process by which the sensor measurement is generated. This model is utilised to obtain the measurement probability of $p(\mathbf{z}_t|\mathbf{x}_t)$, often referred to as the *likelihood observation function*. In the particle filter, this function is used to incorporate a measurement update into the particle weight w_t^i.

In [86] [87], a measurement model is obtained by an extended version of the NN algorithm. However, the model does not properly take into account some physical characteristics of signal propagation in indoor environments. It leads to an inaccurate model which makes the localisation estimation less accurate.

The work described in this thesis proposes a measurement model which considers the physical characteristics of signal propagation in indoor environments based on the fingerprinting method.

3.5.1 Fingerprint

A fingerprint is a database of stored RSS measurements throughout the coverage area of all discrete possible states (section 2.1.2). These discrete states are often referred to as a *grid*. The fingerprint acts as the "true" RSS values obtained by the sensor, denoted by $\mathbf{z}_t^+$, at the state $\mathbf{x}_t$. Figure 3.6 illustrates a RSS fingerprint throughout a coverage area from 1 AP which was measured at every 1m grid[1].

[1]Theoretically, smaller grid size gives better localisation accuracy since the measurement model will be more distinct between grids. However, it is technology dependent. Based on the observations, WLAN RSS values are discernible when they are measured in a grid $\geq$ 1m.

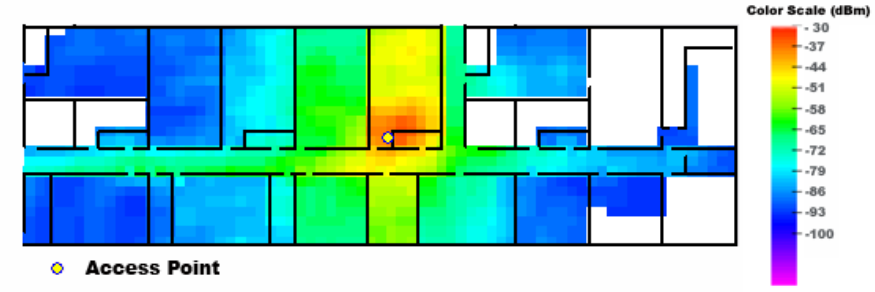

Figure 3.6: A fingerprint illustration from 1 AP.

To obtain the likelihood observation function, statistical inference is performed between a *true* value stored in the fingerprint and recent RSS measurement (termed as *signature*).

The mobile device is able to simultaneously retrieve RSS measurements from different APs, therefore $\mathbf{z}_t$ is a set of measurements which is described as:

$$\mathbf{z}_t = \{z_t^1, z_t^2, z_t^3, \ldots, z_t^K\} \tag{3.19}$$

where z_t^k denotes RSS value z_t at time t from AP with identification k[1]. The probability $p(\mathbf{z}_t|\mathbf{x}_t)$ is obtained as the product of the individual likelihood observation function.

$$p(\mathbf{z}_t|\mathbf{x}_t) = \prod_{k \in \mathbf{z}_t} p(z_t^k|\mathbf{x}_t) \tag{3.20}$$

3.5.2 Algorithm for the Measurement Model

The measurement model comprises three types of probability densities, each of which corresponds to a type of dissimilarity:

1. **Measurement with noise.** Assuming that the sensor can capture the true RSS measurement, the returned value is still subject to error caused by shadowing (or slow fading) and multipath fading [88]. This fading, which

[1]MAC address is used for WLAN AP

appears as a time-varying process, makes the RSS value fluctuate even when it is measured at the same position.

Since the sensor (i.e. WLAN interface) has an internal mechanism to suppress multipath fading, the received error is largely caused by shadowing which has a Gaussian distribution [89]. Therefore, the noisy measurement may be modelled with a Gaussian distribution with mean value of z_t^{+k} and standard deviation of σ_+. The Gaussian is denoted by p_{hit} as described in Figure 3.7 below.

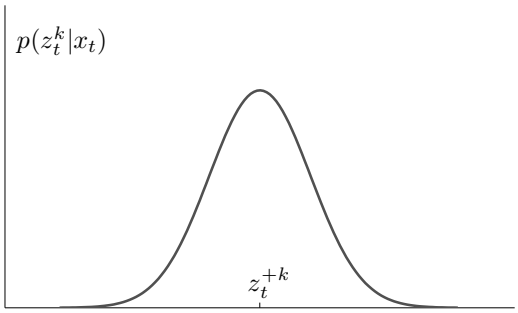

Figure 3.7: Gaussian distribution p_{hit}.

The value of z_t^{+k} is given by the RSS measurement stored in the corresponding grid of the fingerprint. The measurement probability is governed by

$$p_{hit}(z_t^k|\mathbf{x}_t) = \mathcal{N}(z_t^k; z_t^{+k}, \sigma_+) \tag{3.21}$$

$$= \frac{1}{\sigma_+\sqrt{2\pi}} \exp\left(-\frac{(z_t^k - z_t^{+k})^2}{2\sigma_+^2}\right) \tag{3.22}$$

where z_t^{+k} is the RSS value stored in the fingerprint and z_t^k is the recent signature such that $\{k \in \mathbf{z}_t \cap \mathbf{z}_t^+\}$ or, to put it differently, the RSS value from an AP which appears in both signature and fingerprint. Notation σ_+ is the intrinsic noise parameter for the measurement model.

2. **Missing RSS.** Considering that it may be the case that not all of the RSS values that appear in the fingerprint grid and signature coming from

the same APs, a question arises as to how to account for such data. This condition can happen when the signature is taken at a different location or there is an extra/missing AP. In the case of no extra/missing AP, a different set of RSS values in the fingerprint grid and signature means that they are taken at different locations. Incorporating this information into the measurement model will eventually lead to better localisation accuracy.

In the case of RSS measurements from an AP which is missing in the signature but which is present in the fingerprint, the measurement probability is modelled by a Gaussian denoted by p_{miss}. The measurement probability is governed by:

$$p_{miss}(z_t^k|\mathbf{x}_t) = \mathcal{N}(\eta; 0, \sigma_+) \tag{3.23}$$

$$= \frac{1}{\sigma_+\sqrt{2\pi}} \exp\left(-\frac{\eta^2}{2\sigma_+^2}\right) \tag{3.24}$$

where η is the penalty parameter given for the missing RSS. The density p_{miss} is calculated for missing z_t^k such that $\{k \in \mathbf{z}_t^+ - \mathbf{z}_t\}$.

3. **Extra RSS.** In the case where there is an extra RSS value of an AP which exists in the signature but which is absent in the fingerprint, the measurement probability is also modelled by a Gaussian denoted by p_{extra} and governed by:

$$p_{extra}(z_t^k|\mathbf{x}_t) = \mathcal{N}(\eta; 0, \sigma_+) \tag{3.25}$$

$$= \frac{1}{\sigma_+\sqrt{2\pi}} \exp\left(-\frac{\eta^2}{2\sigma_+^2}\right) \tag{3.26}$$

where η is the penalty parameter given for the extra RSS. The density p_{extra} is calculated for extra z_t^k such that $\{k \in \mathbf{z}_t - \mathbf{z}_t^+\}$.

These three densities are combined to obtain the likelihood observation function of RSS measurement $p(\mathbf{z}_t|\mathbf{x}_t)$. The likelihood observation function is given by:

$$p(\mathbf{z}_t|\mathbf{x}_t) = \left[\prod_{k\in K} p_{hit}(z_t^k|\mathbf{x}_t)\right]^{\frac{1}{|K|}} . \prod_{k\in L} p_{miss}(z_t^k|\mathbf{x}_t). \prod_{k\in M} p_{extra}(z_t^k|\mathbf{x}_t). \beta \tag{3.27}$$

with

$$\beta = \frac{|K|}{|K| + |L| + |M|}$$

where K is the set of measurement in $(\mathbf{z}_t \cap \mathbf{z}_t^+)$, L is the set of measurement in $(\mathbf{z}_t^+ - \mathbf{z}_t)$, M is the set of measurement in $(\mathbf{z}_t - \mathbf{z}_t^+)$. The expressions of $|K|$, $|L|$, $|M|$ denotes the number of elements in K, L, M respectively. β represents the weighting factor, k denotes AP identification.

Algorithm 3.4 describes the steps necessary to obtain the likelihood observation function. The input of the algorithm is the measurement $\mathbf{z}_t$ and the state $\mathbf{x}_t$. The output is the likelihood observation function of $p(\mathbf{z}_t|\mathbf{x}_t)$.

Algorithm 3.4 Measurement_Model ($\mathbf{z}_t$, $\mathbf{x}_t$)

1: $p = 1$
2: $q = 1$
3: $y = 1$
4: $S = 0$
5: get $\mathbf{z}_t^+$ from the fingerprint
6: **for** $k \in K$ **do**
7: $\quad p = p.p_{hit}(z_t^k|\mathbf{x}_t)$
8: **end for**
9: $p = p^{1/|K|}$
10: **for** $k \in L$ **do**
11: $\quad q = q.p_{miss}(z_t^k|\mathbf{x}_t)$
12: **end for**
13: **for** $k \in M$ **do**
14: $\quad q = q.p_{extra}(z_t^m|\mathbf{x}_t)$
15: **end for**
16: $S = |K| \div (|K| + |L| + |M|)$
17: $y = p.q.S$
18: **return** y

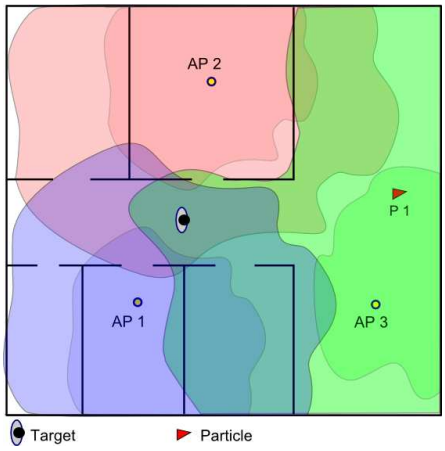

Figure 3.8: Illustration for the calculation of the measurement model.

Examples

Figure 3.8 is used to illustrate how to obtain the likelihood observation function of a particle $p(\mathbf{z}_t|\mathbf{x}_t^1)$. It shows a fingerprint from 3 APs, a target and a particle.

Supposing that the target measured RSS value $\mathbf{z}_t$={AP1 = - 70 dBm, AP2 = - 70 dBm, AP3 = - 75 dBm}. The corresponding fingerprint grid where the particle x^1 is located, has value of $\mathbf{z}_t^+ = \{\text{AP3 = -65 dBm}\}$. If the value of both σ_+ and η are set to 4 dBm[1], the $p(\mathbf{z}_t|\mathbf{x}_t^1)$ can be calculated as follows:
Calculating p_{hit} from AP3 with equation (3.24):

$$\begin{aligned} p_{hit}(z_t^3|\mathbf{x}_t^1) &= \frac{1}{\sigma_+\sqrt{2\pi}} \exp\left(-\frac{(z_t^k - z_t^{+k})^2}{2\sigma_+^2}\right) \\ &= \frac{1}{4\sqrt{2\pi}} \exp\left(-\frac{(-75-(-65))^2}{2.4^2}\right) = 0.0044 \end{aligned}$$

Calculating p_{extra} from AP1 and AP2 with equation (3.26):

$$\begin{aligned} p_{extra}(z_t^1|\mathbf{x}_t^1).p_{extra}(z_t^2|\mathbf{x}_t^1) &= \left(\frac{1}{\sigma_+\sqrt{2\pi}} \exp\left(-\frac{\eta^2}{2\sigma_+^2}\right)\right)^2 \\ &= \left(\frac{1}{4\sqrt{2\pi}} \exp\left(-\frac{(4)^2}{2.4^2}\right)\right)^2 = 0.0037 \end{aligned}$$

Calculating $p(\mathbf{z}_t|\mathbf{x}_t^1)$ with equation (3.27):

$$p(\mathbf{z}_t|\mathbf{x}_t^1) = 0.0044 \,.\, 0.0037 \,.\, \frac{1}{1+2} = 0.0000054$$

[1]Determination of the intrinsic parameters are discussed in section 3.5.3.

Measurement Model & Particles Distribution

The likelihood observation function update to the particle distribution is illustrated in Figure 3.9. Figure 3.9(a) shows 3 APs and its RSS measurement throughout the coverage area which is used as the fingerprint. In the initial time, the particles will be uniformly distributed as shown in Figure 3.9(b). Once measurement $\mathbf{z}_t$ is obtained, the likelihood observation function or measurement probability is calculated based on equation (3.27). The result is illustrated in Figure 3.9(c). Higher likelihoods are shown with bigger blue circles. Furthermore, the particles' weight is updated with the likelihood observation function and subsequently is resampled. The new particle distribution and estimated target location are shown in Figure 3.9(d).

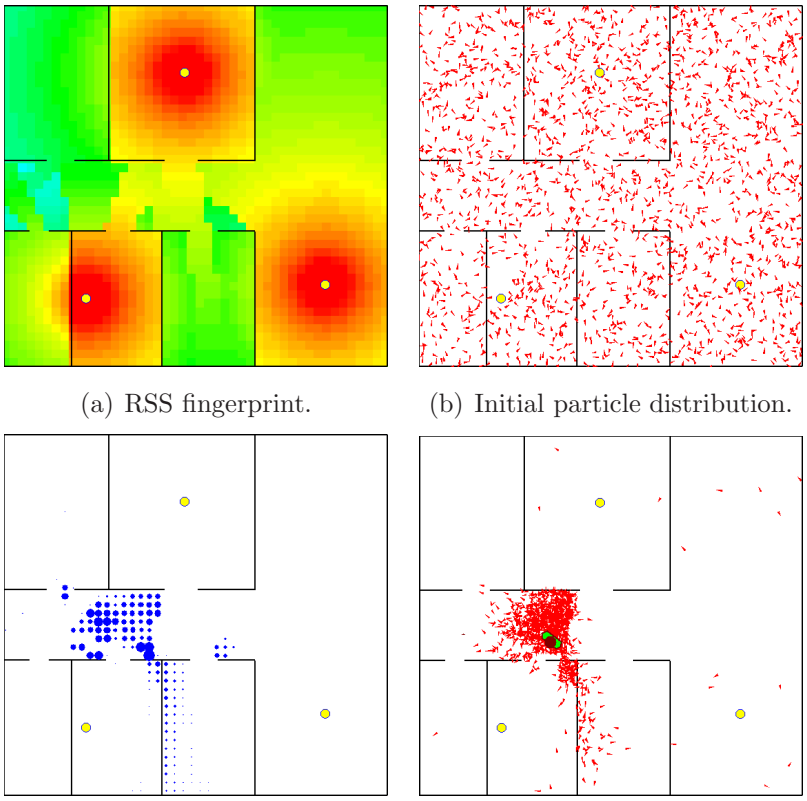

(a) RSS fingerprint. (b) Initial particle distribution.

(c) Measurement probability. (d) Updated particle distribution.

Figure 3.9: Update of the particles distribution with the likelihood observation function.

3.5.3 Intrinsic Parameter of the Measurement Model

To obtain the intrinsic parameters of the measurement model, such as σ_+, measurement data is used. Figure 3.10(a) depicts a scatter plot of 2000 RSS measurement from the same location. Figure 3.10(b) shows the Gaussian distribution of this data.

Such measurements need to be taken in various places in the environment in order to be able to properly characterise the RSS measurements in that environment. From these measurements, standard deviations are averaged to obtain the σ_+. This is illustrated in Figure 3.10(c) which shows the standard deviations of RSS measurements across the environment (4226 measurements is used). Averaging the standard deviations will give σ_+ value of 4.025 dBm.

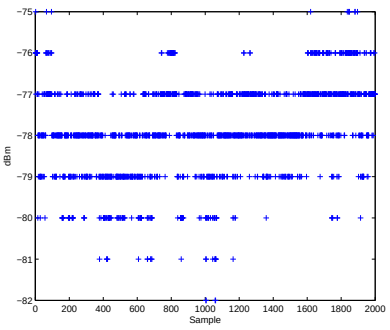

(a) Plot of RSS values.

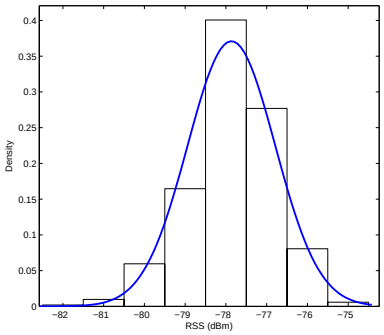

(b) Gaussian fitting.

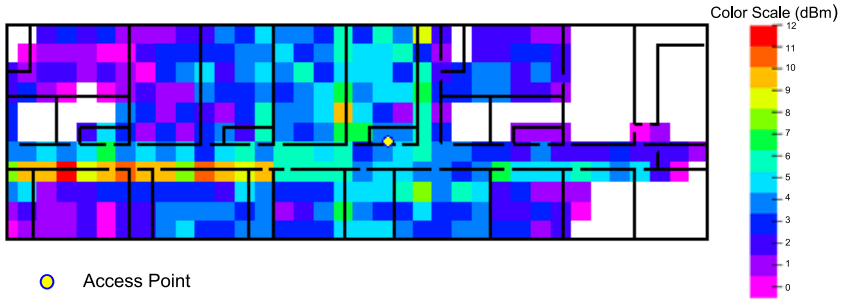

(c) Standard deviation of RSS measurements in the environment.

Figure 3.10: Acquire parameter from measurements.

The value of the penalty η in equation (3.24) of p_{miss} and (3.26) of p_{extra} is

governed by the following expression

$$\eta = \begin{cases} (5/30)(z_t + 100), & z_t \leq -70 \\ (15/25)(z_t + 70) + 5, & -70 < z_t \leq -45 \\ 20, & z_t > -45 \end{cases} \tag{3.28}$$

The aforementioned equation is formulated to mimic the tail part of a Gaussian distribution. The RSS range is taken from maximum and minimum RSS values measurable from a WLAN interface (-100dBm and -45dBm). Maximum penalty is given by the maximum signal loss caused by people shadowing (20 dBm) [90]. Linear interpolation is used to obtained penalty η values.

The result is that the value of η is in proportion to the RSS value missing in the fingerprint $\mathbf{z}_t^+$ or extra in $\mathbf{z}_t$. Greater missing/extra RSS values will have a proportionately higher penalty η (Figure 3.11).

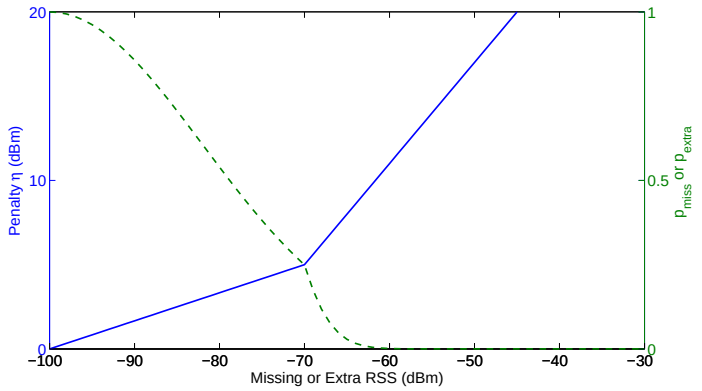

Figure 3.11: Penalty η for missing or extra RSS value.

The value of intrinsic parameters of standard deviation σ_+ and penalty η can be applied to environment similar with office setting (characterised by many walls, corridors and rooms), such as hospital, campus or apartment.

3.6 Estimation of Target State

Once the posterior probability is obtained, an estimation of the state is made based on equation (3.10). The state is estimated using a particle set $\mathcal{X}_t$ which is distributed in proportion to $p(\mathbf{x}_t|\mathbf{z}_t)$ ($\mathcal{X}_t$ is a return value of algorithm 3.2 of particle filter). Algorithm 3.5 below describes steps to estimate this state.

Algorithm 3.5 State_Estimation($\mathcal{X}_t$)

1: $\hat{\mathbf{x}}_t = 0$
2: **for** $i = 1$ to $|\mathcal{X}_t|$ **do**
3: $\quad \hat{\mathbf{x}}_t = \hat{\mathbf{x}}_t + \mathbf{x}_t^i . w_t^i$
4: **end for**
5: **return** $\hat{\mathbf{x}}_t$

3.7 Conclusion

This chapter described the implementation of a particle filter algorithm to improve the accuracy of opportunistic indoor localisation. The ability to deal with a non-linear and non-Gaussian system, the suitability for estimation of dynamic state with large process noise, and the robustness of the algorithm make the particle filter an ideal approach for RSS-based opportunistic system.

Furthermore, motion and measurement models were devised to enable the implementation of particle filter into opportunistic system. The approach for the motion model is a combination of the Brownian movement and the first-order motion model. This approach is novel and more accurately reflects the target's kinematics behaviour in opportunistic system. The proposed measurement model properly considers the physical characteristics of signal propagation in indoor environments. It leads to more accurate model which in turn leads to more accurate location estimation.

The implementation of a particle filter in an opportunistic system through the invention of measurement and motion models is novel and become one of the research contributions.

To improve further the accuracy of opportunistic indoor localisation, this research looks at other information beyond the available signal in the environment. This research also advances current approaches in fingerprinting to significantly enhance the usability of the system.

The collection of algorithms to further increase the accuracy and usability of the opportunistic system is the next contribution of the research and will be described in the following chapter.

Chapter 4

Learning Data Fusion

The previous chapter presented the implementation of the particle filter to increase the accuracy of opportunistic indoor localisation. It was achieved through the application of novel measurement and motion models.

To further improve the accuracy, this research examines other information beyond the available signal in the environment, i.e. map information and particle trajectory. The fusion[1] of extra information, in addition to RSS measurement, is the distinct characteristic of the algorithms explained in this chapter.

Filtering particle motion with map information is used to further increase the accuracy of opportunistic system (section 4.1). Moreover, particle trajectory is fused to refine state estimation with backtracking particle filter algorithm (section 4.2).

Furthermore, the research advances current methods in fingerprinting to address the usability problem (section 4.3). The novelty of the algorithm lies in the ability to automatically build and maintain the fingerprint up-to-date, thus significantly enhancing the usability of the opportunistic indoor localisation.

The collection of algorithm presented in this chapter is one of the most important contributions of this research.

[1] See section 2.2.2 for the definition of data fusion.

4.1 Map Filtering

To enhance the accuracy of localisation, the system can be constrained based on the characteristics of the target or restrictions imposed by external conditions. For example, kinematic constraints of the target, such as constant speed, has been formally incorporated as pseudo-measurement [91]. Constraints can also be introduced by external conditions, such as a road for car driving, air corridor for commercial plane flight or belt conveyor systems in airports.

A map, as a representation of the area or environment description, therefore can be used to restrict target movement along an allowable corridor or path. In [92], a map-aided particle filter was used to track car movement in an urban area. Target motion was restricted along a 1-dimensional line defined as a path representing the road.

In [93], the constraint is represented as a prior probability introduced to the map. The map is divided into zones with weight. The priori weight is used to bias the motion model toward areas of higher probability or put differently, to constraint the motion model from areas with lower probability. This approach is similar to [91], in a way that it incorporates constraint information by augmenting the motion model. However, it needs additional effort to manually build a map with weighted zones.

The present work proposes usage of indoor map information to constrain target motion. The target moves within a 2D plane in a manner restricted by indoor obstacles. For example, the target cannot cross solid objects (e.g.: walls, windows and furniture) and is only allowed to move within rooms, through doors and corridors.

4.1.1 Representation of the Map

A map or environment description is a basic necessity for map filtering. A map is essentially a skeleton description of the floor plan structure. It provides the main constraint for restricting target movement and can allow basic visualisation of localisation estimation in the context of the environment. Hence, the simplest form of the map is conveyed as a combination of walls (Figure 4.1).

Furthermore, maps are also used as an input for indoor propagation modelling which estimates electromagnetic propagation throughout the environment. The details of this parameter are dependent on the propagation model used, which will be discussed in more detail in section 4.3.1.2.

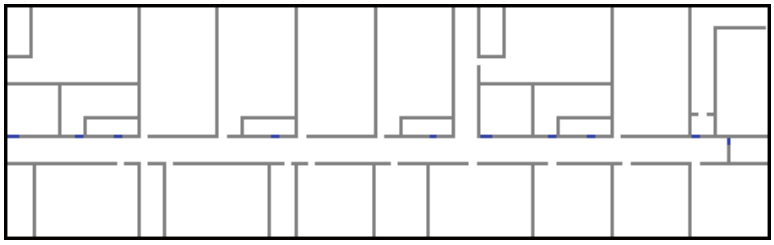

Figure 4.1: Environment description.

4.1.2 Algorithm for the Map Filtering

Fusing the map with the particle filter algorithm is achieved by including the constraint rule in the motion model of the particle. The new particle state, predicted by the motion model, should not cross walls or other obstacles. The prediction will be attempted a pre-determined number of times. If the attempts still fail, the particle will be categorised as invalid.

A similar method, called collision avoidance, has also been used in robotic localisation [56]. This thesis extends this approach by introducing and optimising the variable of a predetermined number of attempts.

The difference between subsequent attempts is the amount of random noise applied into the particle's direction (see equation 3.16 in chapter 3). The newly added noise should not make particle's direction deviate too much from true state's direction. A big deviation of particles' direction has an adverse effect on localisation accuracy.

Moreover, the number of attempts is proportional to the computational time required. The more attempts performed, the longer time needed to perform one cycle of particle filtering. Therefore, there is a trade-off between attempts, accuracy and speed. The number of attempts is determined empirically and evaluated in section 6.1.3.

Figure 4.2 illustrates evolution of particles with and without map filtering from a known state in 2D space ($v_0 = 3$ m/s, $N = 2000$). Map filtering constrains particle movement within the walls, as can be seen in Figure 4.2(b).

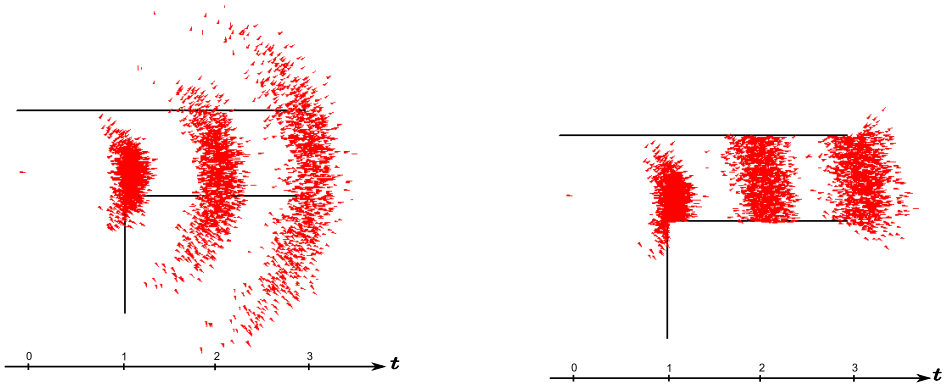

(a) Without map filtering. (b) With map filtering.

Figure 4.2: Particle evolution without and with map filtering.

Fusion of the map is formally performed in the update stage of the particle weight w_t^i. The particle weight will be updated with the following rule:

$$w_t^i = \begin{cases} 0, & \textit{crossing wall particle} \\ p(\mathbf{z}_t|\mathbf{x}_t^i), & \textit{otherwise} \end{cases} \tag{4.1}$$

where $p(\mathbf{z}_t|\mathbf{x}_t^i)$ is the likelihood observation function.

Algorithm 4.1 describes the map filtering steps for single particle. The input of the algorithm is the previous particle state $\mathbf{x}_{t-1}$ and measurement $\mathbf{z}_t$. The output is a new particle state $\mathbf{x}_t^i$ and its weight w_t^i.

1. Lines 1 and 2 represent initialisation of the algorithm
2. Lines 3 to 14 are the main loop for the map-filtering algorithm. Line 4 shows a motion model application based on equation 3.18. Lines 5 to 10 shows evaluation of new particle position constrained by walls.
3. Line 16 shows how the particle weight is set to 0, when all attempts fail.
4. Line 18 shows the update of the particle weight with algorithm 3.4 of the measurement model (see section 3.5.2).

5. Line 20 shows the algorithm return, i.e. current particle state with its associated weight.

Algorithm 4.1 MapFiltering ($\mathbf{x}_{t-1}^i$, $\mathbf{z}_t$)

1: A = number of attempts
2: c = false
3: **for** $a = 1$ to A **do**
4: given $\mathbf{x}_{t-1}^i$, predict the particle state $\mathbf{x}_t^i$ {with the motion model}
5: **for** $j = 1$ to number of wall **do**
6: c = particle state $\mathbf{x}_t^i$ cross the wall$_j$
7: **if** c = true **then**
8: **break**
9: **end if**
10: **end for**
11: **if** c = false **then**
12: **break**
13: **end if**
14: **end for**
15: **if** c = true **then**
16: $w_t^i = 0$
17: **else**
18: $w_t^i = p(\mathbf{z}_t|\mathbf{x}_i^t)$ {given by the measurement model}
19: **end if**
20: **return** $\mathbf{x}_t^i$, w_t^i

4.2 Backtracking Particle Filter

Fusing map information to increase the accuracy of the opportunistic system has been proposed in the previous section. Information that can be fused to further increase the accuracy is particle trajectory[1].

Backtracking particle filter (BPF) is a technique for refining state estimates based on particle trajectory. Incorporation of the map filtering technique allows

[1]Trajectory is set of time-ordered states representing the path taken by each particle

the BPF to exploit the long-range geometrical constraints of a map[1] and a long-term likelihood observation function.

If some particles $\mathbf{x}_t$ are not valid at some time t, the previous state estimates back to b time steps $\hat{\mathbf{x}}_{t-b}$ can be refined by removing the invalid particle trajectories. This is based on the assumption that an invalid particle is the result of a particle that follows an invalid trajectory or path. Therefore, recalculation of the previous state estimation $\hat{\mathbf{x}}_{t-b}$ without invalid trajectories will produce better estimates. In order to enable backtracking, each particle has to remember its state history or trajectory.

BPF implementation for opportunistic localisation is illustrated in the following figures. Figure 4.3(a) shows a typical phenomenon when a standard particle filter is used for opportunistic localisation. It shows the posterior density of the particles at four time-steps. The position estimates and the ground truth are shown in the diagram as well.

A particle deemed to be invalid when it is filtered out by the map filtering technique or by the likelihood function (performed in the 3rd time-step). For instance, a crossing wall particle will be categorised as invalid by map filtering technique and its weight is set to zero. A particle is also deemed as invalid if its weight, given by likelihood function, is very low. The invalid particles subsequently are not resampled in the 4th time-step.

Figure 4.3(b) shows how the BPF removes the invalid trajectories. Figure 4.3(c) illustrates the recalculation of the state estimation after backtracking. It is evident that, under certain conditions, BPF can improve the state estimation relative to a normal PF. This condition will be evaluated in section 6.1.3.

Algorithm 4.2 describes the steps necessary for BPF:

1. Line 1 refers to the increment of counter B, which shows how many estimations have been made.

2. Line 2 refers to the prediction stage of particle with the motion model. During the prediction stage, a new particle is sampled from the transition density $p(\mathbf{x}_t|\mathbf{x}_{t-1})$ with the map filtering technique. The new particle $\mathbf{x}_t$ will save the previous state $\mathbf{x}_{t-1}$.

[1] A wall used to filter current particle state x_t^i can affect previous states.

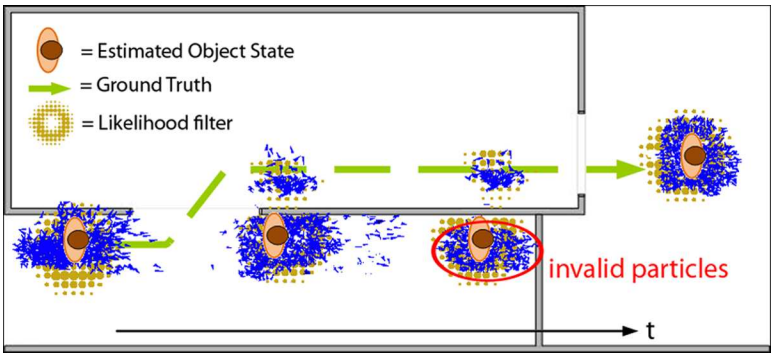

(a) Detecting the invalid particles

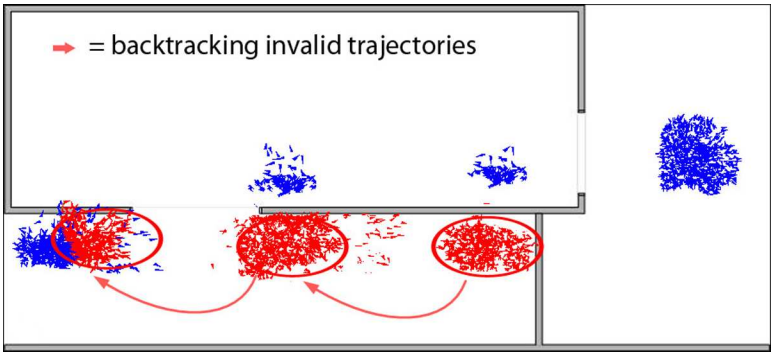

(b) Backtracking the invalid trajectories

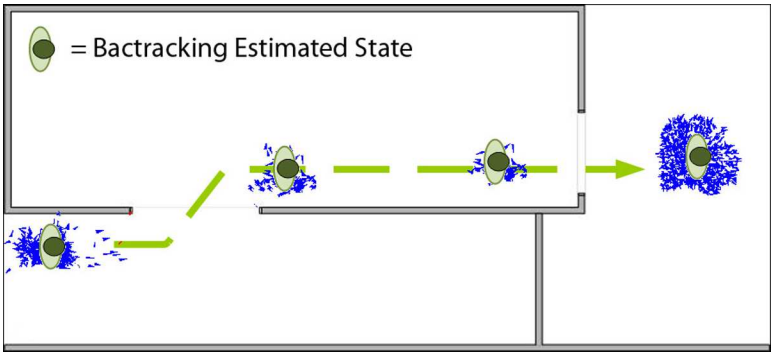

(c) Backtracking the estimated states

Figure 4.3: Illustration of BPF for opportunistic indoor localisation

Algorithm 4.2 Backtracking_PF ($\mathcal{X}_{t-1}$, $\mathbf{z}_t$)

1: $\bar{\mathcal{X}}_t = \mathcal{X}_t = \emptyset$
2: Increment B
3: **for** $i = 1$ to N **do**
4: **MapFiltering**($\mathbf{x}^i_{t-1}$, $\mathbf{z}_t$)
5: **end for**
6: calculate total weight $k = \sum_{i=1}^{N} w^i_t$
7: **for** $i = 1$ to N **do**
8: normalise $w^i_t = k^{-1} w^i_t$
9: $\bar{\mathcal{X}}_t = \bar{\mathcal{X}}_t + \{\mathbf{x}^i_t, w^i_t\}$
10: **end for**
11: $\mathcal{X}_t =$ **Resample** ($\bar{\mathcal{X}}_t$) with state inheritance
12: **if** $B \geq b$ **then**
13: **return** $\mathcal{X}_t$, $\mathcal{X}_{t-b}$
14: **else**
15: **return** $\mathcal{X}_t$
16: **end if**

3. In line 11, resampling is followed by inheritance of the state history. The resampling algorithm is performed with algorithm 3.3 as described earlier (section 3.3.1). The inheritance step makes the newly-sampled particle inherit its parent state history and enables each particle to remember its path trough the state-space. It does not expire over time.

4. Lines 12 to 15 show the output of the algorithm. The backtracked particle set $\mathcal{X}_{t-b}$ is returned when the number of calculations performed B is more than b (called the 'tail' or 'back-step'). The previous state estimate $\hat{\mathbf{x}}_{t-b}$ may be calculated from this set. The current particle set $\mathcal{X}_t$ is returned when the condition is not fulfilled.

The fusion of trajectory implies that BPF can only refined past state x_{t-b}. From application perspective, BPF can be useful for application that tolerant to the introduced delay, such as an application that studies user movement pattern in indoor environment.

4.2.1 Summary

Fusing map information to increase the accuracy of the opportunistic system had been proposed with the map filtering technique. Information that can be fused to further increase the accuracy is particle trajectory.

The fusion of particle trajectory is performed with the BPF algorithm. BPF is a technique for refining state estimates based on particle trajectory histories. This is based on the assumption that an invalid particle is the result of a particle that follows an invalid trajectory or path. Therefore, recalculation of the previous state estimation without invalid trajectories will produce better estimates.

Furthermore, the trajectory concept is expanded further to advance current fingerprinting methods. Set of hypothetical trajectories are proposed, evaluated and weighted in self-calibration fingerprinting algorithm to address usability problem in opportunistic system. The following section will elaborate self-calibration fingerprinting algorithm in detail.

4.3 Self-Calibration Fingerprinting

The objective of a self-calibration fingerprinting algorithm is to advance current approaches in fingerprinting in order to address the usability problem of opportunistic system.

The self-calibration for the opportunistic system eliminates labour-intensive and cumbersome manual calibration and makes the fingerprint adaptive to any change in the system or environment configuration. The algorithm maintains the fingerprint up-to-date, thus achieving self-calibration of the localisation system. Self-calibration fingerprinting is one of the most important contributions of this research.

The self-calibration fingerprint takes advantage of a fingerprint prediction with propagation model. However, it enhances this further by automatically re-calibrating parameters required for the propagation model across the environment and time. The algorithm learns from the history of measurement, target movement pattern and map description to accurately adjust the parameter of the propagation model.

The system assumes knowledge of the layout of dominant obstacles (walls) and system infrastructure within the environment (i.e.: the floor plan and system's fixed node positions). A mobile device carried by a moving target gathers RSS measurements and sends them to an opportunistic localisation system server with a self-calibrating algorithm to estimate target state. The target states and the gathered RSS measurements (together with additional information[1]), in turn are used to calibrate the localisation system (i.e.: the fingerprint). The system thus has a *closed loop* characteristic as illustrated in Figure 4.4.

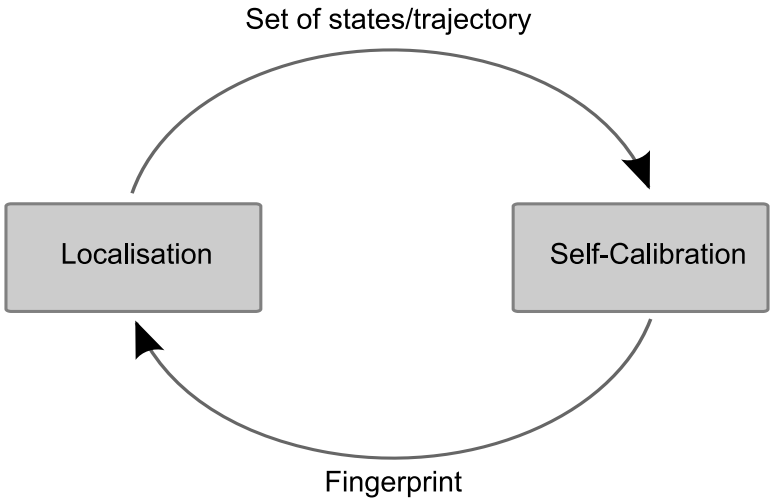

Figure 4.4: Closed loop characteristic of the self-calibration fingerprint.

4.3.1 Algorithm for Self-Calibration Fingerprint

The algorithm has a sequential characteristic and can be described with the flow chart shown in Figure 4.5. This algorithm consists of several steps which, for clarity, can be grouped into stages based on their immediate purpose.

1. **Initialisation.** This includes steps 1 and 2. It deals with system initial input, setting and parameter.

2. **Fingerprint prediction.** This includes step 3. The purpose of this stage is to predict the fingerprint with a propagation model.

[1]For instance, Voronoi graph, trajectories and fitness function.

3. **Trajectory creation.** Steps 4 to 6 of the algorithm are included here. A set of possible trajectories is the output of this stage.

4. **Ranking of trajectory.** Steps 7 to 14 are included in this stage. The purpose is to find the most likely trajectory which in turn is used to optimised-wall parameters.

5. **Adjustment of wall parameter.** Steps 15 to 16 are included here. The aim is to select the most likely trajectory and to update the wall parameter used for fingerprint prediction with the one in the most likely trajectory.

4.3.1.1 Initialisation

The self-calibration algorithm assumes knowledge of wall layout with their wall parameters. The wall parameters are the attenuation signal-loss of walls which will be discussed in more detail in section 4.3.1.2. The algorithm also assumes the knowledge of APs layout which is used for localisation and the initial position of mobile device.

Step 1 performs initialisation of the algorithm with inputs as follows:

- layout of main obstacles such as building floor plans or wall layout
- initial attenuation signal-loss of walls
- layout of APs used for localisation

The layout of walls and APs are represented as an indoor map described in section 4.1.1. However, to describe more accurately the behaviour of the environment, the wall is segmented into smaller sizes. This segmented wall reflects the mean local behaviour of the wall and its surrounding obstacles (such as furniture and people moving around the wall) which will influence the propagation model as depicted in Figure 4.6. This approach is taken from the 2D grid wall called 'motif' in [61].

The corresponding parameters of all environment walls are set to the same default value. Default values are reasonable values characterised by the prediction model. The absolute values are not as important as their initial uniformity throughout the environment.

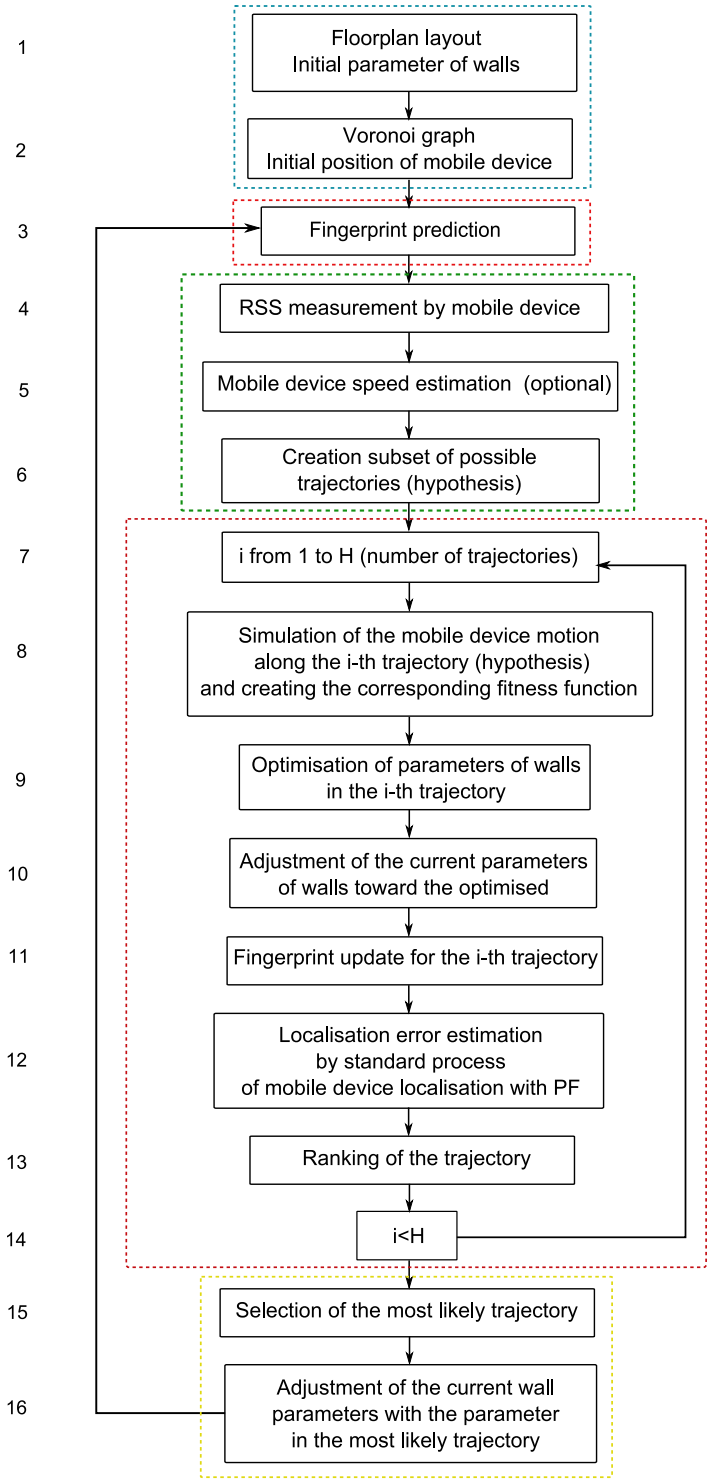

Figure 4.5: Flowchart describing the self-calibration fingerprint algorithm.

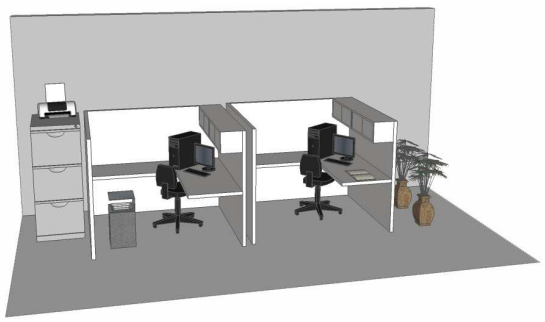

Figure 4.6: Wall surrounded by many obstacles.

Step 2 of the algorithm is a development of a Voronoi graph and a placement of initial position of the mobile device. A Voronoi graph (i.e.: the generalised Voronoi graph) is defined as a set of points in m dimensions, equidistant to m convex obstacles [94].

The Voronoi graph is represented as a set of vertices and edges.

$$G = \{\mathcal{V}, \mathcal{E}\} \tag{4.2}$$

where $\mathcal{V}$ is a set of vertices $\mathcal{V} = \{v^1, v^2, v^3, \ldots, v^I\}$ and $\mathcal{E}$ is a set of edges $\mathcal{E} = \{e^1, e^2, e^3, \ldots, e^J\}$ such that each edge connect two vertices, called the *endpoint* of the edge. Two vertices in a graph are said to be *adjacent* if there is an edge from one to the other. The position of vertices in the floor plan and edges' lengths are known.

The Voronoi graph is used for the constructing a set of possible trajectories in the next stage. The initial position of a mobile device is aligned with the Voronoi graph and can be input manually or by additional sensor measurement (such as RFID and GPS). Figure 4.7 shows an environment description with the Voronoi graph, APs and the initial position of the mobile device in the Electronic Department of CIT.

4.3.1.2 Fingerprint Prediction

The aim of this stage is to predict the fingerprint based on a propagation model.

Step 3 of the self-calibration algorithm is the fingerprint prediction. In this step, estimation of the expected RSS fingerprint, taking into account the (de-

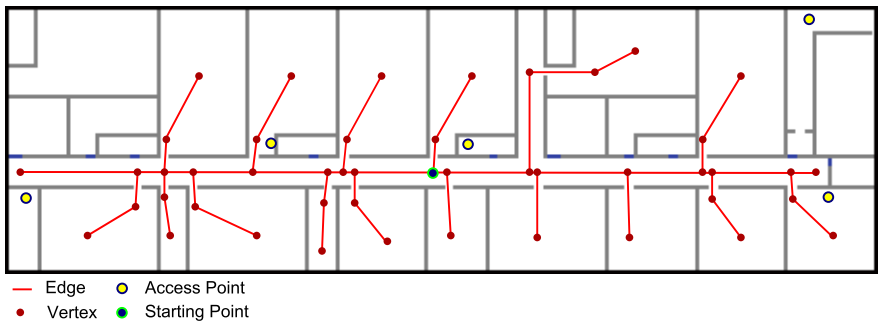

Figure 4.7: Map with Voronoi graph, APs and initial position of mobile device.

fault) parameters of the wall, is performed by appropriate empirical or physical propagation models.

A simple empirical approach, the MWM, is utilised for fingerprint prediction. MWM is chosen because of its simplicity and fast propagation prediction. Furthermore, it allows the application of linear optimisation (section 4.3.1.4). These factors contribute to the speed of overall algorithm, which is important factor for increasing the usability of opportunistic system.

In the MWM, the path loss is given by the following equation [95]:

$$L = L_1 + 20\ log(d) + L\mathsf{w} + L\mathsf{f} \tag{4.3}$$

where

$$L\mathsf{w} = \sum_{i=1}^{I} Lw^i = \sum_{i=1}^{I} a_w^i k_w^i \tag{4.4}$$

$$L\mathsf{f} = a_f k_f \tag{4.5}$$

L denotes the predicted signal loss, L_1 is the free space loss at a distance of 1 m from the transmitter, d is the distance from the transmitter to the receiver, $L\mathsf{w}$ is the contribution of walls to the total signal loss, $L\mathsf{f}$ is the contribution of floors to the total signal loss. Lw^i denotes the contribution of wall of i^{th} type to the total signal loss, a_w^i denotes the transmission loss factor of one wall of i^{th} type, k_w^i denotes the number of walls of i^{th} type, I is the number of wall types, a_f is the transmission loss factor of one floor, k_f is the number of floors.

This model takes into account the loss factor of wall and floor depending on their thickness and material composition. Figure 4.8 shows fingerprint prediction

with MWM from 5 APs. Only the strongest RSS in a fingerprint grid is shown. In this research, fingerprinting is used for localisation in 2D single floor, therefore signal-loss of floors Lf are not considered. The initial prediction uses a uniform

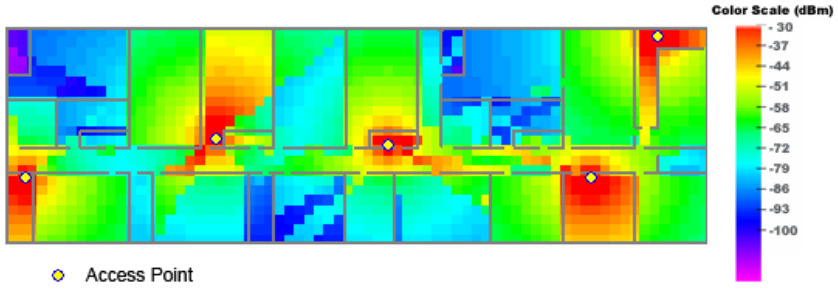

Figure 4.8: Fingerprint prediction with MWM

wall parameter (attenuation signal-loss) which is not accurate enough to represent site-specific wall parameters and its surrounding obstacles for fingerprint prediction.

Therefore, subsequent steps are performed to tune the initial wall parameters towards their optimised values. In the self-calibration fingerprinting algorithm, walls are divided into segments of smaller size. Each wall segment is optimised individually, to accurately reflect mean local behaviour of the wall and its surrounding obstacles.

The conventional method to optimise the MWM is to take a few measurements and then use it to optimise the model. It differs in several aspects with self calibration fingerprint: first, it only optimises wall signal attenuation without considers surrounding obstacles; second, it groups walls by their material type, therefore, it ignores individual wall characteristic; third, it needs manual measurements in known positions, which need to be performed for every environment; fourth, it can not optimise the wall parameter automatically if the environment change.

4.3.1.3 Trajectory Creation

The output of this stage is a set of possible trajectories of the mobile device. Trajectories are used because the inaccurate initial fingerprint will make erro-

neous estimated location. Therefore, this estimation is unreliable to be used to optimised the wall parameter.

Step 4 of the algorithm is the RSS measurement by a mobile device. The mobile device, subject to the pinpointing by the localisation system, gathers observed RSS measurements along the motion trajectory.

Step 5 is an optional step. The set of RSS measurements could be optionally used to estimate the motion behaviour (i.e.: speed and direction) of the mobile devices. The speed also can be estimated with additional sensor (such as accelerometer). In this research, mobile device was attached to a person who was moved in a constant speed (1m/s).

Based on the length of the time-interval of RSS measurements (and optional mobile device's motion behaviour), the distance travelled (d) by the mobile device can be estimated.

Step 6 is the trajectory creation step. Once the distance travelled, initial position of the mobile device and the Voronoi graph of the environment are known, a number of motion trajectories (hypotheses) H of the mobile device are proposed. A trajectory is defined as a set of time-ordered states expressed by

$$\hat{\mathcal{X}}_t = \{\hat{\mathbf{x}}_t, \hat{\mathbf{x}}_{t-1}, \hat{\mathbf{x}}_{t-2}, \ldots, \hat{\mathbf{x}}_{t-l}\} \tag{4.6}$$

where l is the number of time intervals of RSS measurement gathering.

The algorithm used to create trajectories is an adaptation of the depth-first traversal of an undirected graph [96]. The depth of the traversal is determined by the distance travelled. The traversal algorithm is naturally formulated as a recursive algorithm. Algorithm 4.3 shows the steps for creation of possible trajectories. The input of the algorithm is a vertex v in the Voronoi graph G and the distance travelled d by a mobile device. The output of the algorithm is a set of vertices $\mathcal{V}$, which is basically a set of way-points inside the trajectory.

1. Line 1 shows inclusion of vertex v in the set $\mathcal{V}$. Line 2 calculates the total edges lengths between adjacent vertices stored in $\mathcal{V}$.

2. Lines 4 to 6 describe the traversal of all adjacent vertices, w to v, as long as the total edge length $D <$ distance travelled d. Distance travelled d is obtained from previous step (step 5).

3. Line 8 shows when $\mathcal{V}$ becomes a candidate trajectory if $D > d$. To mimic normal walking trajectory and to reduce the number of possible trajectories, edges only can be traversed in a limited number.

Algorithm 4.3 Traverse(v, $\mathcal{V}$, d)

```
1: V = V + {v}
2: D = total of edges length in V
3: if D < d then
4:    for each vertex w adjacent to v do
5:       Traverse(w, V, d)
6:    end for
7: else
8:    save V {V is a candidate of trajectory}
9: end if
```

Figure 4.9 shows an example of the creation of possible trajectories in the CIT floor plan. The Voronoi graph and an initial position are shown in Figure 4.9(a).

Graph vertices and edges with their distances are shown in Figure 4.9(b). The target, which carries a WLAN enabled mobile device, did an 8m walk starting from the initial position. Possible trajectories are calculated with algorithm 4.3 and the result is illustrated in figure 4.9(c).

4.3.1.4 Ranking of Trajectory

The aim of this stage is to find the most likely trajectory which consists of a set of optimised-wall parameters. Step 7 to 14 are included in this stage.

Step 7 of the flowchart 4.5 starts at an inner loop evaluating the likelihood (ranking) of all proposed trajectories (hypotheses).

Step 8 of the algorithm is a simulation of the mobile device motion along the i^{th} trajectory and creation of the corresponding fitness function. The fitness function describes how similar RSS values estimated along the i^{th} trajectory by the propagation model (which uses current wall parameters) to the RSS measurements gathered by a mobile device along the i^{th} trajectory. The fitness function

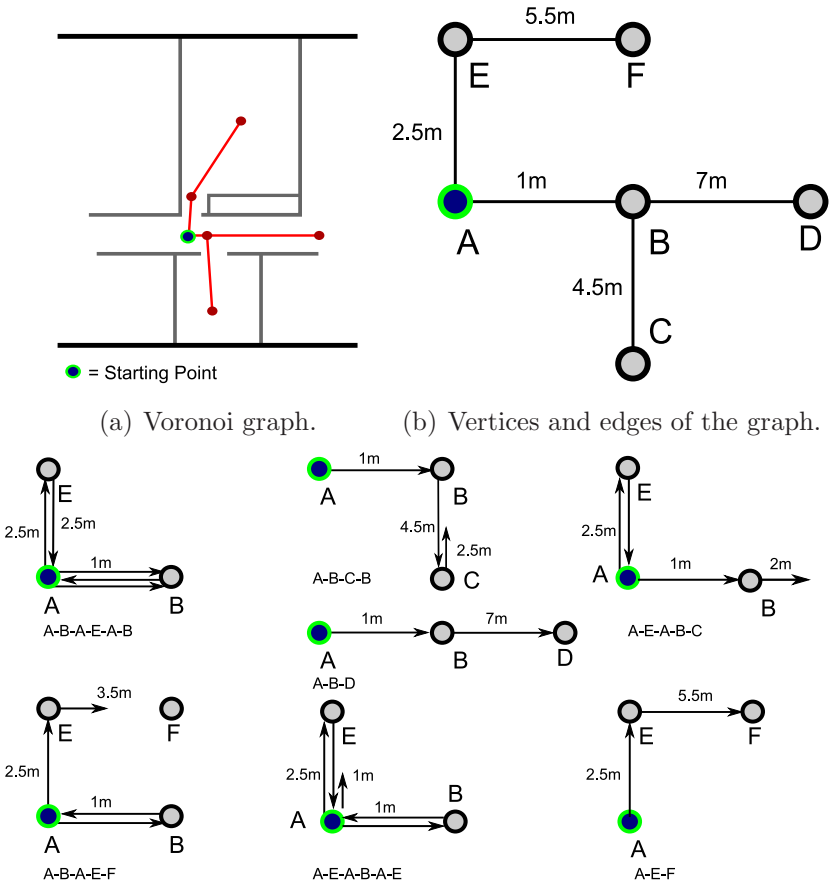

(a) Voronoi graph. (b) Vertices and edges of the graph.

(c) Proposed trajectories.

Figure 4.9: Trajectory creation of a mobile device with 8m distance travelled

takes the form of a set of linear equations suited to the optimisation method used in step 9.

In this work localisation is performed in 2D on single floor. Therefore, to create the fitness function, equation (4.3) of MWM may be rewritten as follows:

$$L = L_1 + 20\ log(d) + Lw \tag{4.7}$$

$$P^k - z_t^k = L_1 + 20\ log(d) + Lw_{t-1} + \Delta Lw_t \tag{4.8}$$

$$\Delta Lw_t = P^k - z_t^k - L_1 - 20\ log(d) - Lw_{t-1} \tag{4.9}$$

where

$$Lw = \sum_{i=1}^{I} Lw^i, \quad \Delta Lw = \sum_{i=1}^{I} \Delta Lw^i \tag{4.10}$$

ΔLw denotes the delta of wall loss, P^k denotes the power transmitted from AP k, z_t^k represents the RSS measurement gathered by the mobile device from AP k, L_1 is the free space loss at a distance of 1 m from the transmitter, d is the distance from the transmitter to the receiver, Lw is the contribution of the walls to the total signal loss and t denotes time. Lw^i represents a wall segment loss, ΔLw^i denotes the delta of a wall segment loss.

The purpose of the fitness function is to obtain the value of ΔLw^i, the delta of a wall segment loss. Figure 4.10 illustrates the fitness function creation when the target with mobile device is simulated along a trajectory.

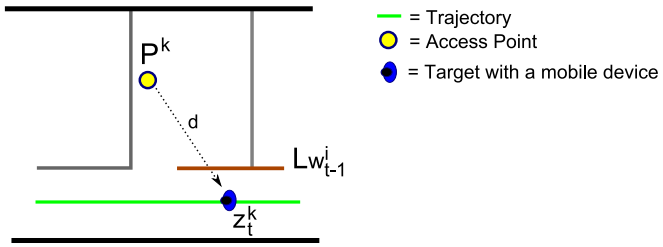

Figure 4.10: Illustration of fitness function creation with MWM.

Step 9 of the algorithm is the optimisation of the wall parameter in the i^{th} trajectory. Based on the RSS measurements gathered along the simulated i^{th} trajectory, a set of linear equations can be created. Since mostly the number of measurements is greater than the number of wall segments, the resulting set of linear equations will form an over-determined system. This means that the number of equations is greater than the unknown (i.e: ΔLw). A fast and robust algorithm to solve an over-determined linear system is least-squares method [97]. Consider the overdetermined system:

$$\sum_{j=1}^{n} X_{ij}\beta_j = y_i (i = 1, 2, \ldots, m) \tag{4.11}$$

where m represents the number of linear equations, n is the number of unknown coefficients, $\beta_1, \beta_2, \ldots, \beta_n$, with $m > n$. Recalling the fitness function in equation (4.9), β is the $\Delta L\mathsf{w}$, and y_i represent the right hand side of the equation.

The linear system can be written in matrix form:

$$\mathbf{X}\beta = \mathbf{y} \tag{4.12}$$

where

$$\mathbf{X} = \begin{bmatrix} x_{11} & x_{12} & \cdots & x_{1n} \\ x_{21} & x_{22} & \cdots & x_{2n} \\ \vdots & \vdots & \ddots & \vdots \\ x_{m1} & x_{m2} & \cdots & x_{mn} \end{bmatrix}, \ \beta = \begin{bmatrix} \Delta Lw_t^1 \\ \Delta Lw_t^2 \\ \vdots \\ \Delta Lw_t^m \end{bmatrix} \text{ and}$$

$$\mathbf{y} = \begin{bmatrix} P^1 - z_t^1 - L_1 - 20\ log(d^1) - Lw_{t-1}^1 \\ P^2 - z_t^2 - L_1 - 20\ log(d^2) - Lw_{t-1}^2 \\ \vdots \\ P^m - z_t^m - L_1 - 20\ log(d^m) - Lw_{t-1}^m \end{bmatrix}$$

This matrix has a unique solution if n columns in matrix $\mathbf{X}$ is linearly-independent[1], which is given by [98]

$$\hat{\beta} = (\mathbf{X}^T\mathbf{X})^{-1}\mathbf{X}^T\mathbf{y} \tag{4.13}$$

Step 10 is the adjustment of the current parameters of walls towards their optimised parameters which influence the RSS along the i^{th} trajectory. The adjustment is given by:

$$Lw_t^i = Lw_{t-1}^i + \Delta Lw_t^i \tag{4.14}$$

where Lw_t^i represents i-th wall segment loss at time t, Lw_{t-1}^i represents i-th wall segment loss at time $t-1$, ΔLw_t^i denotes the delta of a wall segment loss at time t. If a wall segment is optimised more than once, the delta ΔLw^i is an average value given by:

$$\Delta\bar{L}w^i = \frac{1}{n}\sum_{t=1}^{n}\Delta Lw_t^i \tag{4.15}$$

[1]A column in the matrix is not a result of linear combination of another column

where n is the number of optimisations performed in a wall segment i.

Step 11 is the prediction (re-calculation) of the fingerprint in the area of interest with the propagation model and adjusted parameters of walls.

Step 12 is the calculation of localisation error with the PF algorithm (algorithm 3.2), which takes into account the re-calculated fingerprint and gathered RSS measurements and the i^{th} trajectory as a ground truth. Figure 4.11 illustrates the calculation of localisation error along a trajectory.

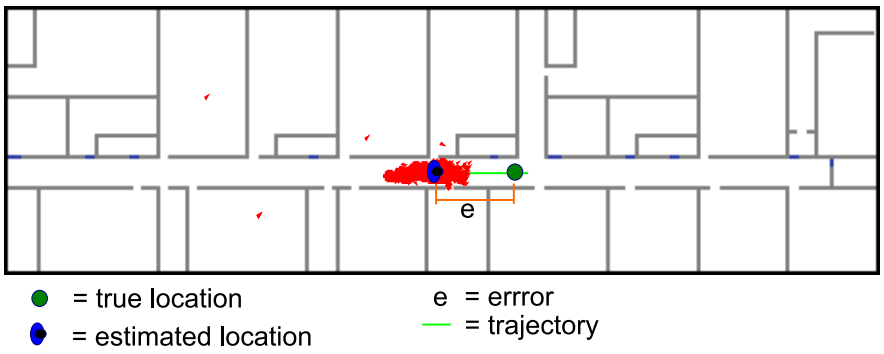

Figure 4.11: Illustration of localisation error.

Step 13 is the actual ranking (the likelihood estimation) of the i^{th} trajectory. It is calculated primarily by taking into account the localisation error and is governed by the following expression:

$$\omega^i = \frac{1}{\sigma\sqrt{2\pi}} \exp\left(-\frac{\epsilon^2}{2\sigma^2}\right) \tag{4.16}$$

where ω^i denotes trajectory likelihood and ϵ represents the localisation error. The trajectory likelihood is a probability with Gaussian distribution with mean localisation error of 0m.

Step 14 is the end of the trajectories (hypotheses) likelihood evaluation loop.

4.3.1.5 Adjustment of Wall Parameter

The aim of this stage is to choose the most likely trajectory and update the wall segments parameter with the parameter in the most likely trajectory. Beforehand, the trajectories need to be ordered based on their likelihood by a standard sorting method, such as the bubble sort or merge sort methods [96].

Step 15 is a selection of a limited number of most likely trajectories (hypotheses) for the mobile device. The other trajectories are discontinued at this stage.

Step 16 is the adjustment of the current wall segments parameter with the parameter in the most likely trajectory. Figure 4.12 illustrates the difference between the initial and calibrated fingerprints. Figure 4.12(a) shows the map with the actual trajectory. While Figure 4.12(b) shows the initial fingerprint, Figure 4.12(c) shows the fingerprint where some wall segment parameters have been optimised based on the most likely trajectory.

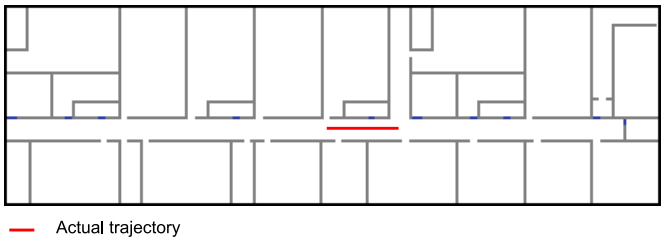

(a) Map with an actual trajectory.

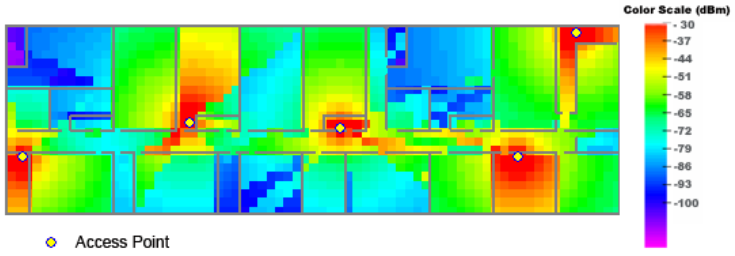

(b) Initial Fingerprint.

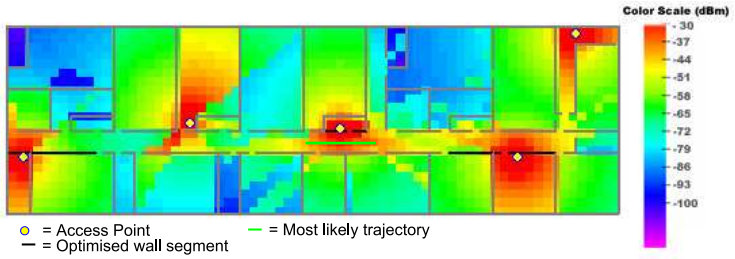

(c) Optimised fingerprint with the optimised wall segments.

Figure 4.12: Map, and fingerprint before and after self-calibration.

4.4 Conclusion

This chapter described the fusion of map information, particle trajectory and RSS measurement. The fusion is performed to further improve the accuracy of opportunistic system.

Map information is used to constrain particle motion with the map filtering algorithm. Fusing the map with the particle filter algorithm is achieved by including the constraint rule in the motion model of the particle. The new particle state, predicted by the motion model, should not cross walls or other obstacles.

Furthermore, the fusion of particle trajectory is performed with BPF algorithm. BPF is a technique for refining state estimates based on particle trajectory histories. Recalculation of the previous state estimation without invalid trajectories will produce better estimation.

The development of map filtering and backtracking particle filter in opportunistic system is novel contribution of this research.

Furthermore, this chapter presented an advancement of current fingerprinting methods with the self-calibration algorithm. The objective of the self-calibration fingerprinting algorithm is to significantly enhance the usability of an opportunistic system.

The self-calibration algorithm combines several advanced techniques, such as an indoor propagation model, Voronoi graph, graph traversal, trajectory concept, linear optimisation with least-square method and a particle filter. This algorithm advances state-of-the-art fingerprinting methods in several key areas: it removes the necessity to collect initial training data; it elevates the necessity to place dedicated RF receivers used for constantly measuring RSS values; it automatically optimises wall parameter for the propagation model.

Using single type of measured phenomenon may not offer required accuracy, but they can be fused with other sensor measurements to achieve better accuracy. The particle filter algorithm is used to fuse different sensory data when more fine-grained accuracy is desirable or when required for different application domains. The next chapter will describe the particle filter-based sensor data fusion to increase the accuracy of indoor localisation system.

Chapter 5

Multi Sensor Data Fusion

The data fusion algorithm presented in the previous chapter fuses RSS measurement, map information and particle trajectory to improve the accuracy of opportunistic indoor localisation. However, using a single type of measured phenomenon may not offer sufficient accuracy required for a particular application domain. Fusion with different localisation technologies is needed to enhance the accuracy of the opportunistic system.

Sensor data fusion[1] described in this chapter is conducted in the context of the Wearit@Work project[2]. The project investigated indoor localisation systems required in an industrial setting (car factory) and fire-fighter scenario.

Fusion of WSN and WLAN is investigated to achieve more fine-grained accuracy in an industrial setting (section 5.1). Furthermore, fusion of PDR, ultrasound and WSN is investigated for indoor localisation for fire-fighters (section 5.2). The fusion of an opportunistic system with different technologies is a novel approach and one of the contributions of this research.

To enable the implementation of particle filter-based fusion, motion models and measurement models for different measured phenomenon have to be devised. The novelty of the algorithm lies in the invented probabilistic models and will be further described in the following sections.

[1] See section 2.2.2 for the definition of data fusion.

[2] www.wearitatwork.com

5.1 Fusion of WSN and WLAN

WSN based on the IEEE 802.15.4 standard [99], are intended principally for monitoring and control applications that demand very low power consumption from a battery source. The range of coverage of a WSN node in indoor use is typically 10-20m.

Based on the standard, a WSN node provides a measured value, called link quality indication (LQI), which can be used for localisation purposes. The LQI can be implemented as RSS, signal-to-noise ratio or a combination of the two. The LQI of WSN is received for each message data-packet and is the result of averaging over eight symbols [9]. Furthermore, a WSN receiver typically has no special mechanism to suppress fading as in WLAN. Both factors make a WSN RSS measurement provide a potentially better profile for localisation purposes.

Figure 5.1(a) and 5.1(b) show the RSS measurements of WSN and WLAN, respectively. This illustrates the RSS in every 0.5m grid. The measurement campaign was performed in a room[1] of dimensions 22m x 9m. It can be seen there is more variation in RSS values of WSN when they were taken at different points compared to the WLAN counterpart.

In the NN algorithm, the variation makes distance measurement M (equation 2.1) more discernible between fingerprint grids, whereas in the particle filter algorithm, the variation causes more distinctive measurement probability $p(\mathbf{z}_t|\mathbf{x}_t)$ between the grids. Eventually, it leads to a better localisation accuracy. Therefore, RSS values of WSN was judged to give a better RSS profile for localisation purposes.

In this work, the WSN RSS is used for localisation based on the fingerprint and distance measurements using RSS lateration (section 5.2).

5.1.1 Fusion Algorithm of WSN and WLAN

The fusion between WSN and WLAN is performed in the calculation of the particle weight as follows (represented in the algorithm 4.1, steps 15-18, of sec-

[1]The measurement was performed in power electronic laboratory, ETH Zurich, Switzerland

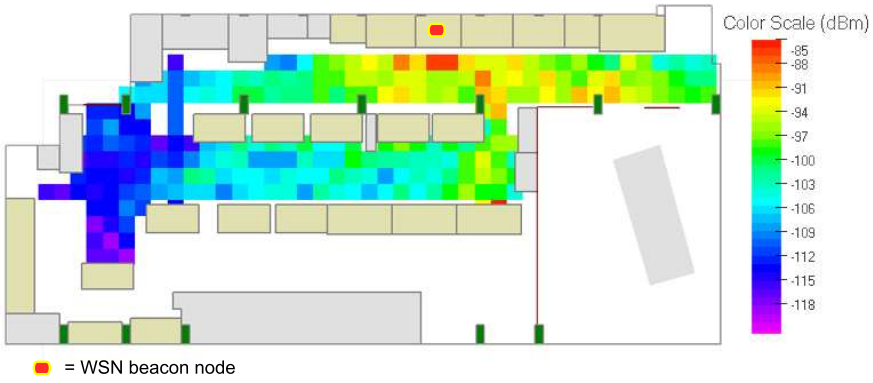

(a) WSN RSS measurement.

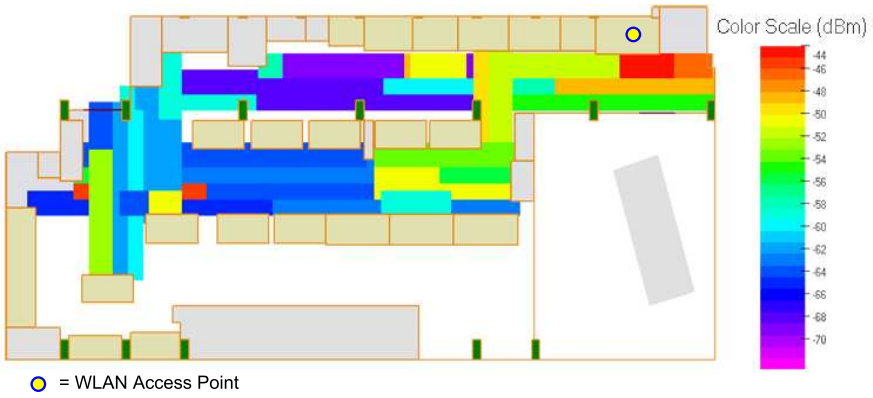

(b) WLAN RSS measurement.

Figure 5.1: RSS measurements from WLAN and WSN.

tion 4.1.2):

$$w_t^i = \begin{cases} 0, & \textit{crossing wall particle} \\ p(\mathbf{z}_t|\mathbf{x}_t^i), & \textit{otherwise} \end{cases} \tag{5.1}$$

where w_t^i represents a particle weight at time t, $p(\mathbf{z}_t|\mathbf{x}_t^i)$ is the likelihood observation function for WLAN and WSN measurement.

In the data fusion algorithm, the RSS of WLAN and WSN were treated as the same *type* of data, only that they were differentiated from their AP or WSN beacon[1] identification.

$$\mathbf{z}_t = \{z_t^1, z_t^2, z_t^3, \ldots, z_t^K\}$$

where z_t^k denotes RSS value z_t at time t from WLAN AP **and** WSN beacon with

[1]WSN beacon is analogue to the WLAN AP.

identification k. When both WLAN and WSN using the fingerprint technique, algorithm 3.4 is used for obtaining the likelihood observation function or the measurement model $p(\mathbf{z}_t|\mathbf{x}_t)$ of both WLAN and WSN.

5.2 Fusion of PDR, Ultrasound & WSN

In the context of indoor localisation for the fire-fighter scenario, fusion of PDR, ultrasound and WSN is investigated. To enable the implementation of particle filter-based fusion, motion models and measurement models for different technologies have to be devised.

Furthermore, to accurately construct the probabilistic models, internal mechanisms of each technology to infer location/displacement/range need to be understood. Section 5.2.1 presents measured data processing used in each fusion modalities. The modalities used are contributions of several partners involved in the Wearit@Work project. Section 5.2.2 describes the probabilistic model and the algorithm for sensor data fusion. The probabilistic model and the algorithm for sensor data fusion are the contribution of this research.

5.2.1 Modality

Positioning and navigation for fire-fighters and other emergency first-responders are mission-critical function. Utilising indoor localisation that needs pre-installed infrastructure (such as WLAN, RFID or UWB) is not suitable for this application domain since the infrastructure might not be available in the building or the existing infrastructure may not survive during a fire [17].

PDR has emerged as an alternative technology for indoor localisation and navigation for rescue/emergency scenarios. PDR is a localisation system based on inertial phenomenon processed by dead-reckoning principle. It is intended to locate a pedestrian (a person going on foot). PDR has a self-containment characteristic which makes this method particularly well suited to tracking in places where there is little or no localisation infrastructure.

However, this technique still lacks robustness, particularly with regards to heading. This shortcoming could cause a skewed path and produce an increasing

position error over time (see Figure 5.2). The sensor data fusion algorithm based on the particle filter can alleviate this problem by fusing PDR positions with other localisation modalities (i.e.: WSN and ultrasound technology).

Figure 5.2: Skewed path of PDR caused by heading error.

The following sections will explain PDR, ultrasound technology and WSN. The most advance type of PDR, foot-inertial PDR, is used in this research.

5.2.1.1 Foot-Inertial Pedestrian Dead Reckoning

In the foot-inertial approach to pedestrian navigation, the distance between footfalls is estimated from 3D acceleration and orientation measurements sensed directly at the foot. An inertial measurement unit (IMU), containing triaxial accelerometers, rate gyros and magnetometers, is solidly attached to, or mounted in, footwear (Figure 5.3).

In order to reduce accumulation of error due to the integration of accelerations our algorithm performs zero velocity updates at each step. Every time the product of acceleration and rate of turn drops below a threshold, it is inferred that the foot is in contact with the ground and therefore not moving. At this point the velocity can be reset to zero.

Figure 5.3: The orange XSens motion sensor is held on by the shoe laces [17].

This is illustrated in Figure 5.4. Each step has a stance phase (shaded) and a swing phase. Velocity is reset to zero during the stance phase, acceleration is double integrated during the swing phase.

The benefits of foot-mounted inertial sensors combined with zero velocity updates are described in more detail in [100] [101] [102].

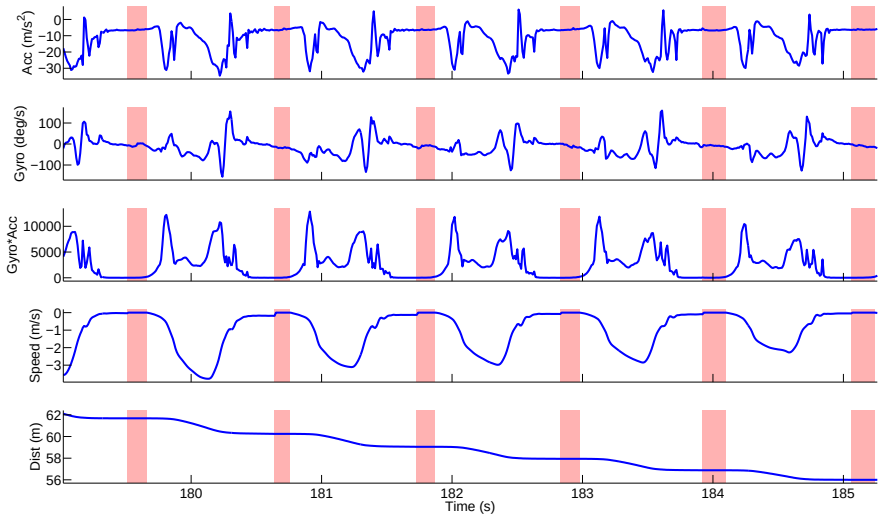

Figure 5.4: Zero velocity updates in pedestrian dead reckoning [103]

5.2.1.2 The Ultrasound Nodes

The Relate ultrasound sensor network[1] is a set of nodes capable of estimating distance and angle to neighbour nodes, and a bridge node connecting a laptop to

[1]The node was developed in the Relate project, a FP6 IST Programme funded by the EU

the node network. These are shown in Figure 5.5.

These nodes are based on the same sensing hardware described in [104] where the error is reported as 11cm and 48° with 90% confidence. The radio module has an indoor transmission range of approximately 15m at 868 MHz. The node periodically emits ultrasound pulses. All nodes in the ultrasound transmission range of the emitter node return the measured relative distance and angle.

Figure 5.5: Components of a Relate ultrasound sensor network.

5.2.1.3 WSN RSS-based Localisation

WSN is used as a complement of ultrasound nodes. It has a wider coverage range (10m-20m) than ultrasound node (<5m), therefore it is useful to extend the range of localisation system.

WSN provides RSS values which can be used to infer distance or location. In the context of localisation of fire-fighter, fingerprinting is not a feasible approach. Therefore, RSS-lateration (see section 2.1.2) is used to infer distance.

Since any infrastructure information (including map) is not available in this context, a simple OSM propagation model [95] is used to estimate distance from RSS value:

$$L = L_1 + 10nlog(d) \tag{5.2}$$

where L_1 (dB) is a reference loss value of 1m distance, n is a power decay factor (path loss exponent) defining slope, and d is the distance in meters.

5.2.2 Fusion Algorithm

Particle filtering for PDR is implemented by incorporating displacement estimates into the particle transition function. For each stride[1], a new particle position x_t^i is generated from the stride length and stride azimuth (heading) estimated from the inertial calculations and is governed by the following motion model:

$$\mathbf{x}_t^i = \begin{bmatrix} x_t^i \\ y_t^i \end{bmatrix} = \begin{bmatrix} x_{t-1}^i + s_t^i cos(\theta_t^i) \\ y_{t-1}^i + s_t^i sin(\theta_t^i) \end{bmatrix} \tag{5.3}$$

where s_t^i is the stride length of the i-th particle at time t, sampled from normal distribution $N(s_t, \sigma_s)$, with mean stride length s_t and standard deviation σ_s. σ_s is a constant value valid over a wide range of stride lengths. Particle heading θ_t^i is sampled from a normal distribution $N(\theta_t, \sigma_{\theta t})$ with a mean stride heading θ_t and standard deviation $\sigma_{\theta t}$. $\sigma_{\theta t}$ is set to a fixed percentage of the stride-to-stride heading change. The net effect is that, in straight paths, the particles remain on their previous course and during turns, particles tend to spread out [105].

Data fusion of PDR, map information, Relate ultrasound and WSN RSS sensor data is formally performed during the calculation of particle weights with the likelihood observation function. The particle weight w_t^i is changed according to the following rule:

$$w_t^i = \begin{cases} 0, & for \quad crossing\ wall\ particle \\ 1/N, & for \quad PDR \\ p(\mathbf{z}_t|\mathbf{x}_t^i), & for \quad ultrasound\ or\ RSS \end{cases} \tag{5.4}$$

where N is the number of particles, and $p(\mathbf{z}_t|\mathbf{x}_t^i)$ is the likelihood observation function.

If, at time t, there is more than one measurement of ultrasound or WSN RSS available, the probability $p(\mathbf{z}_t|\mathbf{x}_t)$ is obtained as the product of the individual

[1]Since the motion sensor is on one foot only, the PDR algorithm calculates the distance between footfalls for the same foot. This is the definition of a stride. For adults, one normal stride is between 1.2 and 2.0 m in length.

likelihood observation function.

$$p(\mathbf{z}_t|\mathbf{x}_t) = \prod_{k=1}^{K} p(z_t^k|\mathbf{x}_t) \tag{5.5}$$

where K represents the number of individual measurements obtained at time t.

The measurement model of an ultrasound measurement is obtained by multiplication of two Gaussian density functions of distance and angle measurement. The measurement model $p(\mathbf{z}_t|\mathbf{x}_t^i)$ of ultrasound node measurements is given by:

$$p(\mathbf{z}_t|\mathbf{x}_t^i) = \frac{1}{\sigma_d\sqrt{2\pi}} \exp\left[-\frac{(X_{z_t} - X_{x_t^i})^2}{2\sigma_d^2}\right] . \quad \frac{1}{\sigma_a\sqrt{2\pi}} \exp\left[-\frac{(\theta_{z_t} - \theta_{x_t^i})^2}{2\sigma_a^2}\right] \tag{5.6}$$

with X_{z_t} represents the distance measured from a Relate ultrasound node, $X_{x_t^i}$ denotes the actual distance of the ith particle at time step t from the ultrasound node, σ_d denotes the distance measurement standard deviation, θ_{z_t} denotes the angle measured from the ultrasound node, $\theta_{x_t^i}$ denotes the actual angle of the ith particle at time step t from the ultrasound node, and σ_a denotes the angle measurement standard deviation.

Figure 5.6(a) illustrates the Relate ultrasound node measurement likelihood observation function.[1]

The measurement model of WSN measurement is obtained by Gaussian density functions of RSS-to-distance value (obtained with equation 5.2). The likelihood observation function $p(\mathbf{z}_t|\mathbf{x}_t^i)$ for a WSN RSS measurement is given by the following expression:

$$p(\mathbf{z}_t|\mathbf{x}_t^i) = \frac{1}{\sigma\sqrt{2\pi}} \exp\left[-\frac{(X_{z_t} - X_{x_t^i})^2}{2\sigma^2}\right] \tag{5.7}$$

with X_{z_t} denotes the RSS-to-distance measured from a WSN, $X_{x_t^i}$ denotes the actual distance of the ith particle at time step t from the WSN node and σ denotes the RSS-to-distance standard deviation.

In indoor environments, phenomena like reflection of obstacles, diffraction around obstacles, and transmission (accompanied by refraction) into the obstacle

[1] ultrasound node is positioned in the centre of the plot, 2m of measured distance (1m of σ_d), 210 of degree angle measurement (45 degree of σ_a).

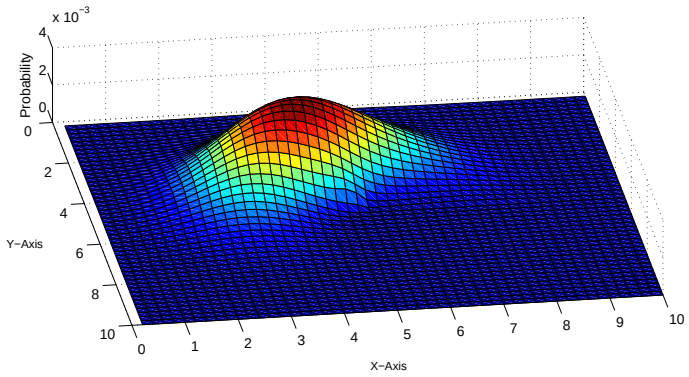

(a) Likelihood observation function of ultrasound measurement

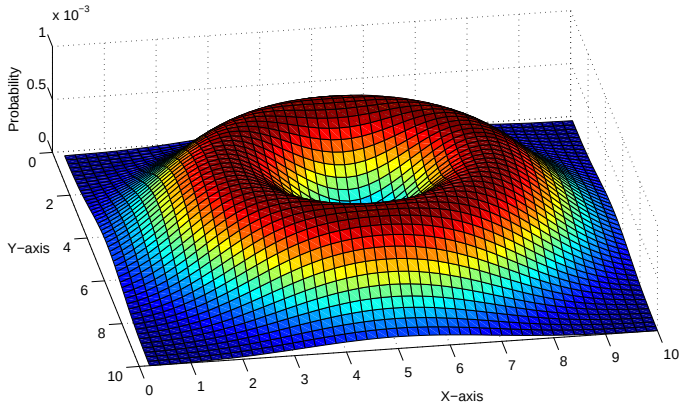

(b) Likelihood observation function of WSN RSS measurement

Figure 5.6: Likelihood observation functions of the ultrasound and WSN measurement

or medium, considerably reduce the reliability of distances computed from RSS values.

To cope with this, a relatively high value for the standard deviation σ of the RSS-to-distance measurement (0.5 of d) is used. Figure 5.6(b) illustrates the WSN node likelihood observation function.[1]

[1]WSN node is positioned in the centre, 2m of RSS-to-distance measurement (1m of σ).

5.3 Conclusion

In this chapter, the usage of particle filter-based algorithm for sensor data fusion of multi-modal localisation technology was described. The sensor data fusion was investigated to achieve more fine-grained of an opportunistic indoor localisation.

In the context of localisation in car industry, fusion of WSN and WLAN was investigated. It was found that RSS values of WSN gives distinctive measurement probability between fingerprinting grids. Eventually, it leads to better localisation accuracy when WLAN and WSN are fused. In the data fusion algorithm, the RSS of WLAN and WSN use the same measurement model explained in algorithm 3.4.

Fusion of PDR, ultrasound and WSN was investigated to increase the accuracy of indoor localisation for the fire-fighters. Motion and measurement models of PDR, ultrasound and WSN were devised to enable the fusion. Fusion for PDR was implemented by incorporating displacement estimates into the particle motion model. Novel motion models based on Gaussian density function were devised for ultrasound and WSN to enable the fusion.

The fusion of opportunistic systems with different technologies through the development of sensor-specific probabilistic models is one of the contributions of this research.

The next chapter will present the evaluation of the developed algorithms in the opportunistic indoor localisation system.

Chapter 6

Evaluation

The collection of algorithms described in Chapter 3, 4 and 5 were implemented into software packages, designed as part of this work, to allow for appropriate evaluation.

The evaluation consists of four parts: The first part will evaluate algorithm performance on the accuracy of indoor localisation (section 6.1); the second part will describe the evaluation of the algorithm addressing the fingerprint usability problem (section 6.2); the third part will evaluate algorithm performance when implemented for multi sensor data fusion (section 6.3); the last part will conclude the evaluation. This chapter describes only the most representative experiments that were conducted for the evaluation.

6.1 Accuracy

This section evaluates particle filter (PF), map filtering (MF) and BPF on the accuracy of indoor localisation. WLAN is utilised as the technology platform for evaluating the algorithms.

The evaluation scenario is shown in Figure 6.1. It shows a person carrying a mobile device as a target of localisation in the area covered by WLAN APs. The mobile device measures the RSS of the APs, sends the measured data *via* WLAN to a central processing unit, where an opportunistic localisation system is executed resulting in pinpointing of the mobile device's location.

The localisation system also records information about the ground-truth[1] of the target, which in turn is used to estimate the error or accuracy of the algorithm.

Ground truth is saved as a part of the floor plan. It recorded as poly lines, with known length s and travel time t. User walks at a same pace, therefore user's speed was a deduction from the length and travel time ($v = s/t$). RSS scan frequency is constant (1 m/s) with known timestamp, therefore user's ground truth of each measurement can be interpolated in the poly line from the speed v and timestamp of the measurement.

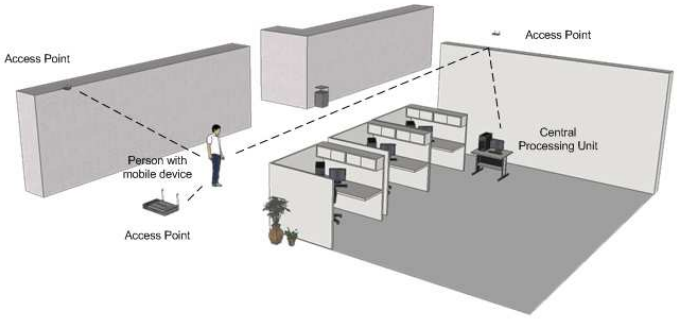

Figure 6.1: Evaluation of opportunistic indoor localisation.

6.1.1 System and Tools

The location system works in two phases. Firstly, *calibration* builds a database of the RSS fingerprint. Secondly, *localisation*; the mobile device measures RSS, sends the measured data to a processing system resulting in pinpointing of the mobile device's location. A block-diagram of the system and related tools are illustrated in Figure 6.2(a).

Several tools have also been built using the C++ language. They include a site-survey tool for the calibration phase (i.e. building the RSS fingerprint), a client tool and a fusion engine.

Figure 6.2(b) shows the client tool that is used for RSS measurement. The client tool also can be used to visualise the target states, particle distribution and likelihood observation function as shown in Figure 6.2(c).

[1]True location of the target.

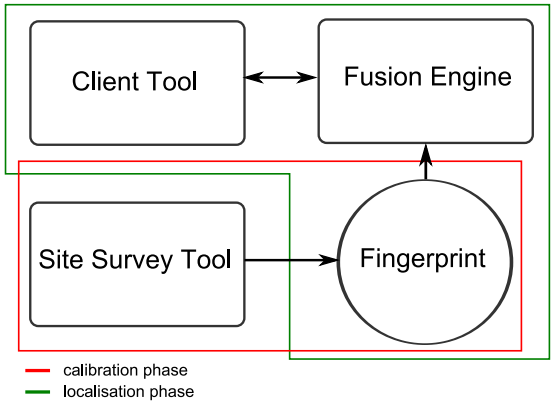

(a) Block diagram of the localisation system.

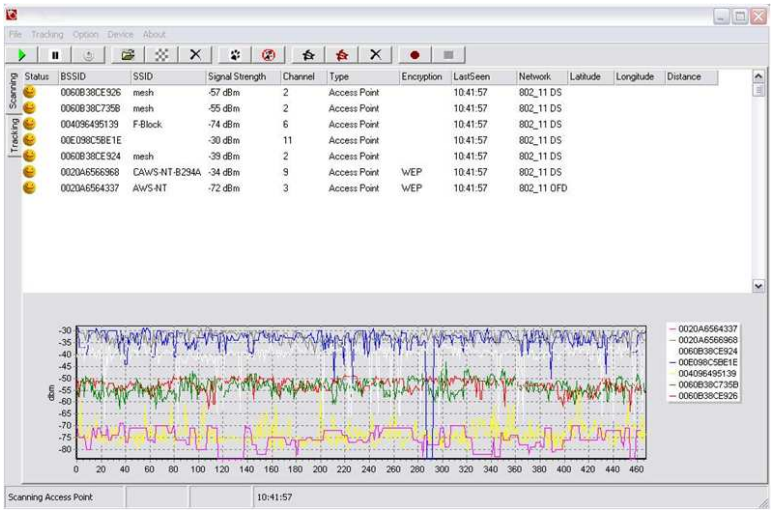

(b) Client tool for gathering the RSS.

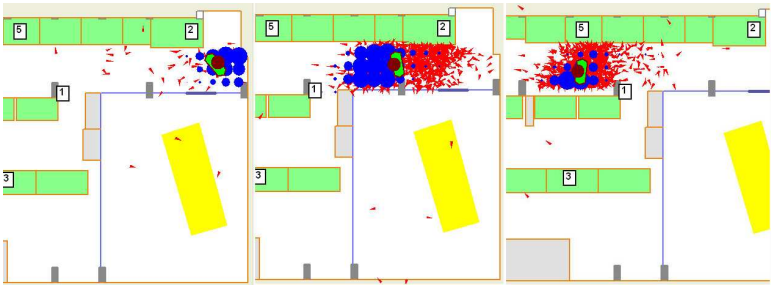

(c) Example of visualisation in the client tool.

Figure 6.2: Diagram and tools for indoor localisation.

6.1.2 Experimental Setup

The Department of Electronic Engineering (73 m x 22 m) at Cork Institute of Technology (CIT) was used as a test-bed to analyse the proposed algorithm. Wireless infrastructure with 5 Orinoco AP-700 access points was installed at the test-bed. A Dell Latitude D505 laptop with Intel PRO/Wireless 2200 BG WLAN interface was used for both calibration and localisation phases. Both access points and WLAN card were set in IEEE802.11g mode.

Three 105m-walks were performed in the EE department of CIT. The map of the department with the ground truth is shown in Figure 6.3. RSS measurements in 238 points along the ground truth were gathered which in turn were used to estimate their location.

Figure 6.3: Map with ground truth in EE CIT building.

To build the fingerprint, RSS measurements were collected while walking between two points back and forth in a slow and constant pace. The location of the measurement was an interpolation between the points. A fingerprint with 1m grid size was used. The density of RSS values between grids was not uniform, the densest had 20 RSS measurement came from 4 APs.

6.1.3 Results

The proposed algorithm was compared to existing algorithm of NN and KF (section 2.2.1). The NN method is an implementation of Motetrack approach (equation 2.3 section 2.2.1). The KF was taken from robotic localisation described in (equation 2.7 section 2.2.1). The localisation accuracy is summarised in Table 6.1.

The BPF can take advantage of long-term likelihood observation function and long-range (geometrical) constraint information yielding excellent localisation

Table 6.1: Localisation error (metres)

	NN	KF	PF	BPF
without MF	μ =5.14 σ =3.16	μ =4.67 σ =3.84	μ =3.25 σ =1.91	μ =2.83 σ =1.28
with MF	-	-	μ =2.15 σ =1.08	μ =1.98 σ =1.11

performance (1.98 m mean 2D error), it shows enhancement up to 40% compared to PF only (3.25 m mean 2D error) and a performance nearly 3 times better than that of NN (see Figure 6.4).

The cumulative distribution function (CDF) of the errors is shown in Figure 6.5. It can be seen that, when using BPF with the MF algorithm, 80% of the errors are below 3m.

More significantly, the BPF without MF yields improved localisation performance (2.83 m mean 2D error) compared to PF-only (3.25 m mean 2D error). This result confirms that BPF can be performed *via* elimination of trajectory errors based on the likelihood observation function.

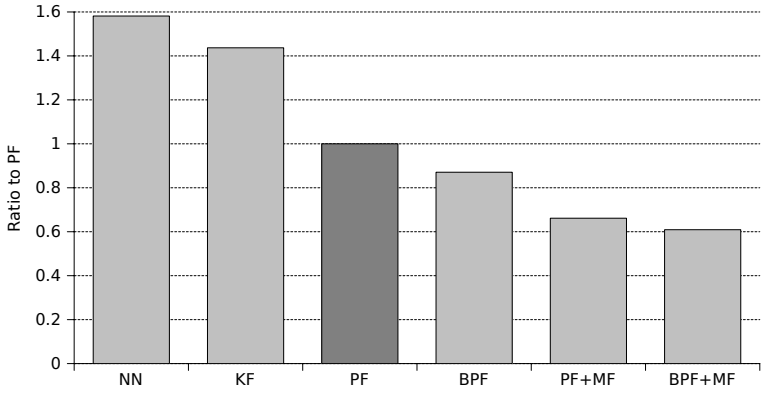

Figure 6.4: Location error in proportion to PF.

As was expected *a priori*, the conventional NN estimation method showed a large position scatter all along the ground truth. The KF, PF and BPF have better trajectory, see Figure 6.6. The trajectory evolution over time is shown in Figure 6.6(b) for estimation without MF. It can be seen that PF trajectory is

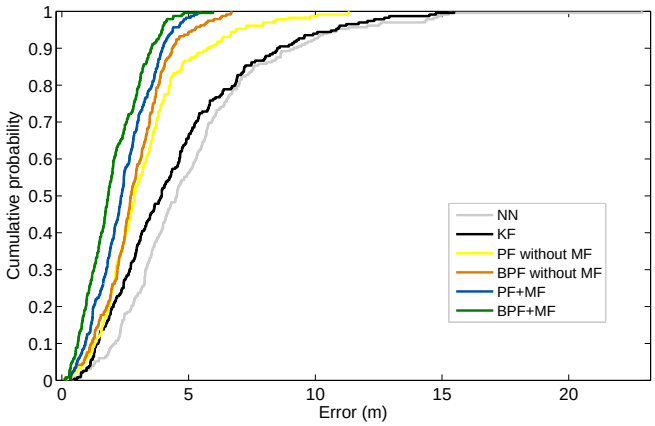

Figure 6.5: CDF of the error.

more scattered than BPF. Trajectories of filtering with MF shown in Figure 6.6(a) are better since they are constrained by the building's walls.

6.1.3.1 Influence of Parameters

The influence of algorithm parameters to the localisation accuracy was also investigated. These parameters were: standard deviation σ_+, number of attempts and tail length.

Standard deviation

Standard deviation σ_+ is used to calculate the likelihood observation function $p(\mathbf{z}_t|\mathbf{x}_t)$ in equation (3.27) and its value can be estimated from measurement as described in section 3.5.3.

The influence of differing σ_+ values on the localisation accuracy is summarised in Figure 6.7. It can be seen that the localisation error decreases as the σ_+ value changes from 1 dBm up to 5 dBm. Afterwards, the error tends to increase.

A value of σ_+ reflects the magnitude of error in the measurement. A big value of σ_+ is assigned when it is believed that the measurement is more prone to error. It will give the update of the measurement model less influence and give the motion model more emphasis. The net effect is that particles will spread more over time (see Figure 3.5) and that the localisation error will increase.

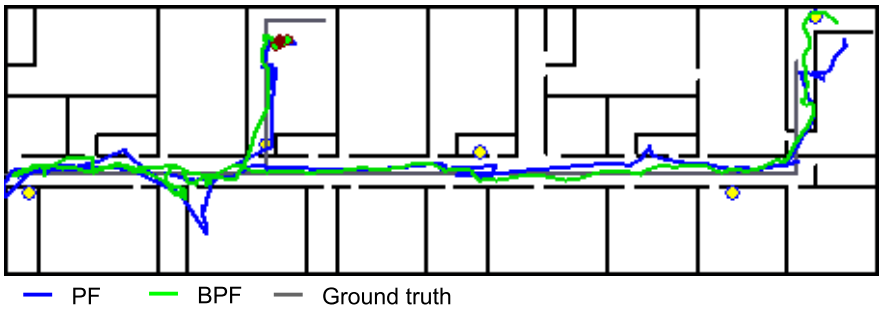

(a) PF and BPF trajectory with Map Filtering.

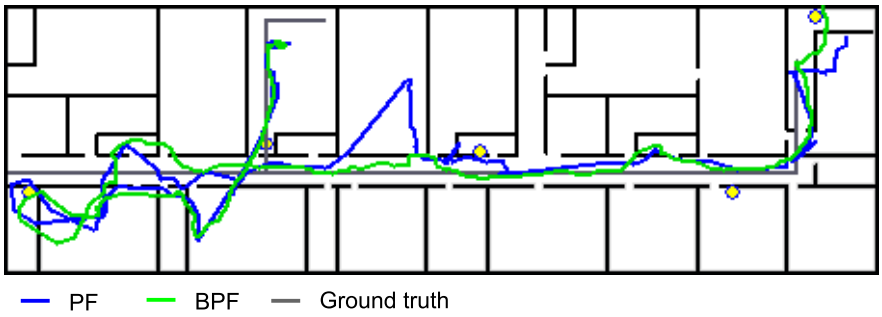

(b) PF and BPF trajectory without Map Filtering.

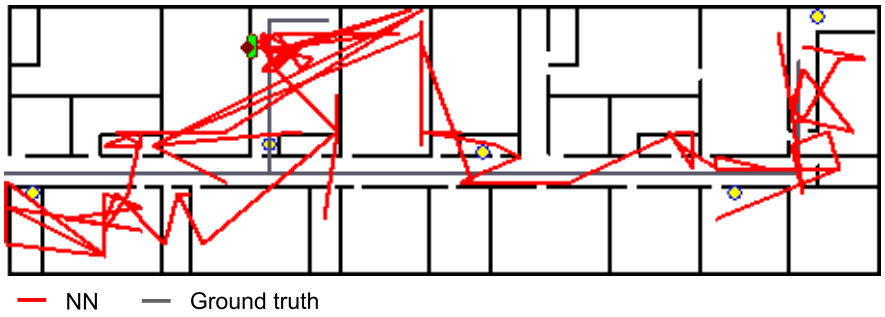

(c) NN trajectory.

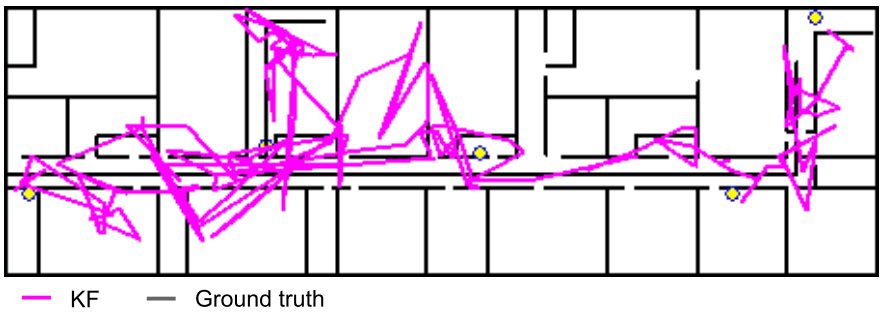

(d) KF trajectory.

Figure 6.6: Trajectories from different algorithm.

Based on the estimated value described in section 3.5.3 and the evaluation, a recommended value of σ_+ can be proposed. Standard deviation σ_+ between 4dBm - 5 dBm is suggested for indoor localisation in an environment similar with office setting (characterised by many walls, corridors and rooms), such as hospital, campus or apartment.

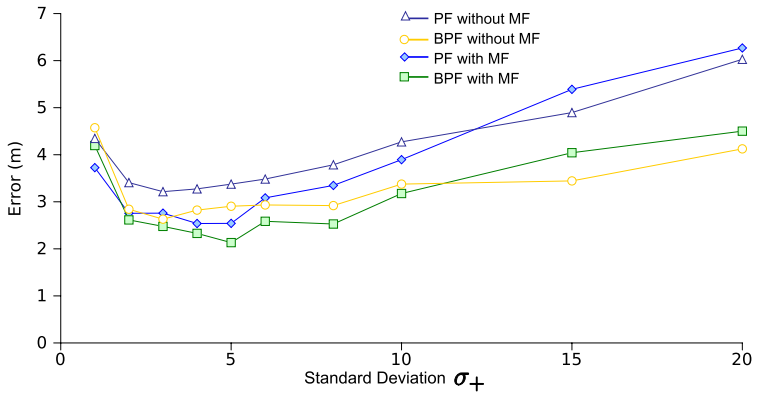

Figure 6.7: Influence of standard deviation σ_+

Number of Attempts

The number of attempts determines how many times a new particle state is predicted with the motion model (algorithm 4.1 of map filtering, section 4.1.2).

The influence of the number of attempts on accuracy is summarised in Figure 6.8. It shows ratios to the PF and BPF accuracy with a single attempt (2.99 m and 2.89 m mean error, respectively). The accuracy improves from 1-4 attempts and is optimum between 5-8 attempts. Afterwards, the error tends to increase. Calculating one cycle of map filtering[1] with 8 attempts requires 1 second of computational time[2].

The differences between consecutive attempts are the direction used in the motion model of a particle. If the preceding attempt failed, the subsequent attempt was performed by changing the particle's direction (equation (3.16)) and noise (equation (3.18)). After 8 attempts, the amount of random noise applied

[1] N =1000 particles

[2] Using Dell Latitude D630 Laptop, Intel Core Centrino Duo CPU, 2GB of RAM

into particles' direction, made particles' direction more deviated from their true state. A big deviation has an adverse effect on localisation accuracy.

Optimum attempt value of 8 is suggested for indoor localisation in a typical office environment. It gives the best accuracy and only needs modest computational power.

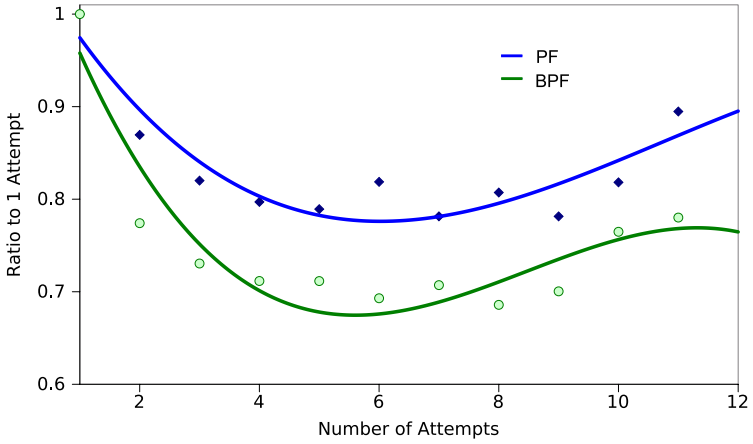

Figure 6.8: Influence of number of attempts in Map Filtering

Tail

Tail length b determines the number of back-steps in time in which the previous target state estimation $\hat{\mathbf{x}}_{t-b}$ can be refined by removing invalid particle trajectories with the BPF algorithm (see section 4.2).

The influence of tail length on accuracy is shown in Figure 6.9(a) and Figure 6.9(b) for BPF with and without MF, respectively. In the BPF without MF accuracy increases until a tail length of 50 before it then decreases. In the BPF with MF, accuracy increases until a tail length of 20, and it decreases after a tail length of 100.

If the value of the tail is too big, the number of surviving particles (as the result of removing the invalid trajectories) become too small. Therefore, the particles distribution is not sufficient to represent the posterior distribution, which makes the accuracy worsen. Based on the result, tail length of 15-20 is suggested to give the best accuracy.

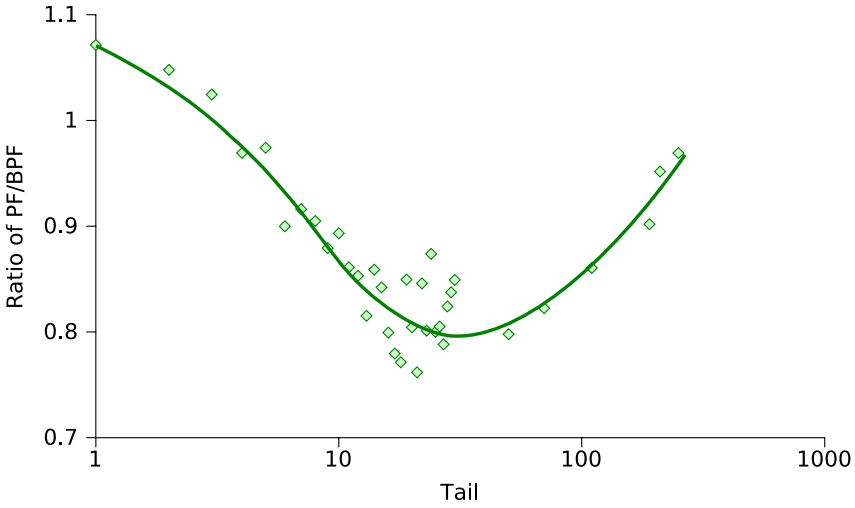

(a) Influence of tail in BPF accuracy without MF.

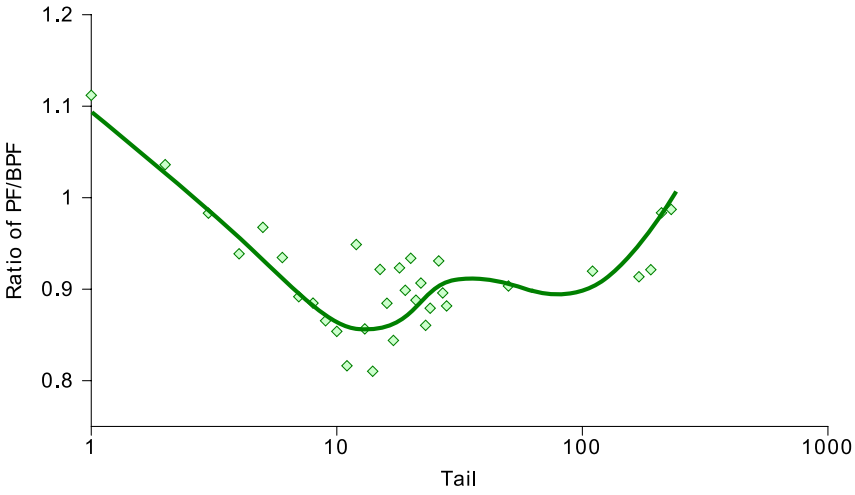

(b) Influence of tail in BPF accuracy with MF.

Figure 6.9: Tail influence on BPF accuracy.

6.1.4 Summary

This section examined how the PF, MF and BPF algorithm influenced on the accuracy of indoor localisation. The proposed algorithms were evaluated and compared with the existing NN and KF algorithms.

The evaluation of the proposed algorithms show favourable results. The PF algorithm gave an accuracy of 3.25m (compared to NN accuracy of 5.14m). The best performance was given by BPF+MF (1.98 m mean 2D error), it shows enhancement up to 40% compared to PF only and a performance nearly 3 times better than that of NN. Furthermore, in 80% of cases, the accuracy of BPF+MF is below 3m.

The influence of algorithm parameters to the localisation accuracy was investigated. These parameters were: standard deviation, number of attempts and tail length.

Standard deviation σ_+ between 4dBm - 5 dBm is recomended for indoor localisation in an environment similar with office setting (characterised by many walls, corridors and rooms), such as hospital, campus or apartment. Attempt value of 8 is suggested since it gives minimum localisation error and only needs a modest computational power. Based on evaluation the result, tail length of 15-20 is proposed to give the best accuracy.

In this section, it was demonstrated that the implementation of a particle filter, map filtering and backtracking particle filter significantly enhances the accuracy of the opportunistic indoor localisation system.

Another contribution of the research is the self-calibration fingerprinting to improve the usability of an opportunistic system. The next section will describe the evaluation of the algorithm in more detail.

6.2 Usability

6.2.1 System and Tool

The architecture of the localisation system with the self-calibration algorithm is described in Figure 6.10. There are four main components of the self-calibration system: the client tool, fusion engine, self-calibration engine and fingerprint. The

client tool collects RSS signatures and passes them on to the fusion and self-calibration engines. The fusion engine is responsible for the pinpointing of the target position based on the PF. The self-calibration engine is the component that performs the self-calibration. The last component is the database of the generated RSS fingerprint.

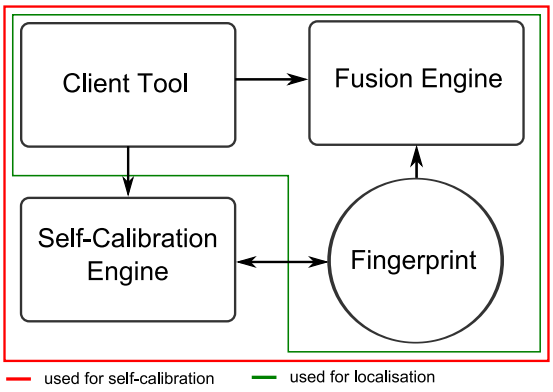

Figure 6.10: Block diagram of the self-calibration system.

6.2.2 Experimental Setup

The Department of Electronic Engineering (73 m x 22 m) at CIT was used as a test-bed to analyse the proposed algorithm. The CIT floor plan with Voronoi graph (as shown in Figure 4.7) was used.

RSS measurements were gathered along the ground-truth (Figure 6.11) to be used for self-calibration. The data was evaluated off-line with the self-calibration system. The walls were divided into 6m of segments.

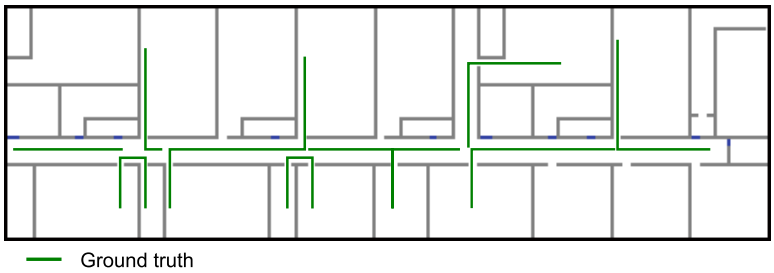

Figure 6.11: Measurement ground truth for self-calibration fingerprinting.

6.2.3 Results

The self-calibration algorithm used to enable an automatic generation and calibration of the RSS fingerprint was evaluated and compared with a predicted and a manual fingerprint (Figure 6.12(c)). MWM was used to predict the fingerprint (shown in Figure 6.12(a)). This, in turn, was also used for the initial fingerprint in the self-calibration algorithm (section 4.3). The calibrated fingerprint and optimised walls are shown in Figure 6.12(b).

Mean signal differences between MWM prediction and manual fingerprint is -5.53 dBm with $\sigma = 7.12$ dBm. Whereas, mean signal differences between self-calibration and manual fingerprint is -1.38 dBm with $\sigma = 9.03$ dBm. Therefore, the self calibration fingerprint is able to refine the fingerprint towards its optimum value.

Histograms and CDFs of the differences are shown in Figure 6.2.3. PDF and CDF signal level differences between MWM and manual fingerprint is illustrated in Figure 6.13(a), meanwhile self-calibration versus manual fingerprint is shown in Figure 6.13(b).

Localisation accuracy with different fingerprinting methods are summarised in Table 6.2. It can be seen that localisation accuracy using a self-calibrated fingerprint improved significantly compared with that obtained using a MWM-predicted fingerprint. BPF with the calibrated fingerprint yielded improved performance (3.57 m error) compared to that obtained with MWM prediction (7.44 m error) or 50% better (shown in Figure 6.14(a)). Despite the fact that PF/BPF manual fingerprint yielding a good result, PF/BPF accuracy with self-calibration fingerprint still out-performs NN and KF with manual fingerprint (see Table 6.1). The CDF of the error is shown in Figure 6.14.

Table 6.2: Localisation error from different fingerprinting methods (metres)

	MWM Prediction	**Self Calibration**	**Manual**
PF	μ =7.74 σ =4.48	μ =3.75 σ =3.04	μ =2.15 σ =1.08
BPF	μ =7.44 σ =3.70	μ =3.57 σ =2.77	μ =1.98 σ =1.11

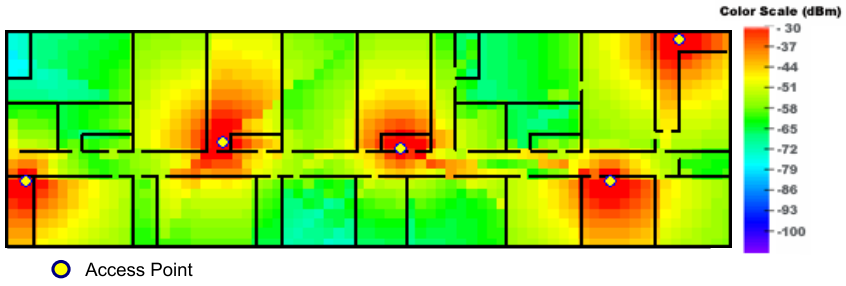

(a) Predicted fingerprint with MWM.

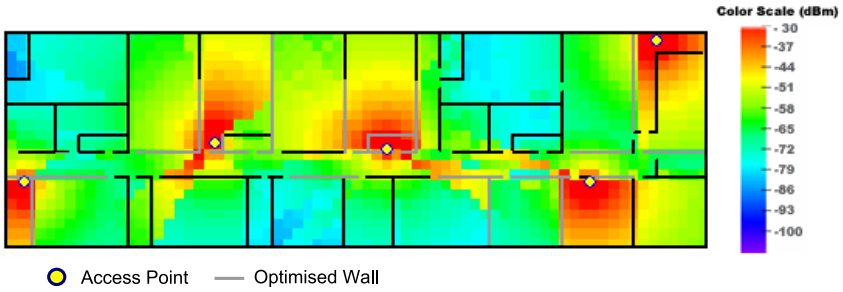

(b) Self-calibrated fingerprint.

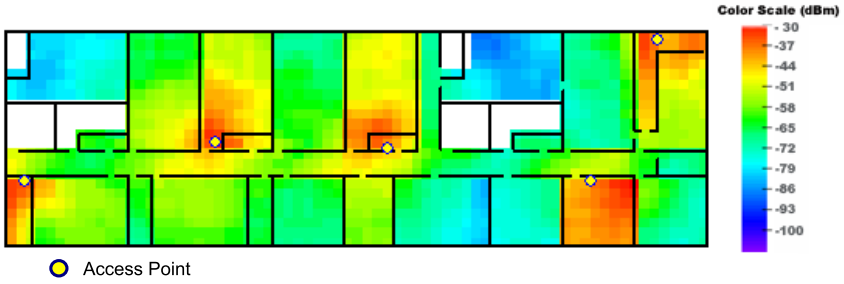

(c) Manually calibrated fingerprint.

Figure 6.12: Fingerprints before and after self-calibration and a manually calibrated fingerprint.

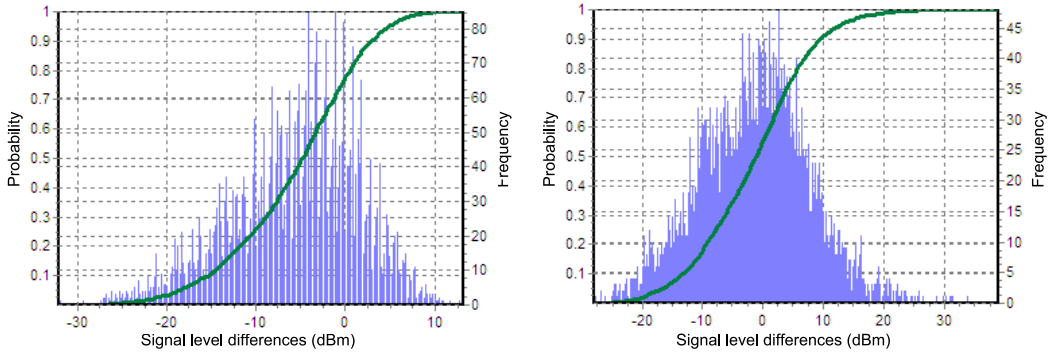

(a) MWM vs. manual fingerprint. (b) Self-calibration vs. manual fingerprint.

Figure 6.13: Histogram and CDF of signal level differences between fingerprints.

The principal advantage offered by the self-calibration fingerprint is its ability to make the fingerprint adaptive to any change in system or environment configuration and to avoid labour-intensive and cumbersome manual calibration. The manual fingerprint took 5 days to build, whereas the self-calibration fingerprint took less than 30 minutes[1].

6.2.4 Summary

This section described the evaluation of the self-fingerprinting algorithm to enhance the usability of opportunistic indoor localisation. The self-calibration algorithm used to enable an automatic generation and calibration of the RSS fingerprint was evaluated and compared with a predicted and manual fingerprint.

The localisation accuracy using a self-calibrated fingerprint was two times better compared with that obtained using a MWM predicted fingerprint (BPF error of 7.44m and 3.57m for prediction and self calibration, respectively). PF/BPF accuracy with self-calibration fingerprint also out-performs NN and KF with empirical fingerprint.

However, the principal advantage offered by the self-calibration fingerprint is its ability to avoid labour-intensive and cumbersome manual calibration. The empirical fingerprint took 5 days to build, whereas the self-calibration fingerprint took less than 30 minutes.

[1]Using Dell Latitude D630 Laptop, Intel Core Centrino Duo CPU, 2GB of RAM

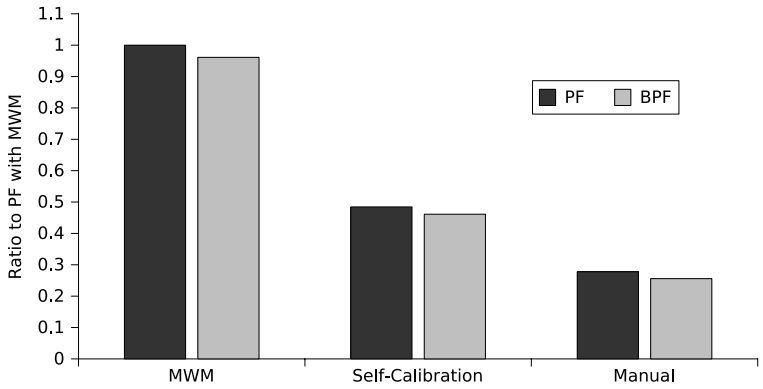

(a) Location error in proportion to MWM prediction fingerprint.

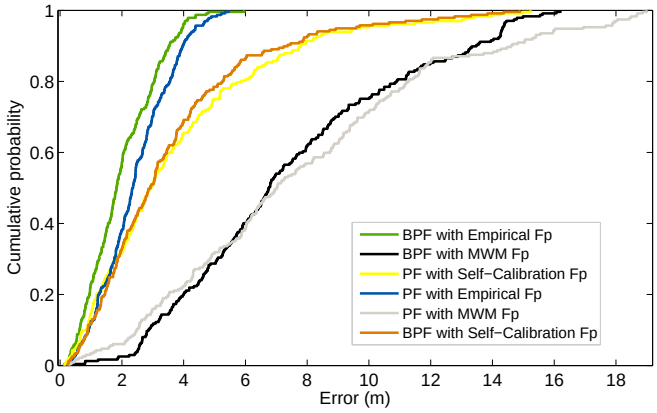

Figure 6.14: CDF of localisation error with different fingerprinting methods.

The ability to automatically build and optimise the fingerprint, to improve accuracy and to alleviate cumbersome manual-calibration make the self calibration algorithm a significant enhancement to the usability of opportunistic indoor localisation.

Furthermore, the particle filter algorithm is used to fuse different sensory data when more fine-grained accuracy is required. The next section will describe the evaluation of the particle filter-based sensor data fusion.

6.3 Multi Sensor Data Fusion

6.3.1 WLAN & WSN

6.3.1.1 Experimental Setup

The Adaptive Wireless Group (AWS) laboratory at CIT was used as a test-bed to evaluate fusion between WLAN and WSN. Three access points and 11 WSN nodes were installed in the test-bed. A fingerprint of WLAN and WSN was collected in every 0.5m grid.

A walk between 2 rooms and a corridor along the ground-truth (Figure 6.15) was performed to evaluate the algorithm. Three 30m-walks were performed to gather RSS measurements, which in turn were processed off-line in the fusion engine. RSS measurements in 200 points along the ground truth were gathered which in turn were used to estimate their location.

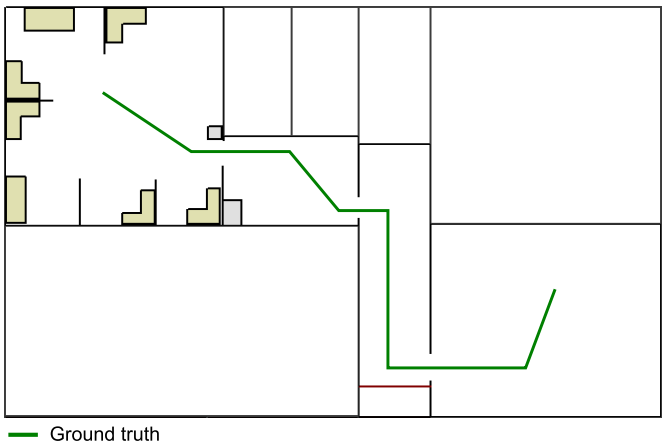

Figure 6.15: Ground-truth for the WLAN and WSN data fusion.

6.3.1.2 Results

In the context of localisation in a car factory, the algorithm provides reasonably good localisation accuracy (see Figure 6.16(a)). Localisation with WLAN-only was considered sufficient to provide room containment information whereas WLAN and WSN fusion provide better accuracy (1.16 m and 0.96 m mean error

for PF and BPF, respectively). It was sufficient to distinguish a worker's location relative to a car[1].

As previously described (section 5.1), since WSN RSS measurements provide a better profile for localisation purposes, it gives better localisation granularity. Figure 6.16(b) shows the CDF of the error. It can be seen that 100% of the error values of WLAN+WSN fusion using BPF are less than 3m.

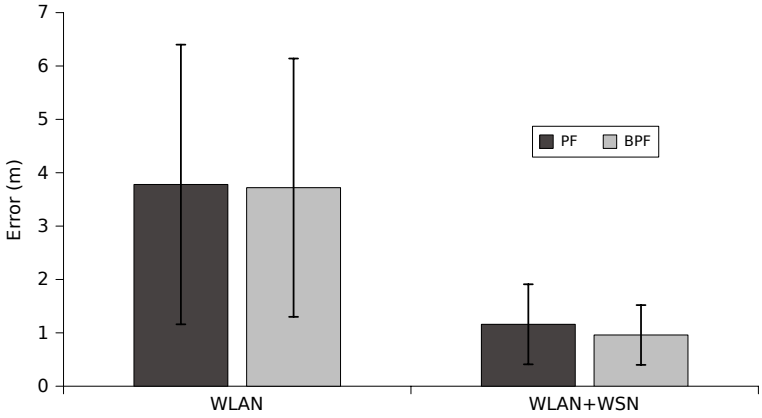

(a) Location error of the WLAN and WSN data fusion.

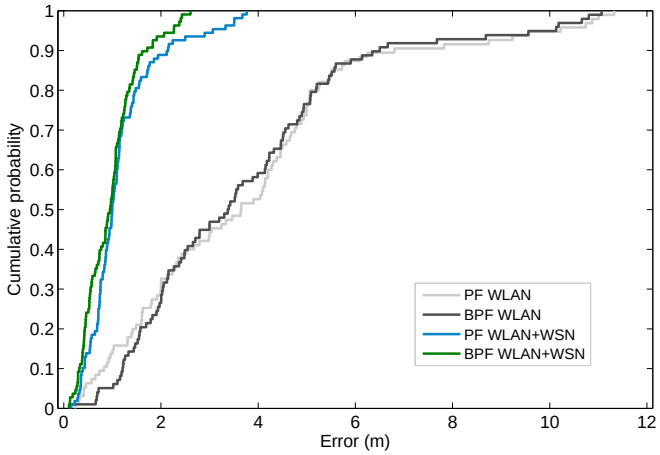

(b) CDF of WLAN and WSN data fusion.

Figure 6.16: Location error and CDF of the WLAN and WSN fusion.

[1]This study was conducted in the context of Wearit@Work project

6.3.2 PDR, Ultrasound & WSN

In typical emergency-response situations (e.g. a building on fire, or earthquake) it is not reasonable to expect built-in infrastructure to work. Therefore, in this setting there is no infrastructure available (e.g. a floor plan or network of pre-deployed nodes). Sensor nodes (Tmote WSN and Relate ultrasound; see section 5.2) are deployed in a dynamic, *ad-hoc* fashion as the user enters a building.

The concept is to use PDR in combination with sensor nodes that users deploy as a ***virtual lifeline*** (analogous to the physical lifelines that fire-fighters often use as "safety ropes"). The lifeline is used to help fire-fighters navigate inside the building. Further explanation about the virtual lifeline concept can be found in [106].

This approach differs from current approaches in fusion schemes for indoor PDR. Woodman and Harle, for instance, have demonstrated a highly-accurate system in which PDR is used in conjunction with a detailed building map [107]. Others have suggested combination of PDR with RFID [108], WLAN [86] and UWB [109]. The limitation of these fusion schemes is that they rely on either prior knowledge of the environment (e.g. maps), or pre-deployment of beacons at known positions.

In contrast, this thesis proposes a technique that relies only on sensors carried and deployed in a *ad-hoc* fashion by the system users (without map and pre-deployed node).

6.3.2.1 Experimental Setup

The experiments were conducted at Passau University, Germany. Data for off-line processing was collected in two different walking modes: normal walking and extended search walking modes[1].

Experiments with Normal Walking

The basement floor of the FIM building was used to collect data using normal walking mode. The overall test-bed dimension were 65 m x 65 m (4225 m^2). Three people did two 80m-walks or 6 walks in total in this building (Figure 6.17(a)).

[1]Random movement mimics fire fighters during search and rescue operations.

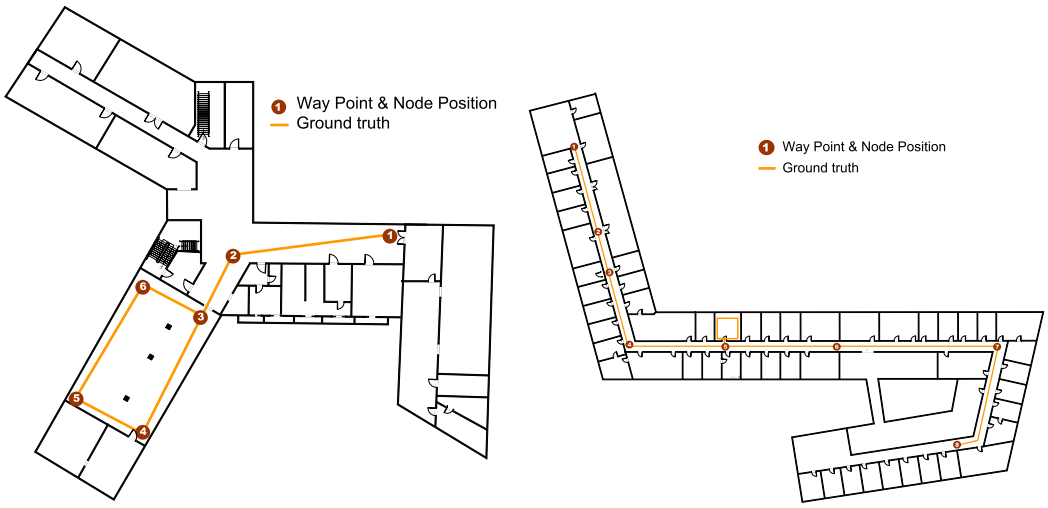

(a) Floor plan of the of the FIM building. (b) Floor plan of the ITZ building.

Figure 6.17: Floor plans for the experiments.

Experiments with Extended Search Inside Rooms

Another data set was recorded on the second floor of the ITZ building. The overall test-bed dimension was 100 m x 80 m (8000m^2). Two people each did four 400m-walks for this data set or 8 walks in total. The path is described in Figure 6.17(b).

The PDR location estimate is expected to drift significantly during this type of movement in a confined space. However, the nearby ultrasound nodes (and the WSN RSS proximity measurements) will be used to correct the position error.

6.3.2.2 Results

The lifeline performance was evaluated together with the data fusion algorithm, i.e: PF and BPF. Several combinations of sensory data, (PDR-only(P), PDR + Relate (P+R), PDR + Tmote (P+T), PDR + Relate + Tmote (P+R+T), were used to evaluate the performance and contribution of each modality.

The default system configuration is that the lifeline nodes (Relate and Tmote) are dropped by the user in *unknown locations* (in absolute location terms).

The localisation accuracy for normal walking mode in the FIM building is summarised in Figure 6.18(a) and for the extended search mode in the ITZ building

in Figure 6.18(b). From the results of both experiments it can be seen that the overall accuracy increases in proportion to the number of modalities being used.

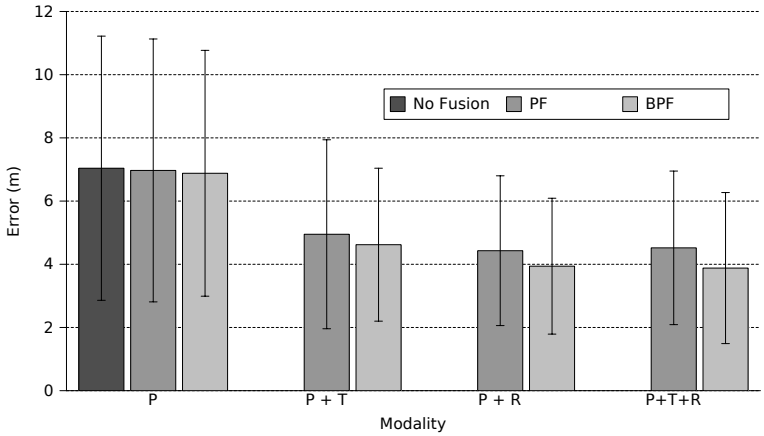

(a) Accuracy in normal walking mode.

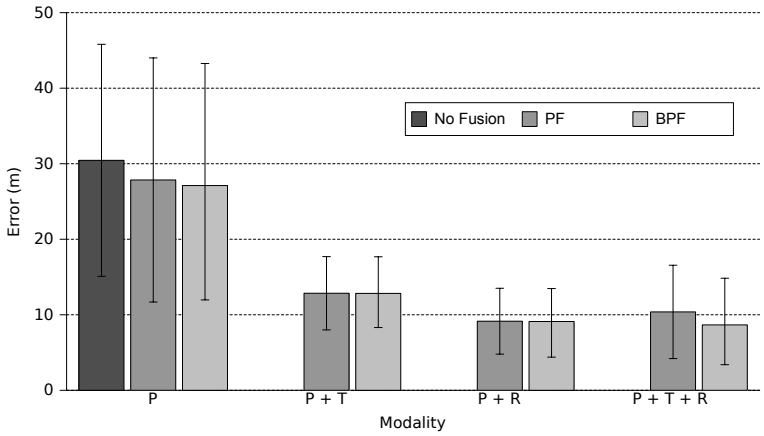

(b) Accuracy in extended search mode.

Figure 6.18: Localisation error with normal and extended search walking mode.

Since RSS-lateration method does not give accurate distance estimation in indoor environment, Tmote WSN does not offer much more accuracy. However, WSN have wider coverage range (10m-20m) than ultrasound node (<5m), therefore it is useful to extend the range of localisation system. In the context of fire-fighter scenario, the WSN can be used to re-align the fire-fighter to the virtual lifeline system in longer distances.

BPF fusion of PDR+Tmote+Relate provide the best accuracy (3.88 m mean

error in normal walking mode and 8.66 m mean error in extended search mode), while the PDR-only mode is worst with 7.04 m mean error in normal walking mode and about 30.45 m mean error in extended search mode.

This data also confirms the assumption that our system is particularly useful to compensate for irregular motion patterns during extended search. While the improvement in position accuracy for normal walking is of a factor of 2, this increases to a factor of about 4 for the extended search mode.

The system accuracy is illustrated by the trajectories as shown in Figure 6.19(a) and Figure 6.19(b) for normal walking and extended search mode respectively. The end of the pure PDR trajectory is inaccurate (by tens of meters) compared to the starting point. If used to guide a first responder back out of the building the system would obviously fail.

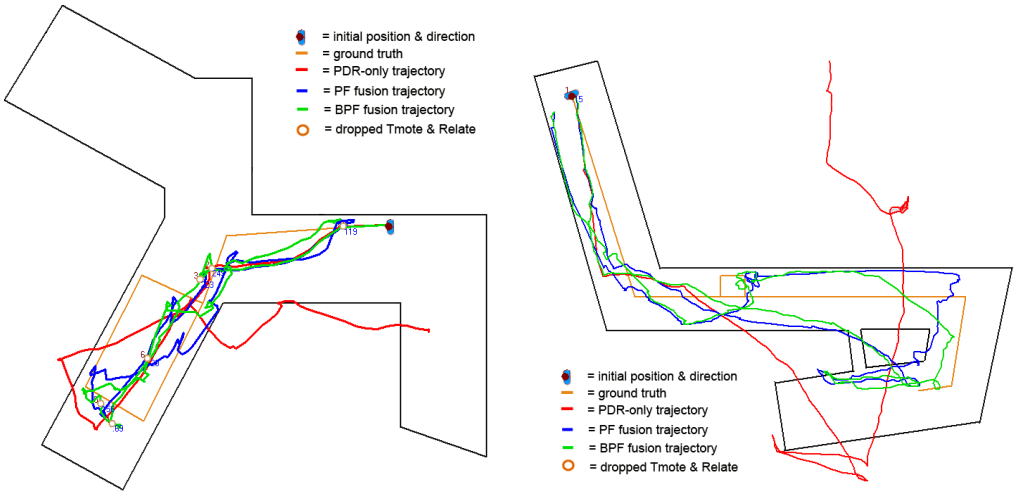

(a) Trajectories for normal walking mode. (b) Trajectories for extended search mode.

Figure 6.19: Trajectories for different walking mode with P+R+T.

In addition to those nodes placed at unknown locations, it is assumed that some nodes can be pre-positioned at known locations (e.g. entry points, windows, other known landmarks) for which an exact position on the map is known. Such nodes can realign the PDR system to the true position. The influence of the number of pre-positioned nodes on system accuracy was investigated during the empirical evaluation.

The location accuracy for differing numbers of pre-positioned nodes is summarised in Figure 6.20(a) and Figure 6.20(b) for normal walking and extended search mode, respectively.

The accuracy is in proportion with the number of pre-positioned nodes. As the number of pre-deployed nodes was increased, the accuracy got better. This is due to the PDR path being corrected more often in proportion to the number of pre-deployed nodes.

In the normal walking mode, the best accuracy is given when all of 6 ultrasound nodes were pre-deployed (BPF mean error of 1.76m). In the extended walking mode, the best accuracy is given when all of 8 ultrasound nodes were pre-deployed (BPF mean error of 6.16m).

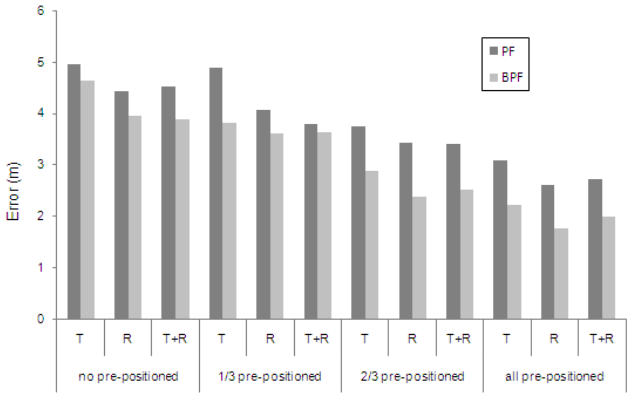

(a) Normal walking mode.

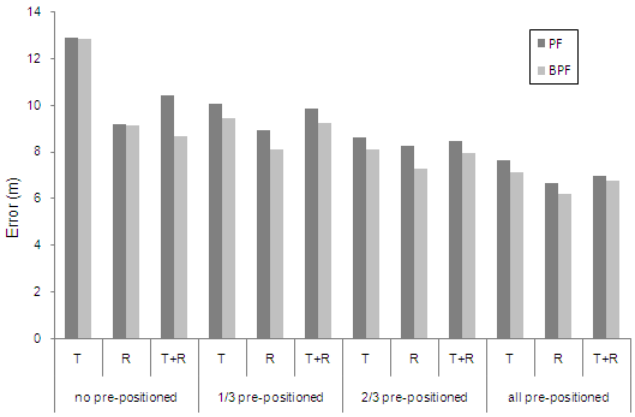

(b) Extended search mode.

Figure 6.20: Influence of the pre-positioned node on the accuracy.

6.4 Conclusion

In this chapter evaluation of the proposed algorithms for improving the accuracy and usability of the indoor localisation system has been performed. In the first part (section 6.1), PF, MF and BPF were evaluated and compared with existing NN and KF algorithms. The best performance was given by the BPF + MF algorithm which achieved nearly 3 times better accuracy than that obtained for the NN algorithm.

Typical applications that require 2-3m accuracies can take advantage of this enhancement. Applications that localises employee in office environment or patient in a hospital setting is one of the possible implementations.

Furthermore, the influence of the algorithm parameters on localisation accuracy was also investigated. These parameters are: the standard deviation σ_+ for the measurement model, the number of attempt for MF and the tail length for BPF.

Standard deviation σ_+ between 4dBm - 5 dBm is recommended for indoor localisation in an environment similar with office setting (characterised by many walls, corridors and rooms), such as hospital, campus or apartment. Attempt value of 8 is suggested since it gives minimum localisation error and only needs a modest computational power. Based on evaluation of the result, a tail length of 15-20 is proposed to give the best accuracy.

Section 6.2 which describes evaluation of the algorithm for addressing the fingerprint usability problem give encouraging results. The self-calibration algorithm was superior to the fingerprint prediction approach. The ability to automatically build and optimise a fingerprint was also demonstrated. It also outperforms the accuracy of state-of the art methods. Moreover, it has a significantly lower computation time compared to manually calibrated fingerprint.

Furthermore, the proposed algorithm could be conveniently used for multi sensor data fusion (section 6.3). Sensor data fusion of WLAN and WSN are implemented when higher accuracy is required. To demonstrate that the algorithm was also useful for multi sensor data fusion in an emergency scenario, a *virtual lifeline* system was proposed. It was used to fuse PDR, ultrasound node and WSN.

The proposed system of virtual lifeline was proved useful for indoor localisation when localisation infrastructure was not available in the environment. Therefore, the system relied on sensors carried and deployed by the users of the system on *an ad-hoc* basis.

It was demonstrated that the implementation of a particle filter, map filtering and backtracking particle filter significantly enhance the accuracy of the opportunistic indoor localisation system.

Furthermore, the ability to automatically build and optimised fingerprint, to improve accuracy and to alleviate cumbersome manual-calibration make the self calibration algorithm a significant enhancement on the usability of opportunistic indoor localisation.

It also showed that the particle filter-based multi sensor data fusion is able to further enhance the accuracy of the opportunistic system.

Therefore, it was demonstrated that the proposed algorithms are able to overcome the drawbacks of current methods in opportunistic systems. The developed algorithms are the foundation in achieving an affordable, accurate and usable opportunistic indoor localisation system. These characteristics enable the large scale adoption of indoor localisation systems. The proposed algorithms are novel and become the thesis contribution to enhance the state of the art of opportunistic systems.

Chapter 7

Conclusion

7.1 Summary

The main objectives of this dissertation as set out in section 1.2 are as follows:

1. *A comprehensive review of the state of the art of indoor localisation systems, with a particular focus on highlighting opportunities for an affordable, accurate, and usable opportunistic indoor localisation system.*

2. *Development and evaluation of a filtering algorithm with a Bayesian approach to enhance the accuracy of opportunistic indoor localisation.*

3. *Development and evaluation of a learning data fusion algorithm to enhance the accuracy and usability of opportunistic indoor localisation.*

4. *Investigation of the sensor data fusion algorithm between different localisation technologies and also algorithm implementation in different application domain.*

5. *Evaluation and comparison of the developed algorithms against current approaches with a particular focus on the implementation of opportunistic indoor localisation.*

Outcomes

The research work documented in this dissertation was performed to achieve the aforementioned objectives. In the next section, the main contributions of this work are outlined and the conclusions that can be drawn from the research are presented.

1. State of the Art of Indoor Localisation

Chapter 2 described current approaches to development of localisation systems. It was found that utilising RSS of the wireless-communication channel for opportunistic indoor localisation offers several advantages, such as affordability (since RSS is virtually free to obtain) and a low technology barrier to implementation (section 2.1).

WLAN has become the dominant local wireless networking technology. Accordingly, majority of the opportunistic indoor localisations use RSS of WLAN as the technology platform of choice.

Section 2.2 focused on current approaches to the opportunistic indoor localisations. It was found that there are some aspects of current approaches in opportunistic indoor localisation that need to be addressed with more research; namely, improvement in the accuracy and usability of the system.

Some algorithms tried to enhance the accuracy of opportunistic indoor localisations. However, it was found that the proposed methods still have many disadvantages. Based on the review of the state of the art, the particle filter algorithm had been identified as the most viable method for the opportunistic system. Therefore, a particle filter-based algorithm was implemented in the opportunistic indoor localisation.

To address the fingerprinting problem, current methods use indoor propagation modellings or machine learning approaches. However, the proposed solutions still have many shortcomings which restrict them from fully addressing the problems associated with an opportunistic system. Therefore, this research constructed novel algorithms for enhancing not only the accuracy but also the usability of the opportunistic localisation system.

2. Particle Filter for Localisation

Chapter 3 described the implementation of the most advanced algorithm, the particle filter, for opportunistic indoor localisation. It was found that the ability to deal with a non-linear and non-Gaussian system, the suitability for estimation of dynamic state with large process noise, and the robustness of the algorithm make particle filter an ideal approach for RSS-based opportunistic system.

Furthermore, novel motion and measurement models were devised to enable the implementation of particle filter into opportunistic system.

Motion Model

A motion model was developed as a combination from both Brownian movement and first-order motion models. This model assumed that the kinematic of a target had random values in it. However, the randomness is constrained by the previous state (section 3.4).

This approach more accurately reflects the target's kinematic behaviour in opportunistic system. It made particles behave more realistic, even in the absence of motion sensor.

Measurement Model

This research proposed a measurement model which properly considered the physical characteristics of signal propagation in indoor environments. The measurement model was derived from statistical inference between a fingerprint and RSS measurements.

Algorithm 3.4 described the steps necessary to obtain a likelihood observation function. Section 3.5.3 further described a method to obtain intrinsic parameters of the measurement model.

The devised measurement model leads to a more accurate representation of the sensor model in the opportunistic system which in turn leads to more accurate location estimations.

The novel motion and measurement models enable the adoption of a particle filter into opportunistic indoor localisation. The implementation of a particle

filter leads into the enhancement of the accuracy of opportunistic indoor localisation.

The limitation of a particle filter is that it needs a relatively high computational power compared to other methods. Recently, this disadvantage becomes less apparent because of the continuous development of more powerful hardware. Implementing a particle filter in resource constrained devices (such as a PDA or a mobile phone) can be a challenge. However, a client-server architecture allows one to distribute the majority of computation to a central server.

3. Learning Data Fusion

Chapter 4 presented a learning data fusion algorithm. To improve further the accuracy, this research examined other information beyond available signal in the environment, i.e. map information and particle trajectory.

Map filtering was used to fuse map information into the particle filter. Moreover, particle trajectory is fused to refine the state estimation with the backtracking particle filter algorithm. Both algorithms were devised to further increase the accuracy of opportunistic systems. Furthermore, with the aim of addressing the usability problem, a self-calibration algorithm was devised to automatically generate and calibrate the RSS fingerprint.

The collection of algorithms to enhance the accuracy and usability of an opportunistic system is one of the most important contributions of this research.

Map Filtering (MF)

Map information is used to constrain particle motion using the map filtering algorithm. Fusing the map with the particle filter algorithm is achieved by including the constraint rule in the motion model of the particle. The map filtering algorithm is presented in algorithm 4.1 in section 4.1.2.

The implementation of a particle filter in opportunistic indoor localisation is a novel approach for opportunistic indoor localisation. It leads to an enhancement of the accuracy of opportunistic indoor localisation.

Backtracking Particle Filter (BPF)

BPF is a technique for refining state estimates based on particle trajectory. The incorporation of the MF technique allowed BPF to exploit long-range geometrical constraints of a map and a long-term likelihood observation function. Algorithm 4.2 describes the steps for BPF algorithm.

The fusion of particle trajectory through backtracking particle filter is one of the novel contributions of this research. It leads to further enhancement of the accuracy of an opportunistic system.

The limitation of BPF is that it can only refine past state x_{t-b}. From application perspective, the BPF technique can be useful for applications that are tolerant to the introduced delay, such as an application that analyses user movement pattern in an indoor environment. For application that real-time localisation is a requirement, PF and MF is more appropriate.

Self Calibration Fingerprint

Self-calibration fingerprinting was devised to eliminate the labour-intensive manual calibration and makes the fingerprint adaptive to any change in the system or environment configuration. The self-calibration algorithm is described in Figure 4.5 in section 4.3.

This algorithm advances state-of-the-art fingerprinting methods in several key areas: it removes the necessity to collect initial training data; it elevates the necessity for placing dedicated RF receivers used for constantly measuring RSS values; it automatically optimises wall parameter for the propagation model.

The novelty of the algorithm lies in the ability to automatically build and optimise the fingerprint, and to make the fingerprint adaptive to any change in the system or environment configuration, thus significantly enhancing the usability of the opportunistic system.

Self-calibration fingerprinting is one of the most important contributions of this research.

4. Multi Sensor Data Fusion

Chapter 5 presented a particle filter-based algorithm for sensor data fusion of multi-modal localisation technology. The sensor data fusion is investigated to achieve more fine-grained accuracy of opportunistic indoor localisation.

Fusion of WSN and WLAN was investigated to achieve more fine-grained accuracy in the context of localisation in the car industry. It was found that RSS values of WSN gives distinctive measurement probability between fingerprinting grids. Eventually, it leads to better localisation accuracy when WLAN and WSN are fused.

Fusion of PDR, ultrasound and WSN was investigated to increase the accuracy of indoor localisation for fire-fighters. Motion and measurement models of PDR, ultrasound and WSN were devised to enable the fusion. Fusion for PDR was implemented by incorporating displacement estimates into the particle motion model. Novel measurement models based on Gaussian density function were devised for ultrasound and WSN to enable the fusion.

The fusion of an opportunistic system with different technologies through the development of sensor-specific probabilistic models is one of the contributions of this research.

5. Evaluation

Chapter 6 described the evaluation of the proposed algorithms for improving the accuracy and usability of the indoor localisation system that had been performed. Evaluation of the algorithms was conducted by means of experiments using a real test-bed in CIT and Passau University, Germany.

The evaluation showed favourable results. In the first part (section 6.1), PF, MF and BPF were evaluated and compared with existing NN and KF algorithms. The best performance was given by the BPF + MF algorithm (μ =1.98m σ =1.11m).

Section 6.2 which describes evaluation of the algorithm for addressing the fingerprint usability problem gives encouraging results. The self-calibration algorithm significantly provided a better result than the fingerprint prediction approach. The ability to automatically build and optimise a fingerprint was also

demonstrated. It also out-performs the accuracy of state-of the art methods (NN and KF). Moreover, it has a significantly lower computation time compared to manually calibrated fingerprint.

Furthermore, the proposed algorithm could be conveniently used for multi sensor data fusion (section 6.3). Sensor data fusion of WLAN and WSN are implemented when higher accuracy is required. To demonstrate that the algorithm was also useful for multi sensor data fusion in an emergency scenario, a *virtual lifeline* system was proposed. It was used to fuse PDR, ultrasound node and WSN.

It was demonstrated that the implementation of a particle filter, map filtering and backtracking particle filter significantly enhance the accuracy of the opportunistic indoor localisation system.

Furthermore, the ability to automatically build and optimise a fingerprint, to improve accuracy and to alleviate cumbersome manual-calibration make the self calibration algorithm is able to significantly enhance the usability of opportunistic indoor localisation.

It also showed that the particle filter-based multi sensor data fusion is able to enhance the accuracy of the opportunistic system.

Therefore, it was demonstrated that the proposed algorithms are able to overcome the drawback of current methods in opportunistic systems. The algorithms were demonstrated to be able to improve the accuracy and usability of the indoor localisation system. The proposed algorithms are novel and become thesis contribution to enhance the state of the art of opportunistic system.

7.2 Future Work

Learning Bayesian Network for the Self-Calibration

As stated in the description of the self-calibration algorithm in section 4.3, optimisation of wall parameters of the MWM is performed by a linear method. This linear optimisation was only applied to a single wall segment at a time, meaning that adjacent walls did not have an influence, or were not in turn influenced by, the optimised wall segment.

Consideration of neighbouring or adjacent walls in the overall optimisation model would potentially produce better optimisation results. This could be achieved by a learning Bayesian network which describes walls by means of a probabilistic graphical model and their conditional independences. This model would allow calculation of interdependencies between wall segments during optimisation.

3D Multi-Floor & Multi-Building

Currently, the implementation of an opportunistic localisation system is suitable for a 2D single floor. Multi-floor environments are stacked as 2.5D structure, but extension into 3D multi-floor and multi-building environments would be highly desirable. The computational requirements for the localisation algorithm and 3D propagation model will increase, but the fundamental PF/BPF and self-calibration algorithm could easily be extended for this purpose.

Smart-Phone based Opportunistic Localisation

Recent mobile phones, in addition to the GSM interface, have been equipped with various sensors such as the WLAN interface, GPS, compass and accelerometer.

Using these sensors for opportunistic localisation would be a logical development of the present study. The multi-modal sensor data fusion could be easily re-used. However, the relatively low computational power of the mobile phone needs to be considered when implementing the algorithm.

7.3 Conclusion

Indoor localisation systems are evolving towards so-called opportunistic localisation systems. These take advantage of any readily available information in the environment and a mobile device, such as RSS. Problems inherent in current approaches to opportunistic localisation that need to be addressed include further improvement of the accuracy and usability of the system. In addition, sensor

data fusion capability is overlooked with existing approaches, even though the accuracy of a single-technology platform often cannot satisfy practical application requirements (see chapter 2 State of the Art).

Hence, development of more advanced algorithms is essential to the wider adoption of a low-cost, accurate and practical indoor localisation system. This thesis offers a solution by enhancing the current particle filter approaches for opportunistic localisation and by constructing a novel algorithm for solving the usability problem (chapter 3 and 4). Furthermore, the algorithm was able to become a framework for the sensor data fusion between multi modal localisation technologies (chapter 5).

To adapt the particle filter algorithm for opportunistic localisation, novel motion and measurement models were devised. The motion model was an enhancement from both Brownian movement and first-order motion model. This work also proposed a measurement model which properly considers the physical characteristics of signal propagation in indoor environments (algorithm 3.4). This evaluation demonstrated that implementation of the particle filter in opportunistic localisation resulted in better localisation accuracy compared to existing conventional algorithms (chapter 6).

The particle filter algorithm was improved further to take advantage of environment description and history of RSS measurement. The algorithms used are called MF and BPF. Implementation of MF and BPF for opportunistic localisation further improved the accuracy of the localisation system.

Self-calibration fingerprinting was devised to significantly enhance system usability. The evaluation shown in chapter 6 demonstrates that the algorithm can overcome the problems of manual fingerprint collection enabling automatic generation and calibration of the RSS fingerprint. The algorithm keeps the fingerprint up-to-date, thus achieving self-calibration of the localisation system.

In addition, the algorithm can be further utilised for sensor data fusion of multi-modal localisation technology to achieve more fine-grained accuracy. Furthermore, a data fusion algorithm was implemented in an indoor localisation system commonly used for first-responders in emergency scenarios. This *virtual lifeline* system could be used for indoor localisation in cases where the infrastructure is not available in the environment.

The work presented in this thesis has demonstrated the ability to address the problem in perfecting an opportunistic indoor localisation system. The new algorithm is not only able to enhance the performance of the system, but also significantly enhanced its usability. This could lead to wider adoption of an affordable, accurate and usable localisation system.

Eventually, knowledge of physical location could open up a wide range of possible applications. For example, tracking people and assets, safety and security or navigating people out of buildings on fire during emergency situations. The aforementioned applications would help to do things more efficiently, save time, money and, perhaps, lives.

References

[1] M. Weiser, "Some computer science problems in ubiquitous computing," *Communications of the ACM*, 1993.

[2] J. Farrell and M. Barth, *The Global Positioning System and Innertial Navigation*. McGraw-Hill Professional, 1999.

[3] G. Roussos and V. Kostakos, "RFID in pervasive computing: State-of-the-art and outlook," *Elsevier Pervasive and Mobile Computing*, vol. 5, pp. 110–131, 2009.

[4] J. Fontana, "Recent system applications of short-pulse ultra-wideband (UWB) technology," *IEEE Transaction on Microwave Theory Technology*, vol. 52, pp. 2087– 2104, 2004.

[5] N. S. Correal, S. Kyperountas, Q. Shi, and M. Welborn, "An ultrawideband relative location system," in *Proceedings of the IEEE Conference Ultra Wideband System Technology*, 2003.

[6] B. B. Peterson, C. Kmiecik, R. Hartnett, P. M. Thompson, J. Mendoza, and H. Nguyen., "Spread spectrum indoor geolocation," *Journal of the Institute of Navigation*, vol. 45, no. 2, pp. 97–102, 1998.

[7] X. Li, K. Pahlavan, M. Latva-aho, and M. Ylianttila, "Comparison of indoor geolocation methods in DSSS and OFDM wireless LAN," in *Proceedings of the IEEE VTC*, vol. 6, September 2000.

[8] C. Drane, M. Macnaughtan, and C. Scott, "Positioning GSM telephones," *IEEE Communications Magazine*, vol. 36, no. 4, pp. 46–54, April 1998.

[9] A. Bensky, *Wireless Positioning: Technologies and Application*, ser. GNSS technology and application series. Artech House Publishers, 2008.

[10] K. J. Krizmant, T. E. Biedkatt, and T. S. Rappaportt, "Wireless position location: Fundamentals, implementation strategies, and sources of error," in *Proceedings of the VTC*, vol. 2, May 1997.

[11] D. Niculescu and B. Nath, "Ad hoc positioning system (APS) using AOA," in *Proceedings of the IEEE INFOCOM*, 2003.

[12] H. Liu, H. Darabi, P. Banerjee, and J. Liu, "Survey of wireless indoor positioning techniques and systems," *IEEE Transaction on Systems, Man, and Cybernetics*, vol. 37, no. 6, pp. 1067–1077, November 2007.

[13] A. Kupper, *Location Based Services: Fundamentals and Operations*. John Wiley & Sons, 2005.

[14] J. Caffery, *Wireless Location in CDMA Cellular Radio Systems*. Kluwer Academic Publishers, 2000.

[15] H. A. Karimi and A. Hammad, Eds., *Telegeoinformatics: Location-based Computing and Services*. CRC, 2004.

[16] D. Titterton and J. Weston, *Strapdown Inertial Navigation Technology*. IEE, 2005.

[17] S. Beauregard, "Omnidirectional pedestrian navigation for first responders," in *Proceedings of the 4th WPNC*, Hannover, Germany, March 22 2007.

[18] M. Kourogi and T. Kurata, "A method of personal positioning based on sensor data fusion of wearable camera and self-contained sensors," in *Proceedings of IEEE MFI*, 2003.

[19] H. Aoki, B. Schiele, and A. Pentland, "Realtime personal positioning system for wearable computers," in *Proceedings of the International Symposium on Wearable Computing*. IEEE Computer Society, 1999, pp. 37–43.

[20] N. Checka and K. Wilson, "Person tracking using audio-video sensor fusion," 2001, MIT Artificial Intelligence Laboratory, 200 Technology Square, Cambridge MA, 02139 USA.

[21] M. Kanaan and K. Pahlavan, "A comparison of wireless geolocation algorithms in the indoor environment," in *Proceedings of the IEEE Wireless Communication Network Conference*, 2004.

[22] B. Fang, "Simple solution for hyperbolic and related position fixes," *IEEE Transaction on Aerospace and Electronic System*, vol. 26, pp. 748–753, September 1990.

[23] A. Goldsmith, *Wireless Communication*. Cambridge University Press, 2005.

[24] R. Want, A. Hopper, V. Falcao, and J. Gibbons, "The active badge location system," *ACM Transactions on Information Systems*, vol. 10, pp. 91–102, January 1992.

[25] M. Porreta, P. Nepa, G. Manara, and F. Giannetti, "Location, location, location," *IEEE Vehicular Technology Magazine*, vol. 3, no. 2, pp. 20–29, June 2008.

[26] (2009, March). [Online]. Available: http://www.ubisense.net

[27] (2009, March). [Online]. Available: http://www.aetherwire.com

[28] (2009, March). [Online]. Available: http://www.timedomain.com

[29] M. Vossiek, L. Wiebking, P. Gulden, J. Wieghardt, C. Hoffmann, and P. Heide, "Wireless local positioning," *IEEE Microwave Magazine*, vol. 4, pp. 77–86, 2003.

[30] (2009, March). [Online]. Available: http://www.symeo.com/English/

[31] N. Patwari, "Location estimation in sensor network," Ph.D. dissertation, University of Michigan, 2005.

[32] K. Romer, "Time synchronization and localization in sensor networks," Ph.D. dissertation, ETH Zurich, 2005.

[33] A. Kotanen, M. Hannikainen, H. Leppakoski, and T. D. Hamalainen, "Experiments on local positioning with bluetooth," in *Proceedings of the IEEE International Conference Infomation Technology*, April 2003, pp. 954–958.

[34] J. Hallberg, M. Nilsson, and K. Synnes, "Positioning with bluetooth," in *Proceedings of the IEEE 10th International Conference on Telecommunications*, 2003.

[35] A. Schwaighofer, M. Grigoras, V. Tresp, and C. Hoffmann, "GPPS: A Gaussian process positioning system for cellular networks," in *NIPS*. MIT Press, 2004.

[36] P. Bahl and V. Padmanabhan, "RADAR: An in-building RF-based user location and tracking system," in *Proceedings of the IEEE INFOCOM*, March 2000, pp. 775–784.

[37] S. Y. Seidel and T. S. Rapport, "914 mhz path loss prediction model for indoor wireless communications in multi-floored buildings," *IEEE Transaction on Antennas & Propagation*, vol. 40, pp. 207 – 217, 1992.

[38] K. Lorincz and M. Welsh, "MoteTrack: a robust, decentralized approach to RF-based location tracking," *Personal Ubiquitous Computing*, vol. 11, no. 6, pp. 489–503, 2007.

[39] A. LaMarca *et al.*, "Place Lab: Device positioning using radio beacons in the wild," in *Proceedings of the Pervasive*, 2005.

[40] R. Battiti, T. L. Nhat, and A.Villani, "Location-aware computing: A neural network model for determining location in wireless LANs," University of Trento, Tech. Rep. DIT-02-0083, February 2002.

[41] A. Kushki, K. N. Plataniotis, and A. N. Venetsanopoulos, "Kernel-based positioning in wireless local area networks," *IEEE Transaction on Mobile Computing*, vol. 6, no. 6, pp. 689–705, June 2007.

[42] M. Brunato and R. Battiti, "Statistical learning theory for location fingerprinting in wireless LANs," *Elsevier Computer Networks and ISDN Systems*, vol. 47, pp. 825 – 845, April 2005.

[43] S. J. Pan, V. W. Zheng, Q. Yang, and D. H. Hu, "Transfer learning for WiFi-based indoor localization," in *Proceedings of the AAAI-08 Workshop on Transfer Learning for Complex Task*, 2008.

[44] M. Youssef, A. Agrawala, and A. U. Shankar, "WLAN location determination via clustering and probability distributions," in *Proceedings of the IEEE PerCom*, 2003.

[45] M. Youssef and A. K. Agrawala, "Handling samples correlation in the Horus system," in *Proceedings of the IEEE INFOCOM*, 2004.

[46] M. B. Kjærgaard, "A taxonomy for radio location fingerprinting," *LCNS*, vol. 4718, pp. 139–156, 2007.

[47] S. Thrun, "Robotic mapping: A survey," in *Exploring Artificial Intelligence in the New Millenium*. Morgan Kaufmann, 2002.

[48] D. Simon, *Optimal State Estimation: Kalman, H Infinity, and Nonlinear Approaches*. Wiley-Interscience, 2006.

[49] D. Fox, J. Hightowerand, L. Liao, D. Schulz, and G. Borriello, "Bayesian filtering for location estimation," *IEEE Pervasive Computing*, vol. 02, no. 3, pp. 24–33, 2003.

[50] N. Sirola, "Mathematical methods for personal positioning and navigation," Ph.D. dissertation, Tampere University of Technology, 2007.

[51] S. Thrun, D. Fox, W. Burgard, and F. Dellaert, "Robust Monte Carlo localization for mobile robots," *Artificial Intelligence*, vol. 128, pp. 99–141, 2001.

[52] M. Heidari, "A testbed for real-time performance evaluation of RSS-based indoor geolocation systems in laboratory environment," Master's thesis, Worcester Polytechnic Institute, 2005.

[53] (2009, March). [Online]. Available: http://www.ekahau.com/

[54] D. L. Hall and J. Llinas, "An introduction to multisensor data fusion," *Proceedings of the IEEE ISCAS*, vol. 85, no. 1, January 1998.

[55] D. L. Hall and J. Llinas, *Handbook on Multisensor Data Fusion*. CRC, 2001.

[56] J. Hightower and G. Borriello, "Particle filters for location estimation in ubiquitous computing: A case study," in *Proceedings of the 6th Ubicomp*, September 2004.

[57] J. Castellanos, J. Neira, and J. Tards, "Multisensor fusion for simultaneous localization and map building," *IEEE Transactions on Robotics and Automation*, vol. 17, pp. 908–914, 2001.

[58] **Widyawan**, M. Klepal, and D. Pesch, "Influence of predicted and measured fingerprint on the accuracy of RSSI-based indoor location systems," in *Proceedings of the 4th IEEE WPNC 2007*, Hannover, Germany, March 2007.

[59] A. Narzullaev, Y. Park, and H. Jung, "Accurate signal strength prediction based positioning for indoor WLAN systems," in *Proceedings of the IEEE/ION Position, Location and Navigation Symposium*, 2008.

[60] M. Lott and I. Forkel, "A multi-wall-and-floor model for indoor radio propagation," in *Proceedings of the IEEE VTC Spring*, 2001.

[61] M. Klepal, "Novel approach to indoor electromagnetic wave propagation modelling," Ph.D. dissertation, Czech Technical University, 2003.

[62] X. Chai and Q. Yang, "Reducing the calibration effort for probabilistic indoor location estimation," *IEEE Transaction on Mobile Computing*, vol. 6, pp. 649–662, 2007.

[63] Z. Xiang, S. Song, J. Chen, H. Wang, J. Huang, and X. Gao, "A wireless LAN-based indoor positioning technology," *IBM Journal of Research and Development*, vol. 48, no. 5/6, pp. 617–626, 2004.

[64] J. Yin, Q. Yang, and L. Ni, "Learning adaptive temporal radio maps for signal-strength-based location estimation," *IEEE Transactions on Mobile Computing*, vol. 7, pp. 869–883, 2007.

[65] S. Thrun, W. Burgard, and D. Fox, *Probabilistic Robotics (Intelligent Robotics and Autonomous Agents)*. The MIT Press, September 2005.

[66] D. P. Bertsekas and J. N. Tsikilis, *Introduction To Probability*. Athena Scientific, 2002.

[67] M. S. Arulampalam, S. Maskell, N. Gordon, and T. Clapp, "A tutorial on particle filters for online nonlinear/non-Gaussian Bayesian tracking," *IEEE Transaction on Signal Processing*, vol. 50, no. 2, pp. 174–188, 2002.

[68] B. D. O. Anderson and J. B. Moore, *Optimal Filtering*. Dover Publications Inc., 2005.

[69] A. Papoulis, *Probability, Random Variables, and Stochastic Processes*. McGraw-Hill Companies, 1984.

[70] P. S. Maybeck, *Stochastic Models, Estimation and Control*. Academic Press, 1982.

[71] R. E. Kalman, "A new approach to linear filtering and prediction problems," *Transactions of the ASME Journal of Basic Engineering*, vol. 82, pp. 35–45, 1960.

[72] R. Kalman, "New methods in Wiener fltering theory," in *Proceedings of the Symposium of Application Random Function Theory and Probability*, 1963.

[73] A. Doucet, N. de Freitas, and N. Gordon, Eds., *Sequential Monte Carlo Methods in Practice*, 1st ed. New York: Springer, June 2001.

[74] B. Ristic, S. Arumpalampam, and N. Gordon, *Beyond the Kalman Filter: Particle Filters for Tracking Applications*. Artech House Publishers, February 2004.

[75] N. J. Gordon, D. J. Salmond, and A. F. M. Smith, "Novel approach to nonlinear/non-Gaussian Bayesian state estimation," *IEE Proceedings F Radar and Signal Processing*, vol. 140, pp. 107–113, 1993.

[76] J. Maccormick and A. Blake, "A probabilistic exclusion principle for tracking multiple objects," in *International Journal of Computer Vision*, 1999, pp. 572–578.

[77] K. Kanazawa, D. Koller, and S. Russell, "Stochastic simulation algorithms for dynamic probabilistic networks," in *Proceedings of the Eleventh Annual Conference on Uncertainty AI*, 1995.

[78] J. S. Liu and R. Chen, "Sequential Monte Carlo methods for dynamic systems," *Journal of the American Statistical Association*, vol. 93, pp. 1032–1044, 1998.

[79] A. Doucet, S. Godsill, and C. Andrieu, "On sequential Monte Carlo sampling methods for Bayesian filtering," *Statistics and Computing*, vol. 10, pp. 197–208, 2000.

[80] G. Kitagawa, "Monte Carlo filter and smoother for non-Gaussian non-linear state space model," *Journal of Computational and Graphical Statistics*, vol. 5, pp. 1–25, 1996.

[81] S. Godsill, A. Doucet, and M. West, "Methodology for Monte Carlo smoothing with application to time-varying autoregressions," in *Proocedings of the International Symposium Frontiers Time Series Modeling*, 2000.

[82] S. T. M. Montemerlo and W. Whittaker, "Conditional particle filters for simultaneous mobile robot localization and people-tracking," in *Proceedings of the IEEE ICRA*, 2002.

[83] E. Meier and F. Ade, "Using the condensation algorithm to implement tracking for mobile robots," in *Proceedings of the Eurobot*, 1999.

[84] A. Bruce, "Better motion prediction for people-tracking," in *Proceedings of ICRA 2004*, 2004.

[85] A. E. Chapman, *Biomechanical Analysis of Fundamental Human Movement*. Human Kinetics Europe Ltd, 2008.

[86] F. Evennou and F. Marx, "Advanced integration of WiFi and inertial navigation systems for indoor mobile positioning," *EURASIP Journal on Applied Signal Processing*, vol. 2006, pp. 1–11, January 2006.

[87] H. Wang, H. Lenz, A. Szabo, J. Bamberger, and W. D. Hanebeck, "WLAN-based pedestrian tracking using particle filters and low-cost MEMS sensors," in *Proceedings of the IEEE WPNC'07*, 2007.

[88] S. R. Saunders and A. Aragon, *Antennas and Propagation for Wireless Communication Systems*, 2nd ed. Wiley & Sons, May 2007.

[89] R. Bansal, Ed., *Handbook of Engineering Electromagnetics*. CRC, 2004.

[90] M. Klepal, R. Mathur, A. McGibney, and D. Pesch, "Influence of people shadowing on optimal deployment of WLAN access points," in *Proceedings of the IEEE VTC*, 2004.

[91] A. Alouani and W. Blair, "Use of a kinematic constraint in tracking constant speed, maneuvering targets," *IEEE Transactions on Automatic Control*, vol. 38, pp. 1107–1111, 1993.

[92] N. Svenzén, "Real time implementation of map aided positioning using a Bayesian approach," Master's thesis, Linköping University, 2002.

[93] S. Oh, S. Tariq, B. Walker, and F. Dellaert, "Map-based priors for localization," in *Proocedings of the IROS*, 2004.

[94] H. Choset, "Sensor based motion planning: The hierarchical generalized Voronoi graph." Ph.D. dissertation, California Insititute of Technology, 1996.

[95] COST Telecommunications, *COST231 Final Report, Digital Mobile Radio: COST231 View on the Evolution towards 3rd Generation Systems*. Brussel: European Commission/COST Telecommunications, 1998.

[96] R. L. Kruse and A. Ryba, *Data Structures and Program Design in C++*. Prentice Hall, 1998.

[97] E. Kreyszig, *Advanced Engineering Mathematics*. John Wiley & Sons, 1999.

[98] A. Björg, *Numerical methods for Least Square Problems*. Siam, 1996.

[99] *802.15.4-2006 Part 15.4: Wireless MAC and PHY specifications for Low Rate Wireless Personal Area Networks (LR-WPANS)*, IEEE Std.

[100] E. Foxlin, "Pedestrian tracking with shoe-mounted inertial sensors," *Computer Graphics and Applications, IEEE*, vol. 25, no. 6, pp. 38–46, 2005.

[101] K. F. Stirling, R. and G. Lachapelle, "Evaluation of a new method of heading estimation for pedestrian dead reckoning using shoe mounted sensors," *Journal of Navigation*, vol. 58, no. 1, pp. 31 – 45, 2005.

[102] F. Cavallo, A. Sabatini, and V. Genovese, "A step toward GPS/INS personal navigation systems: Real-time assessment of gait by foot inertial sensing," in *Proceedings of the IEEE IROS*, Edmonton, Canada, August 2005, pp. 1187 – 1191.

[103] C. Fischer, K. Muthukrishnan, M. Hazas, and H. Gellersen, "Ultrasound-aided pedestrian dead reckoning for indoor navigation," in *Proceedings of the MELT*, California, September 2008.

[104] M. Hazas, C. Kray, H. Gellersen, H. Agbota, G. Kortuem, and A. Krohn, "A relative positioning system for co-located mobile devices," in *Proceedings of the 3rd MobiSys*. New York, NY, USA: ACM Press, 2005, pp. 177–190.

[105] S. Beauregard, **Widyawan**, and M. Klepal, "Indoor PDR performance enhancement using minimal map information and particle filters," in *Proceedings of the IEEE/ION PLAN*, Monterey, California, May 2008.

[106] M. Klann *et al.*, "LifeNet: an ad-hoc sensor network and wearable system to provide firefighters with navigation support," *Proceedings of the UbiComp: Demos Extended Abstracts*, 2007.

[107] O. Woodman and R. Harle, "Pedestrian localisation for indoor environments," in *Proceedings of the 10th UbiComp*. New York, NY, USA: ACM, 2008, pp. 114–123.

[108] L. E. Miller, "Indoor navigation for first responders: A feasibility study," Wireless Communication Technologies Group, Advanced Networking Technologies Devision, Information Technology Laboratory, National Institute of Standards and Technology, Tech. Rep., February 10 2006.

[109] V. Amendolare, D. Cyganski, R. J. Duckworth, S. Makarov, J. Coyne, H. Daempfling, and B. Woodacre, "WPI precision personnel locator system: Inertial navigation supplementation," in *Proceedings of the IEEE/ION PLAN*, Monterey, California, May 2008.